2012

Time-Frequency Analysis of Ongoing and Event Related Potentials

Iordanidou Vasiliki

Supervisor: Prof.

Zervakis Michalis

ABSTRACT

During the past few years there has been an increasing interest in studying and understanding the neural mechanisms behind cognitive brain activity. This kind of knowledge is of great importance in many scientific areas such as clinical prognosis and diagnosis, brain computer interfaces design, etc. In this context, various methodological approaches have been suggested for the analysis of the EEG signal, which is one of the most widely used brain representations.

This work explores two different approaches for the EEG analysis. In the first approach there is a case of ongoing EEG in which we use the power spectrum (PS) and linear coherence (LC) in order to investigate the differences in the channel activations for two mathematical thinking tasks. The goal in this case is to identify differences between the mathematical tasks through the measures of PS and LC and evaluate them through statistical testing. In the second approach there is a case of evoked EEG from a working memory experiment on which populations of control and dyslexic subjects participate. In this case, various synchronization measures are applied on the time-frequency (TF) maps of the corresponding independent components (ICs). Those measures were very important for the evaluation of the components and helped us recognize a number different cases for the generation of our ERPs. We also tried to identify differences between the two populations overall activation comparing the TF maps of the synchronizations measures and evaluate them through statistical testing. For both datasets, we had findings with statistical significance which also are in support and complementary to previous research.

ΠΕΡΙΛΗΨΗ

Κατά τις τελευταίες δεκαετίες υπάρχει ολοένα αυξανόμενο ενδιαφέρον για τη μελέτη και κατανόηση των νευρωνικών μηχανισμών που βρίσκονται πίσω από τη νοητική εγκεφαλική δραστηριότητα. Τέτοιου τύπου γνώσεις είναι εξαιρετικά σημαντικές σε πολλές επιστημονικές περιοχές όπως η κλινική πρόγνωση και διάγνωση, ο σχεδιασμός διασύνδεσης υπολογιστή-εγκεφάλου και λοιπές συναφείς περιοχές. Σε αυτό το πλαίσιο, έχουν προταθεί ποικίλες μεθοδολογικές προσεγγίσεις για την ανάλυση του ηλεκτροεγκεφαλογραφήματος (ΗΕΓ), το οποίο αποτελεί μία από τις πιο διαδεδομένες εγκεφαλικές απεικονίσεις.

Η εργασία αυτή διερευνά δύο διαφορετικές προσεγγίσεις ανάλυσης του ΗΕΓ. Στην πρώτη προσέγγιση έχουμε μια περίπτωση συνεχούς ΗΕΓ στο οποίο χρησιμοποιούμε το μέτρο της φασματικής ισχύος και της γραμμικής συνοχής έτσι ώστε να διερευνήσουμε τις διαφορές στη δραστηριότητα των καναλιών για δύο πειράματα μαθηματικής σκέψης. Το ζητούμενο σε αυτή την περίπτωση είναι να αναγνωρίσουμε τις διαφορές μεταξύ των δύο μαθηματικών πειραμάτων με τη χρήση των παραπάνω μέτρων και να τις αξιολογήσουμε μέσω τεστ αξιολόγησης στατιστικής σημαντικότητας. Η δεύτερη προσέγγιση αφορά την περίπτωση προκλητού ΗΕΓ (ΠΔ) από ένα πείραμα μνήμης στο οποίο συμμετέχουν μη παθολογικά και δυσλεκτικά άτομα. Σε αυτή την περίπτωση, χρησιμοποιούνται διάφορα μέτρα συγχρονισμού στο χρονοσυχνοτικό περιεχόμενο των προκυπτόντων ανεξάρτητων συνιστωσών. Τα μέτρα αυτά είναι ιδιαιτέρως σημαντικά για την αξιολόγηση των συνιστωσών και βοηθητικά στην αναγνώριση των διαφορετικών περιπτώσεων γένεσης των ΠΔ. Επιχειρήσαμε επίσης να αναγνωρίσουμε τις διαφορές μεταξύ των δύο πληθυσμών όσον αφορά τη γενική δραστηριότητα που εμφανίζεται στα ΠΔ συγκρίνοντας τις χρονοσυχνοτικές απεικονίσεις των μέτρων συγχρονισμού και αξιολογώντας τις χρησιμοποιώντας τεστ στατιστικής σημαντικότητας. Εν τέλει, και για τα δύο σετ δεδομένων είχαμε ευρήματα με στατιστική σημαντικότητα τα οποία είναι σε συμφωνία και συμπληρωματικά με προηγούμενα ερευνητικά ευρήματα.

ACKNOWLEDGEMENTS

CONTENTS

PREFACE

Here we will give a brief preview of the structure of this work.

1. **Electroencephalography**: An introduction in the basic concepts of the electroencephalogram such as the electrodes, the artifacts and the frequency bands.

2. **Methods of EEG Analysis**: A mathematical background on the main tools we used for the analysis of the EEG signal.

3. **Dataset 1: Methodology and Results**: Presentation of the first dataset, description of the methodological approach we used and demonstration of our results.

4. **Dataset 2: Methodology and Results**: Presentation of the second dataset, description of the methodological approach we used and demonstration of our results.

5. **Conclusions**: A review of the thesis and suggestions for future work.

INTRODUCTION

During the past few years there has been an increasing interest in studying and understanding the neural mechanisms behind cognitive brain activity. This kind of knowledge is of great importance in many scientific areas such as clinical prognosis and diagnosis, brain computer interfaces design, etc. On this direction the electroencephalogram (EEG) has been developed, which indicates all physiological and neurophysiological activity. Ongoing and event related potentials are the two main EEG representations studied and evaluated for the extraction of important information. In ongoing EEG abnormalities can be detected concerning seizures or other brain disorders by the studying and evaluation of long term recordings. Multiple trial evoked responses can also be encountered as ongoing EEG if general term characteristics need to be extracted from the EEG. The other useful EEG representation involves event related potentials (ERPs) which are in fact responses caused by an external or internal stimulus and give us valuable information on how the brain responds in different occasions such as cognitive, movement, visual and other tasks. In this context, various methodological approaches have been suggested in order to bring forward the interesting characteristics each EEG representation is associated with.

In this work we explore two different approaches for the analysis of the EEG signal using two individual datasets each representing ongoing EEG or ERPs, accordingly. The first dataset (ongoing EEG) consist of EEG recordings during simple mathematical task performance. Power spectrum (PS) and linear coherence (LC) measures are used in this approach in order to investigate the differences in the channel activations for two mathematical thinking tasks. The goal in this case is to identify differences between the mathematical thinking tasks through the measures of PS and LC and evaluate them through statistical testing. This study resulted in the identification of topographic brain locations having statistical significant differences for the different tasks for both measures and correlations indication between the two measures. The second dataset (ERPs) concerns EEG recordings during a working memory experiment for a dyslexic and control group of subjects. In this case, various synchronization measures are applied on the time-frequency (TF) maps of the corresponding independent components (ICs). These measures are used for the evaluation of the components and recognition of a number of different cases for the generation of the ERPs. Furthermore evidence from time-frequency maps of the measures are evaluated via statistical testing in order to evaluate differences between the two populations. The results of this study concern the identification of various types of ERP activations using the measures' results, as well as the identification of ERP components having significant differences for the two populations in specific frequency bands. To sum up, for both datasets, we have

findings with statistical significance which are also in support and complementary to previous research.

1. Electroencephalography

1.1.Introduction

The first electroencephalographic recording (EEG) in humans, performed by the German psychiatrist Hans Berger in 1942, was greeted in skepticism by the scientific community. The recording was achieved by placing electrodes on the surface of the scalp and revealed the existence of rhythmic oscillatory activity.

The conventional EEG shows cortical electrical activity and includes cortical manifestations of the sub cortical regions. More specifically, EEG oscillations are hypothesized to be generated by the summation of excitatory and inhibitory post-synaptic potentials in cortical pyramidal neurons. Tens of thousands of synchronously activated pyramidal cortical neurons are assumed to take part in the generation of an EEG oscillation. The coherent orientation of their dendritic trunks (parallel to each other and perpendicular to the cortical surface) allows summation and propagation to the scalp surface. [1]

The EEG reflects the brain functionality and as such, it can be used from clinicians for the diagnosis of a variety of neurological problems and inspection of the brain integrity. The most commonly diagnosed pathological cases using EEG recordings include common headaches and dizziness, seizure disorders, stroke, brain tumors, epilepsy, multiple sclerosis, sleep disorders and movement disorders.[2]

Even though the first attempt was to exploit spontaneous EEG oscillations, the recent research tendency focuses to EEG activity time-locked to the events such as event related potentials (ERPs). The ERP activity expresses brain activity coming from synchronously active populations of neurons which occurs before or after an internal or external to the subject event. Consequently, ERPs can be interpreted as neural manifestations of specific psychological functions.[1]

The main purpose of this chapter is to review the EEG basic principles (electrode montages, frequency activity etc) and introduce ERPs, which are the brain's electrical potentials mostly analyzed and discussed by the scientific community.

1.2.Electrodes

To allow comparisons among studies it is important to adhere to standardized electrode locations. The most widely used system for the placement of the electrodes on the head is the 10-20 international system proposed by Jasper (1958). The locations for the electrodes are determined in the following way: The reference points are the nasion (the delve at the top of the nose) and the inion (the bony prominence at the base of the skull on the midline at the back of the head).

According to this line, the first electrode is placed 10% of its distance and the others are arranged at 20% intervals (Figure 1.1).[2]

The typical number of electrodes used in the 10-20 international system is 64, though some high-density (128 or 256 electrodes) or low-density (15 or 32 electrodes) systems are also used depending on the application. As far as the names of the electrodes are concerned, each site has a letter to identify the lobe and a number to identify the hemisphere location. The letters F, T, C, P and O stand for frontal, temporal, central, parietal, and occipital lobes, respectively. The C letter is the only case that does not correspond to a lobe and is just used to describe the central area. The usage of letter z refers to an electrode placed on the midline. Even numbers and odd numbers refer to electrode positions on the right and the left hemisphere correspondingly.

Since the EEG signal represents the voltage difference between two electrodes the result may have several different ways to be expressed according to the electrode pair selection. The electrode placement and the different combination patterns of the electrode pairs so as to measure the potential differences on the scalp constitute the electrode montage. The main EEG montage patterns are: referential, average reference and bipolar montage. Referential montage shows the potential difference between an active and a designated non-active electrode. Midline positions are often used because they do not amplify the signal in one hemisphere vs. the other. Another popular reference is linked ears, which is a physical or mathematical average of electrodes attached to either earlobes or mastoids. In the ideal case, the reference electrode should be electrically inactive, allowing the measurement of an absolute EEG value. Though there is no position in the human body following these specifications and as so the reference chosen contributes to the EEG recording. In the bipolar case each electrode potential represents the difference between two adjacent electrodes. Due to the fundamental issue of reference-dependency of EEG waveforms, reference-free transformations have been proposed for an unbiased assessment of EEG measures such as average reference. With the average reference approach EEG signals are re-derived against the average value across all electrodes. [1], [2]
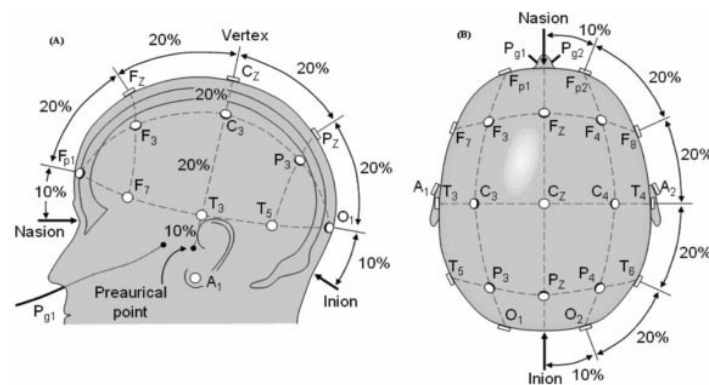
Figure 1.1: 10-20 system representation and electrode positions.[2]

1.3.Artifacts

In most of the cases the raw EEG signal contains along with the desired content, various types of noise and artifacts. These artifacts can either be biological or environmental. The most common biological artifacts are: eye artifacts such eye blink and movement, muscle artifacts (EMG) and cardiac artifacts (ECG). Electrocardiogram (ECG), electrooculogram (EOG), and electromyogram (EMG) can be very important tools for the proper detection and removal of these artifacts. Environmental artifacts mainly derive from interferences from power lines (50/60 Hz), additional electrical noise, poor subject grounding, and poor electrode contact. Though, the use of notch filters, proper subject grounding, and shielding of the recording system can even eliminate their influence.

Removal of eye and muscle artifacts is particularly important, because these artifacts overlap in frequency and amplitude with the EEG. If it is not of great concern, the contaminated EEG part can be removed by cutting out the specific milliseconds. Though, one of the most effective and non-destructive ways to remove the artifacts from the EEG signal is independent component analysis (ICA). ICA works very well on the raw EEG separating the useful EEG components from the artifact components. [1]
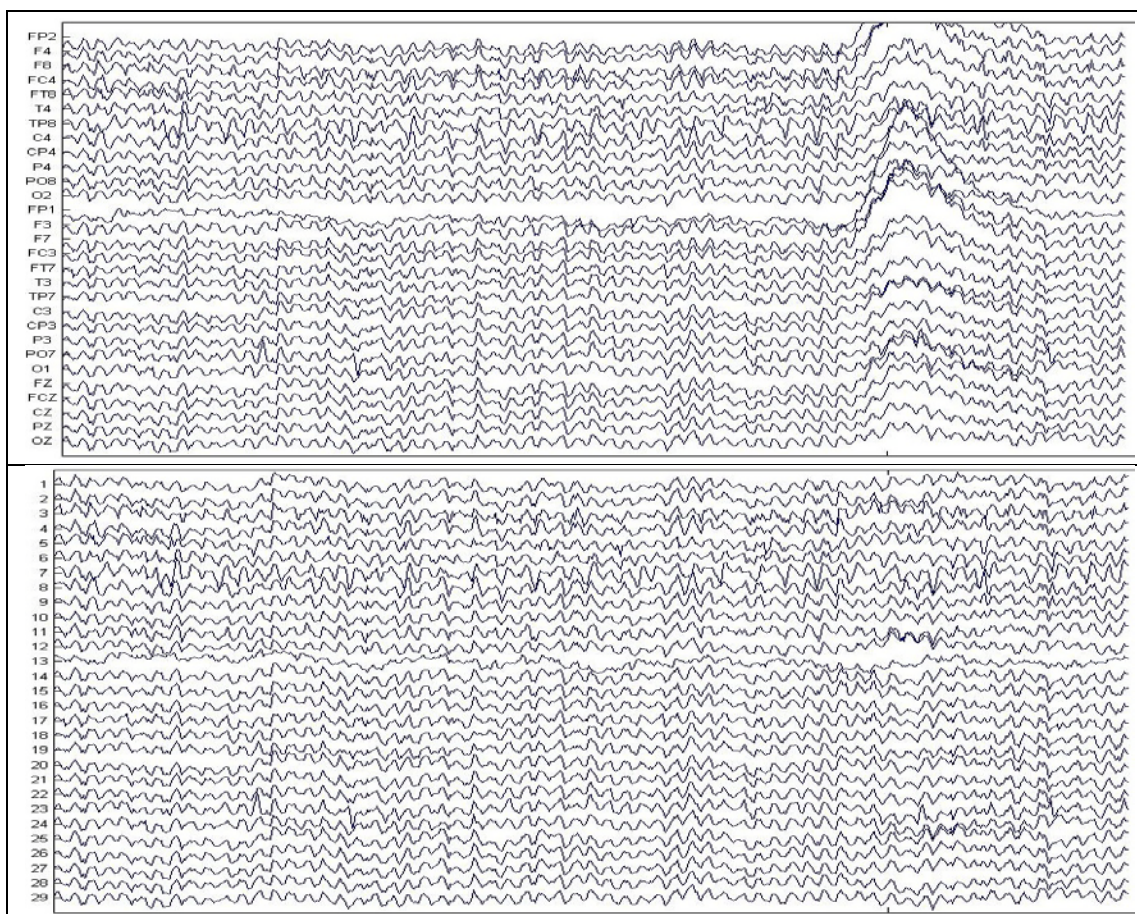
Figure 1.2: Raw EEG with eye artifact (first row) and its clean result after removing the infected component ICA gave (second row).

1.4. EEG Frequency Activity

The EEG is mainly described by its patterns of rhythmic activity which is divided into bands according to the frequency. The cerebral cortex signal typically falls in the range of 1-40Hz. It has been observed that low frequencies (e.g., delta and theta) show large synchronized amplitudes, whereas high EEG frequencies (e.g., beta and gamma) show small amplitudes because of the high degree of desynchronization in the underlying neuronal activity. [1]

The frequency bands can be categorized according to their range (from the lowest frequency range to the higher) as Delta, Theta, Alpha, Beta and Gamma. [2] There follows a quick review of the EEG frequency bands and their functional roles.

1.4.1. Delta Band

Delta is the EEG low-frequency rhythm ranging from 1 to 4 Hz. It is usually associated with healthy human sleep and neurological pathology. Tumors, brain lesions, anesthesia and sleep condition are some cases in which delta power has been reported to increase. [1] Also, in infants during the first two years of their life delta is found to be the predominant activity. Both delta and theta (low frequency bands) relent with increasing age in contrast to alpha and beta band. [1], [3]

In oddball experiments it has been found that the amplitude of the delta response is considerably increased. Accordingly, it has been concluded that the delta response is related to signal detection and decision making. More specifically, in response to stimuli at the hearing threshold delta oscillations are observed in human subjects something that confirms the hypothetical role of the delta response in signal detection and decision making. [4]
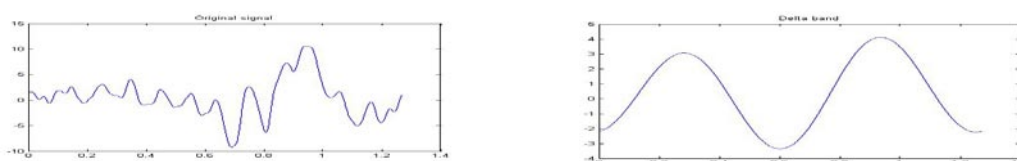

Figure 1.3: An original EEG signal (left figure) and its delta activity (right figure) isolated.

1.4.2. Theta Band

The EEG activity within the 4-8 Hz range is referred as theta activity. The power of theta is increased and alpha power lowered in subject with a variety of different

neurological disorders (not only demented subjects but also children with reading/writing difficulties) as compared to subjects of the same age. [3]

Theta activity is prominently seen during sleep. Two different types of theta have been reported during wakefulness in adults. In the first one, theta seems to have a widespread distribution and is affiliated with drowsiness and impaired information processing. On the other hand, the second type of theta is located midline frontally (frontal midline theta activity) and it is associated with focused attention, mental effort, and effective stimulus processing. More specifically, theta synchronization has been connected to cognitive tasks where mental effort is required. This attitude relates theta to alpha in an opposite way. [3]

Physiologically, the septo-hippocampal system has been strongly implicated in the generation of theta oscillations, although theta has also been recorded in numerous other limbic regions, including the anterior cingulate cortex (ACC), entorhinal cortex, and the medial septum, among others. [1]
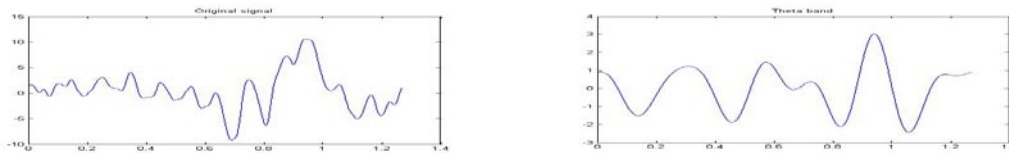
Figure 1.4: An original EEG signal (left figure) and its theta activity (right figure) isolated.

1.4.3. Alpha Band

The EEG activity ranging from 8 to 13 Hz is the so-called alpha band. In healthy adults alpha can easily be detected during relaxing states of wakefulness, although large individual differences in amplitudes are not uncommon. [1] The alpha rhythms show their greater amplitudes in posterior regions, and more specifically in posterior occipito-temporal and parietal regions, and can best be seen during resting periods in which the subjects closed eyes. [1], [3]

Alpha can be greatly diminished or abolished by eye opening, sudden alerting, and mental concentration, a phenomenon known as alpha desynchronization. The alpha rhythm can also be attenuated when alertness decreases to the level of drowsiness. However this attenuation is often accompanied by a decrease in frequency. [1], [3]

Although the physiological role of alpha rhythm remains largely unknown, there have been studies relating alpha synchronization to information processing. [3] Further complicating the physiological interpretation of alpha, emerging evidence indicates that different alpha sub-bands may be functionally dissociated, in particular with increasing task demands (e.g. waiting for a stimulus/task). [1] More specifically, in cognitive tasks lower alpha (8-10 Hz) desynchronization has been affiliated with

tasks that require increased attention. [3] On the other hand, upper alpha desynchronization seems to be associated with processing of sensory-semantic information, increased semantic memory performance, and stimulus-specific expectancy. [3]
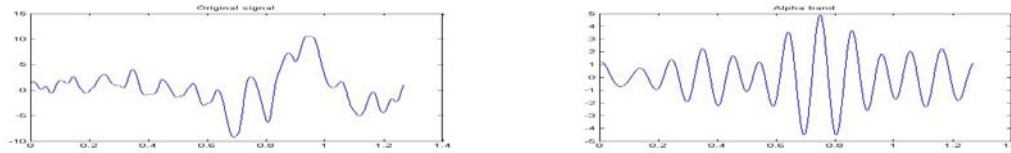
Figure 1.5: An original EEG signal (left figure) and its alpha activity (right figure) isolated.

1.4.4. Beta Band

Beta is the EEG rhythm raging from 13 to 30 Hz and typically topographically located symmetrically in the fronto-central location. Although classically considered as being related to sensorimotor functions, the functional role of beta-band oscillations at present seems to be least understood. It seems to replace alpha rhythm during cognitive activity, as it has been reported that it increases with attention and vigilance. According to the previous, beta increases generally reflect increased excitatory activity, particularly during diffuse arousal and focused attention. [1]

A number of recent studies suggest that interactions in the beta-band predominate in tasks that strongly involve endogenous top-down processes. According to this, the most extreme case is probably provided by the processing of ambiguous stimuli where the percept is fully determined by endogenous factors, whereas stimulus features do not deliver any task-relevant information. [5]
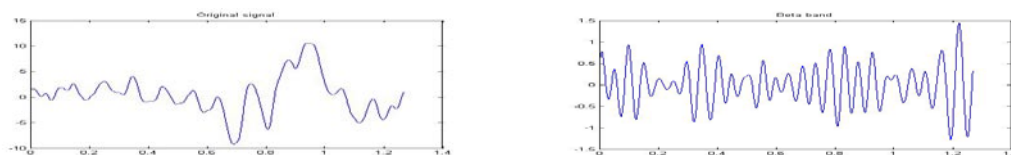
Figure 1.6: An original EEG signal (left figure) and its beta activity (right figure) isolated.

1.4.5. Gamma Band

Gamma EEG oscillations are low amplitude rhythms in the 30–100 Hz range. Gamma oscillations have been associated with attention, arousal, object recognition, top-down modulation of sensory processes, and perceptual binding (integration of information processed in distributed neurons and/or neural circuits and/or cortical areas into a coherent cognitive process/percept). [1], [6], [7] Various findings

indicate that gamma activity is directly associated with brain activation. It has been linked with various mental processes, including perception and learning. [1], [6], [7] There have been described dose-dependent decreases during anesthesia and systematic decreases throughout the sleep-wake cycle. [1]
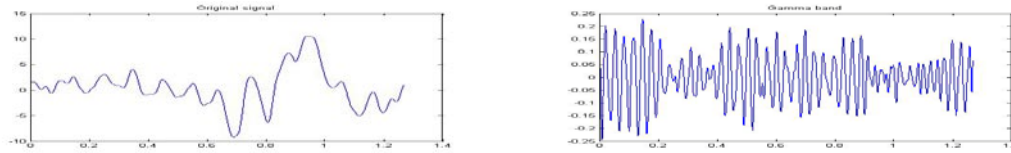
Figure 1.7: An original EEG signal (left figure) and its gamma activity (right figure) isolated.

1.5. Event Related Potentials

Aside from the conventional continuous EEG which represents the ongoing brain activity, another useful EEG that can be recorded is the evoked or event related potential (ERP). It is called so because of its arousal in response to a stimulus (auditory, visual or somatosensory, etc.).

ERPs are very useful as they provide very interesting information on how the sensory processing is achieved in the brain. This information is very important as it gives diagnostic background to clinicians and/or researchers and can also be used for the design of brain computer interface (BCI) for different applications. In contrast to continuous EEG, ERPs are much smaller in amplitude and as such they are difficult to be distinguished. Therefore, there usually has to be a series of trials of the experiment with the stimulus to the subjects so as to have enough repetitions and be able to apply signal averaging method so as to improve the signal-to-noise ratio (SNR) of the recorded signals to allow interpretation. Averaging is one of the most common methods used for the discrimination of the ERP from the noise because the EEG aspects which are not time-locked are assumed to vary among the trials and so taking the average should reduce the noise potentials, rendering the ERPs. [1], [2], [8]

For the averaging technique to be satisfactory, three assumptions have to be accomplished. The ERPs should be consistent across the trials, the noise (ongoing EEG) random and the ERP signals independent of the background noise. In this case, the SNR increases by the square root of the number of trials included in the average. In a typical experiment these assumptions may not be satisfied. For example there is usually reported a latency jitter from trial to trial, so that the average ERP will not be a representative of the actual ERP of any individual trial. To deal with these problems a number of pattern recognition techniques have also been applied to ERP analysis such as independent component analysis [9], principal component analysis and time-frequency techniques [10], [11] (wavelets, Wigner-Ville distribution etc). [1]

The average ERP has many positive and negative peaks that can be subjected to various measurement operations. Positive and negative peaks in the ERP are typically described according to their characteristic scalp distribution, their polarity and latency. In fact, the labels given to the ERP peaks are subject to the polarity (P for the positive peak and N for the negative peak) and latency (50, 100, 300, etc.) of the peaks. [1], [8]

The ERPs are usually described by their amplitudes and latencies of their characteristic waveform. Depending to the time the ERP components appear, they have a different nature. The ERP components which have latency below 10-12ms are called early ERPs (or 'far-fields') and they are associated with the response of the receptors and peripheral nervous system. As late ERPs (or 'near-fields') are distinguished the ERP components with latency greater than 50ms, and they are generated in the brain. In late ERPs there can be distinguished endogenous and exogenous components. The endogenous components are associated with internal cognitive purposes and the exogenous with the characteristics of the external stimulus. Endogenous components of 100-200ms latencies are usually fired by the attention to the stimulus. The later components at about 300ms (usually P300) seem are associated with recognition and discrimination between the stimuli. P300 amplitude is considered as a manifestation of CNS activation that reflects attention to incoming stimulus, when memory representations are updated. P300 latency is dependent on the stimulus classification speed (gets smaller for known stimuli) and the latency is connected with individual cognitive capability. [12]

The generation of an ERP is associated with an integration of the activity of many neurons, as the electrical activity coming from single neurons is comparable small at the scalp. So as for this integrated activity to be expressed the neurons have to be synchronously activated as well as the electric fields generated by each particular neuron must have a specific orientation to give a cumulative effect detectable at the scalp. Taking in account these considerations, ERPs represent only a sample of the brain electrical activity. Thus, there are cases in which the ERPs do not show activity before or after the stimulus even though there occurs information processing in the brain organization. This is the reason why there has to be caution in the interpretation of the ERP results. If an experimental manipulation has no effect on the ERP we cannot conclude that it does not influence brain processes, in the same way that we cannot assume that two experimental manipulations that have the same effect on the ERP are not necessarily influencing the exact same processes. [1]

1.6.Ongoing EEG

One way to go in the EEG analysis is the ERP which we previously described. In the ERP analysis we need to have many trials so as to succeed reliable results (high

SNR). On the other hand, we have other EEG analysis directions, where many trials are not necessary, and even if we have them, we treat them as one by concatenation. The final EEG signal is called ongoing EEG. In particular, when we treat EEG as 'ongoing EEG', power spectrum and coherence behavior of the multiple electrodes are what we are interested in.

Such analysis is very helpful for the clinicians and researchers because the brain topographic behavior is revealed under different kind of situations (cognition, attention, thinking etc.). Results of this analysis can also be used for the discrimination of pathological cases (Alzheimer, neurological disorders etc.). It has to be noted that aside from the definition we gave to the ongoing EEG, there are also other interpretations. In the case of the ERPs, ongoing EEG is conceptualized as noisy activity or else the activity of internal processes not associated with the experiment. From now on, any reference to the ongoing EEG will be associated with the definition presented here.
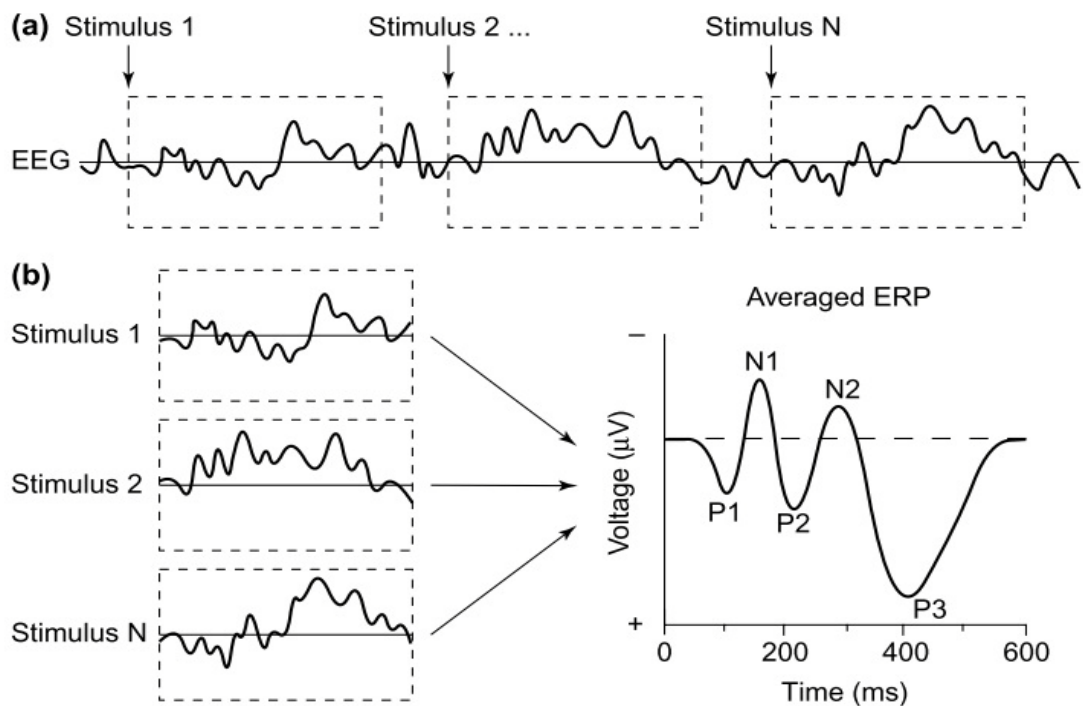
Figure 1.8: a) The ongoing EEG, b) ERP.[8]

2. Methods of EEG Analysis

2.1. Introduction

The EEG signal is one of the most complicated signals to analyze, as it represents the activity of thousand of neurons responding to multiple processes. In order to interpret, visualize and evaluate the content of an EEG signal, the use of different mathematical tools is necessary. Here we will give a brief presentation of some modern methods for the analysis of the EEG signal (wavelets, independent component analysis etc.) which are regularly used in the field, and which we also use in this work.

2.2. Time-Frequency Representation

Spectral analysis (usually achieved via Fast Fourier Transform or FFT) is considered to be a very important tool as it decomposes an EEG signal into a sinusoidal set of functions having different frequencies, amplitudes and phases. Consequently, the spectral analyses can provide valuable information about the frequency compositions of EEG oscillations. Nevertheless, spectral analysis cannot provide any evidence about when in time such frequency shifts occur, which is a drawback because the EEG signal is dynamic, time-varying, and often non-stationary.

For these reasons, approaches allowing the investigation of transient changes in the frequency domain appear particularly important. In order to achieve this, many time-frequency methods have been developed such as short time Fourier Transform (STFT) which computes a time dependent spectrum the so-called spectrogram, Wigner-Ville transform (WVT) which is a principal member of the quadratic time-frequency transformations and computes the so-called scalogram and wavelet analysis which recently is gaining ground in EEG analysis as it allows a more adaptive time-frequency approach affording flexible resolution. [1], [13], [14], [15]

2.2.1. Short-Time Fourier Transform

Short time Fourier Transform (STFT) also known as windowed Fourier Transform is an extension of the Gabor transform, in which we have time-frequency windows (or atoms) to create a window of time from which the spectrum of the local signal values is computed. Mathematically, this is written as:

$$X_w(\tau, \omega) = \int_{-\infty}^{\infty} x(t) w(t - \tau) e^{-j\omega t} dt \qquad (2.1)$$

Where x(t) is the signal in time and w(t) is the window function. Commonly used window functions are the Gaussian and Hanning window functions. There follows a table giving the some widely used window functions.

Name	Definition
Rectangle	$w(t) = \begin{cases} b & \text{if } (\|t\| \le a) \\ 0 & \text{otherwise.} \end{cases}$
Bartlett (triangle)	$w(t) = \begin{cases} \dfrac{b}{a}t + b & \text{if } -a \le t \le 0, \\ -\dfrac{b}{a}t + b & \text{if } 0 \le t \le a, \\ 0 & \text{otherwise.} \end{cases}$
Hanning (von Hann)	$w(t) = \begin{cases} b\cos^2\left(\dfrac{\pi t}{2a}\right) & \text{if } \|t\| \le a \\ 0 & \text{otherwise.} \end{cases}$
Hamming	$w(t) = \begin{cases} 0.54b + 0.46b\cos\left(\dfrac{\pi t}{a}\right) & \text{if } \|t\| \le a \\ 0 & \text{otherwise.} \end{cases}$
Blackman	$w(t) = \begin{cases} 0.42b + 0.5b\cos\left(\dfrac{\pi t}{a}\right) + 0.08b\cos\left(\dfrac{2\pi t}{a}\right) & \text{if } \|t\| \le a \\ 0 & \text{otherwise.} \end{cases}$

Table 2.1: Widely used window functions in STFT. Parameter a > 0 regulates the window width appropriate to the signal features of interest and parameter b > 0 normalizes the window function. [13]

The time-frequency windows having smaller t-dimensions provide higher time resolution. On the other hand, those having tighter ω-dimensions provide higher frequency dimensions. So it is obvious that the smaller the cells are the better resolution is succeeded. Unfortunately there is an offset of how small the cell can be. The time-frequency window used in the STFT has fixed time duration and a fixed frequency resolution. More specifically, the uncertainty principle of Heisenberg states that:

$$\sigma_t \sigma_\omega \ge \frac{1}{2} \qquad (2.2)$$

This holds for the transformation pair $g(t) \leftrightarrow G(\omega)$ where σ_t, σ_ω are the squared variances of $g(t), G(\omega)$. So, STFT can be interpreted as a filtering of signal $x(t)$ by a filter bank in which each filter is centered at a different frequency but has

the same bandwidth (Figure 2.1, first column). In this case there occurs the problem that for both high and low frequency components, we have the same window length, and thus an unsatisfactory overall localization of events is achieved (Figure 2.4, second row and column). More specifically, signals with both low and high frequencies or with abrupt are not conveniently analyzed by STFT. Choosing a window of variable length could be the solution to this problem. That way, a larger window could analyze long-time, low-frequency components while a shorter one could detect high-frequency, short-time components. That exactly is what wavelets transform (WT) came to offer. More specifically, wavelets are very popular in EEG analysis because of their accuracy in resolving resolve EEG waveforms into specific time and frequency components. [1], [13], [14], [15]
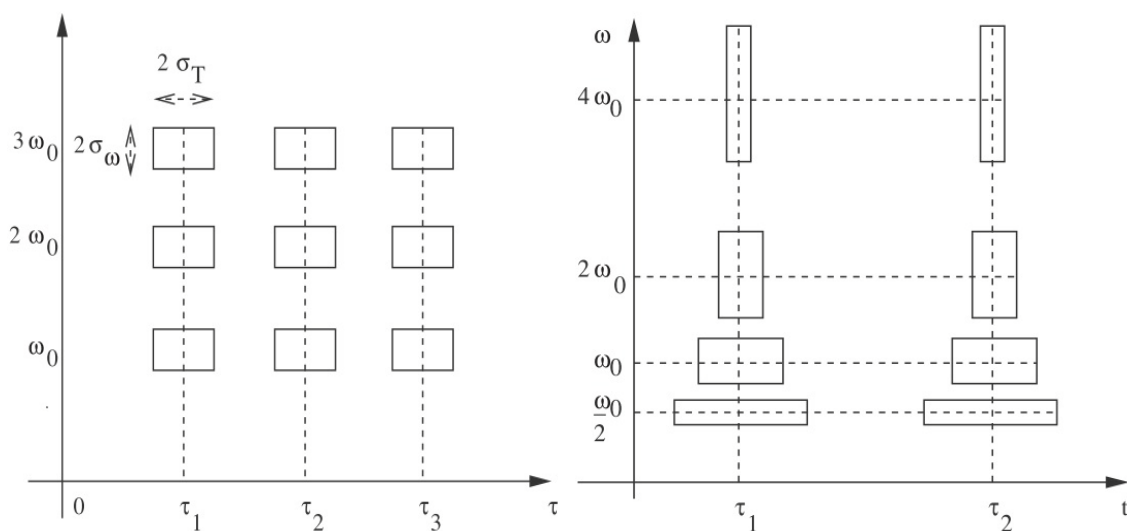
Figure 2.1: The resolution cells for the STFT and the wavelets transform correspondingly. [14]

2.2.2. Wavelets

As we previously mentioned, modern transform techniques such as the wavelet transform are gaining an increasing importance in biomedical signals analysis (e.g. EEG). The wavelets transform (WT) is based on wavelets, which are small waves of varying frequency and limited duration, and thus represents a deviation from the traditional Fourier transform concept that has sinusoids as basis functions. Also, it is clear from the previous section that in contrast to the Fourier Transform (FT) which just shows a frequency representation, WT also contains temporal information of the signal. [13], [14], [16]

A wavelet represents a basis function in continuous time and can serve as an important component in a function representation: any function $f(t)$ can be represented by a linear combination of basis functions, such as wavelets. One of the most important characteristics in the WT is that all the wavelet functions are

generated from a single so-called 'mother' wavelet. Some of the most popular 'mother' wavelets are the Morlet (most widely used in EEG case), Mexican hat and Meyer wavelets. An example of those is presented in the figure below. [13], [14], [16]
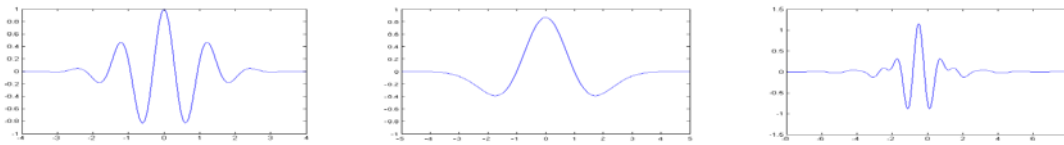
Figure 2.2: Examples of 'mother' wavelets. The first, second and third column show the Morlet, Mexican hat and Meyer wavelets correspondingly.

WT's most important feature is its capability to analyze different frequency components of a signal with different resolution. This attribute requires the notion of functions at different scales. It is obvious that the small scales show the content of the signal with great detail and the large scales show basically coarse features. In such an analysis, we basically use translations and scaling (or dilations) of a basis function $\psi(t)$. A scaled version of a function $\psi(t)$ is the function $\psi\left(\frac{t}{a}\right)$, for any a scale. For $a > 1$, there is obtained a function of lower frequency which can describe slowly changing signals. In contrast, for $a < 1$ there is obtained a function of higher frequency which can detect fast signal changes. It should be noted here, that the scales are inversely proportional to the frequencies. [13], [14], [16]
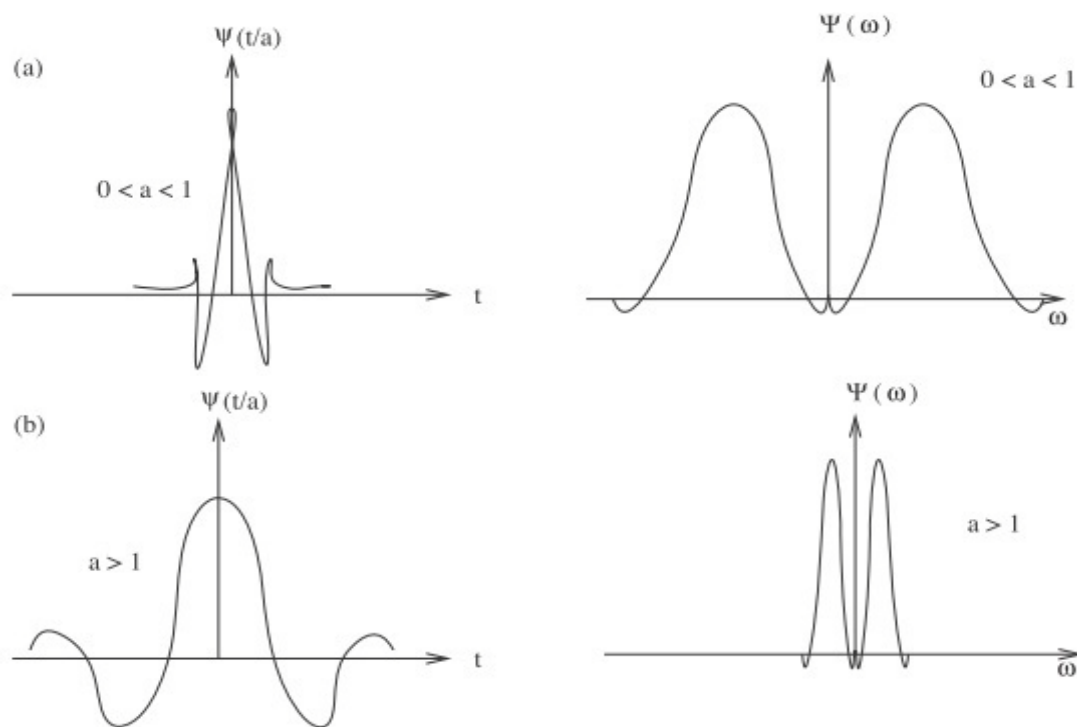
Figure 2.3: The wavelet function in time and frequency domain having, a) scale factor 0<a<1 and b) scale factor a>1. [14]

Wavelet functions are localized in frequency in the same way sinusoids are. The only difference they have from sinusoids is that they are localized in time too. Each of the several families of wavelets has a characteristic shape. The basic scale for each wavelet family covers a specific, standard time interval. The time span, for wavelets of the same family gets wider for larger scales and tighter for smaller scales. Subsequently, wavelet functions can offer either good time resolution or good frequency resolution. Good time resolution is associated with tight, small-scale windows, while good frequency resolution is associated with wide, large-scale windows. In order to estimate what frequencies a signal has and when they emerge, the wavelet functions must be translated through the signal for each scale. The function:

$$\psi\left(\frac{t-b}{a}\right)$$ (2.3)

is a scaled and translated version of the wavelet function $\psi(t)$, for any scale α and translation b. In the case where we have similarity between the signal, there is generated a large WT and in the opposite case, there is generated a small WT. The small scales correspond to high frequencies and the large scales to low frequencies. [13], [14], [16]

So, the WT is produced by a translation and dilation or scaling of the 'mother' wavelet or prototype function $\psi(t)$. As such, according to the Fourier transform we have:

$$\psi(t) \leftrightarrow \Psi(\omega)$$

and

$$\frac{1}{\sqrt{a}}\psi\left(\frac{t}{a}\right) \leftrightarrow \sqrt{a}\Psi(\omega\alpha)$$ (2.4)

with $\alpha > 0$. From this equation it is obvious that as we rescale, the frequency increases by a certain quantity and at the same time the time interval decreases by the same quantity. Also the amplitude in frequency increases by a $\sqrt{a}$ factor which means that we have greater amplitude for the low frequencies (greater a) than for the high frequencies (lower a). Subsequently, the uncertainty principle (equation 2.2) holds. If we define the wavelet function as:

$$\psi_{\alpha,b}(t) = \frac{1}{\sqrt{a}}\psi\left(\frac{t-b}{\alpha}\right)$$ (2.5)

The WT is given by the inner product:

$$W(a,b) = \int_{-\infty}^{\infty} f^*(t)\psi_{\alpha,b}(t)\, dt = \langle f, \psi_{\alpha,b} \rangle$$ (2.6)

with $a \in R^+$ and $b \in R$. The mostly used wavelet functions are the Morlet wavelets which are basically define as the product of a complex exponential wave and a Gaussian envelope:

$$w(t, f) = A exp\left(\frac{-(t - t_0)^2}{2s^2}\right) exp(2\pi i f t) \tag{2.7}$$

Morlet wavelets $w(t, f)$ have a Gaussian shape both in the time (around time t_0) and in the frequency domain (around frequency f).[13], [14], [16]

2.2.3. Wigner-Ville transform

In contrast to STFT and WT, Wigner-Ville transform (WVT) does not depend on the windows functions. Instead it emerges out of the properties of the analyzed signal. The absence of a window in this transform seems to be the asset of WVT, as we do not have the window effect we had in the two other transforms. The WVT is the radial Fourier transform of the product $x(\tau + \frac{t}{2})x^*\left(\tau - \frac{t}{2}\right)$ given by:

$$X_{WV}(\tau, \omega) = \int_{-\infty}^{\infty} x(\tau + \frac{t}{2})x^*\left(\tau - \frac{t}{2}\right)e^{-j\omega t}dt \tag{2.8}$$

When τ is close to zero $x(\tau + \frac{t}{2})$ and $x^*\left(\tau - \frac{t}{2}\right)$ terms are coherent and their product contributes to the integral. On the case where τ is large, those terms are incoherent (in phase) and as such average to zero. [13], [14], [15]

The Wigner-Ville distribution is quadratic in x, so if x is a sum of two individual signals a,b, the Wigner-Ville distribution of x contains an interference term 2ab in addition to the desired quantity $(a^2 + b^2)$. These interference terms result in an increased noise level of the Wigner-Ville distribution relative to the spectrogram. In practice, these interference terms can be dramatically reduced by smoothing in time and frequency. The result is the smoothed-pseudo Wigner-Ville transform (SPWVT) which is defined by:

$$X_{PWV}(\tau, \omega) = g(t) * \int_{-\infty}^{\infty} h(t)x(\tau + \frac{t}{2})x^*\left(\tau - \frac{t}{2}\right)e^{-j\omega t}dt \tag{2.9}$$

Where we have a convolution of g(t) with the integral in time. The function g(t) is the smoothing function in time and h(t) restricts the range of the integral in t. Restricting the range in t is equivalent to smoothing in frequency. The SPWVD reduces to the conventional Wigner-Ville distribution when $h(t) = 1$ and $g(t) = \delta(t)$.

2.2.4. Example

In order to compare the three TF representations we previously described, we made two simulations with three sinusoidal signals. In the first example we have the linear combination of three sinusoidals each having frequency content in different time instants than the others. That way, the linear combination of the three signals.

1 Frequency per time instant
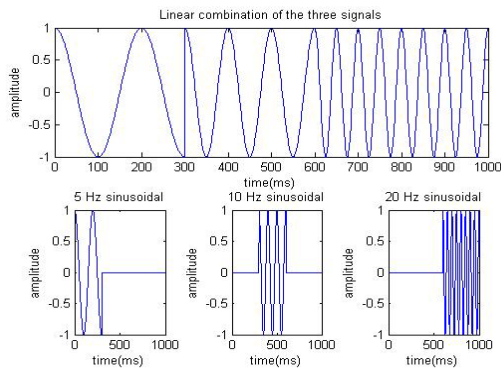
3 Frequencies per time instant
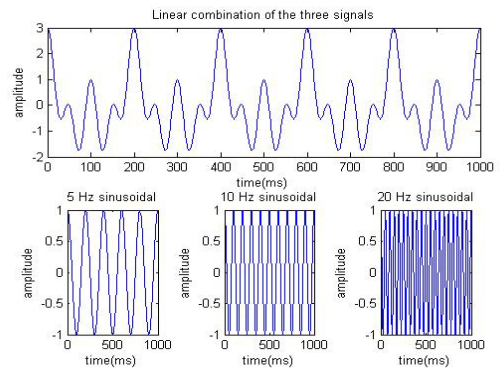
Short Time Fourier Transform (STFT)
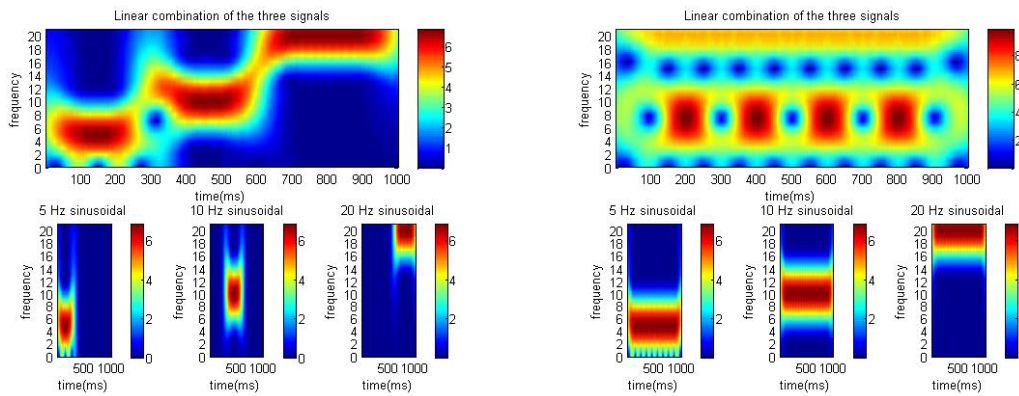
Smoothed-Pseudo Wigner-Ville Transform (SPWVT)
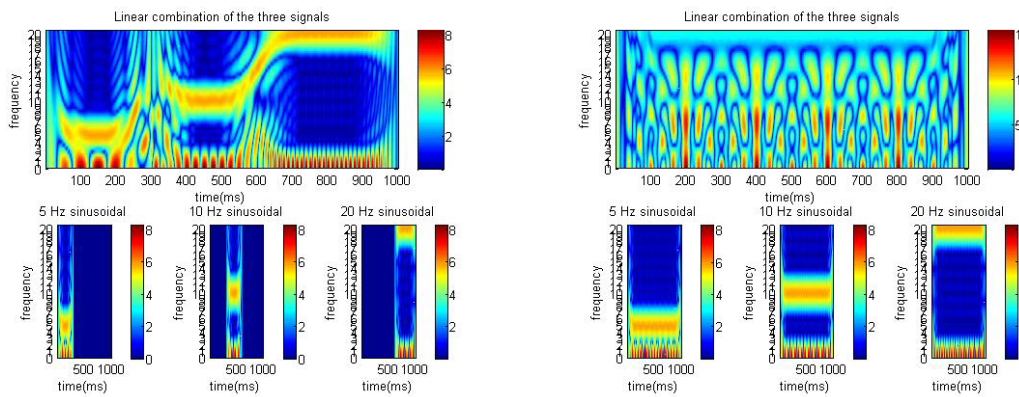
Wavelet Transform (WT)
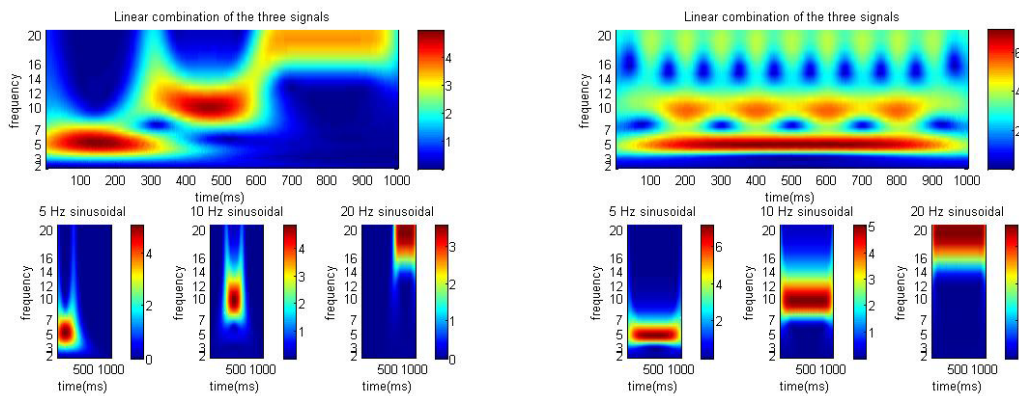
Figure 2.4: STFT, WVT, and WT (Morlet wavelets) on two different linear combinations of sinusoidal signals. The first signal (1ˢᵗ column) has one frequency per time instant and the second three.

has a unique frequency per time instant. In the second example all three sinusoidals have frequency content in the whole time range, such that the linear combination gives three different frequencies per time instant. Those two examples and their TF transforms are given in the previous figure.

In the first example where we have one frequency per time instant, all three TF transforms have satisfactory results. The WVT has sharper results in frequency, though it has inference terms in this case too. In the second example, only the WT has good results as it distinguishes successfully the three different frequencies. On the other hand, in STFT the 20Hz activity is preserved, though it mixes the 5Hz and 10Hz frequency content in a way that they cannot be distinguished. Finally, WVT mixes the frequency content in a way that no frequency can be distinguished sufficiently.

Taking these into consideration and also that EEG signal usually consists of many different frequencies; wavelets seem to be the proper TF tool to decompose an EEG signal to its frequency content.

2.3. Independent Component Analysis

One of the major problems in data analysis is that there is a large amount of data most of which does not contain important information. To a variety of scientists and engineers, the existence of high-dimensional datasets makes it is an important challenge to identify underlying statistical patterns that facilitate the interpretation of the data set using techniques from machine learning. Commonly, linear representations have several potential applications including the decomposition of objects into 'natural' components, redundancy and dimensionality reduction, biomedical data analysis, microarray data mining or enhancement, feature extraction of images in nuclear medicine, etc. [14]

We assume that the data is given by a multivariate time series $x(t) \in \mathcal{R}^m$ where t indexes time (or some other quantity). The definition of data analysis could be as finding a meaningful representation of $x(t)$ as $x(t) = f(s(t))$, with unknown features $s(t) \in \mathcal{R}^m$ and a mixing mapping f. In many cases f is assumed to be linear, so we have the case:

$$x(t) = As(t) \tag{2.10}$$

with mixing matrix $A \in \mathcal{R}^{m \times n}$. Often white noise is added which results in:

$$x(t) = As(t) + n(t) \tag{2.11}$$

Noise $(n(t))$ can be absorbed by $s(t)$ increasing its dimension. The prospect of the decomposition in equation 2.10 is the feature signal $s(t)$ allows more insight into the data than $x(t)$ does.

Source signals

Linear mixture of the source signals

Sourse signal retrieval via ICA
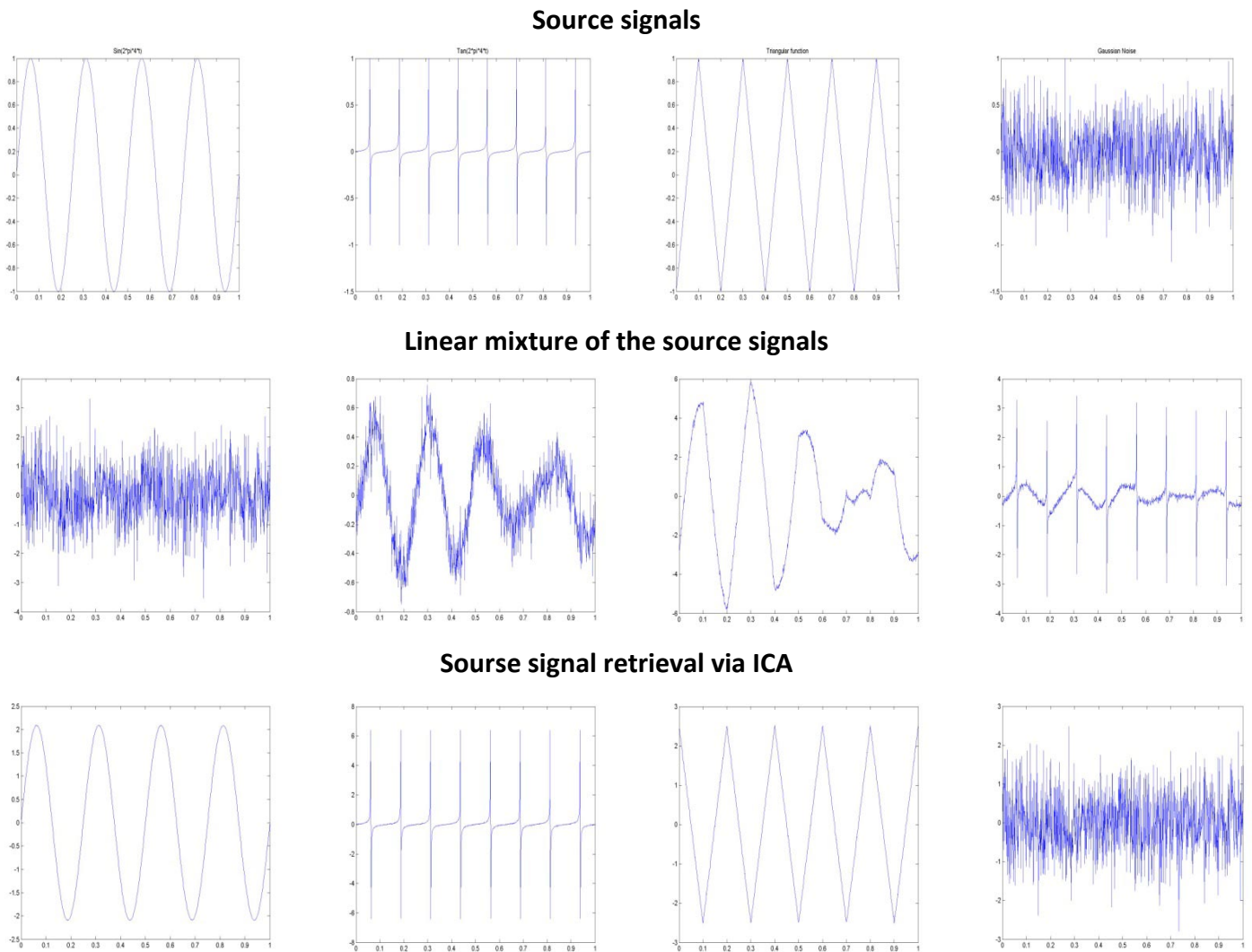
Figure 2.5: Source signals retrieval using ICA. The source signals are a sinusoidal signal, a tangent signal, a triangle signal and Gaussian noise correspondingly.

Typically, there are two approaches in finding data representations the way equation 2.10 does and those are the supervised and unsupervised models. In the supervised models, we have additional information for the input-output pairs $\left((x(t_1), s(t_1)), \cdots, (x(t_M), s(t_M))\right)$, which can be used for interpolation and learning of the map f or the basis A (regression). In the unsupervised models, often called blind source separation (BSS) since neither features or sources $s(t)$ nor mixing mapping f are assumed to be known, we make weak statistical assumptions on either $s(t)$ or f / A. [14], [17]

Independent Component Analysis (ICA) belongs to the category of the unsupervised models and is of great interest, as it promises to reveal the driving forces which underlie a set of observed phenomena. These phenomena include the firing of a set of neurons, mobile phone signals, brain images such as functional magnetic resonance imaging (fMRI), stock prices, and voices. In each case, there needs to be measured a large dataset of signals, affected by a mixture of underlying

factors. These factors are the so-called source signals, which are of great importance and buried in a set of signal mixtures. The ICA is a statistical method which works in a way that the underlying source signals can be extracted from the aggregated signal. The sources revealed through ICA are maximally independent. A schematic representation of ICA is given in Figure 2.6 and a simulation with four signals (original, mixed and recovered via ICA) is given in Figure 2.5 . [14], [17]
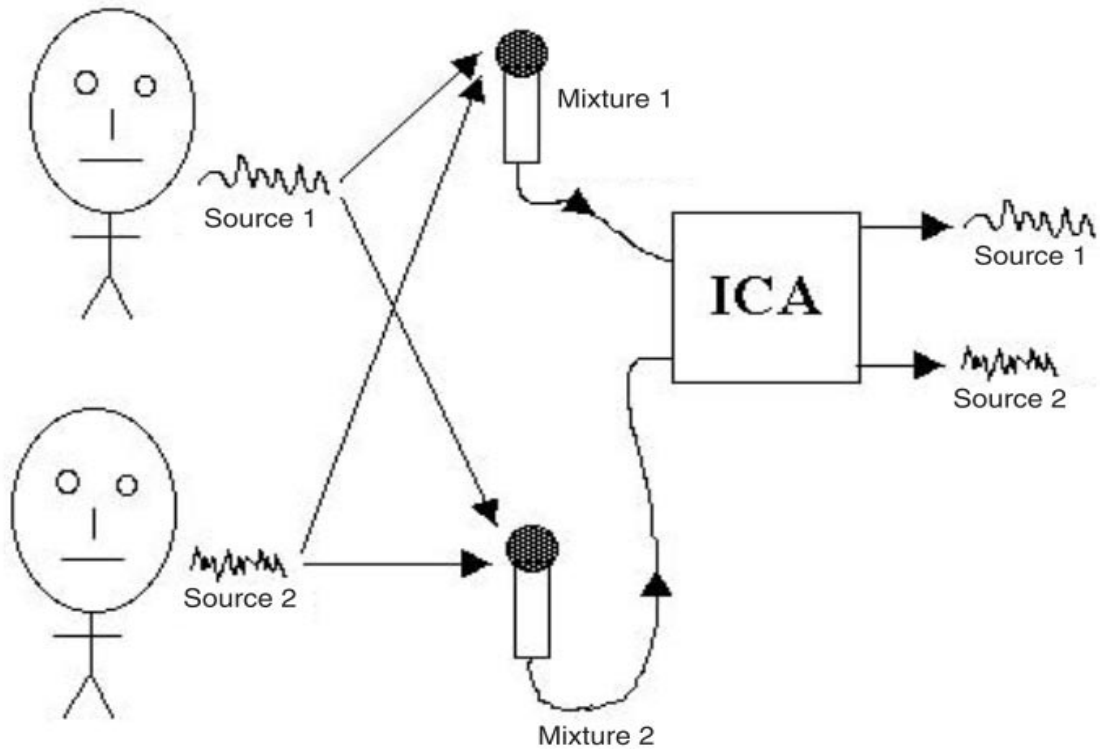
Figure 2.6: A schematic representation of the ICA procedure in a voice example. [18]

Typically, ICA assumes a generative model where observations are assumed to be linear mixtures of independent sources. In contrast to principal component analysis (PCA) which only uncorrelates the data, ICA works with higher-order statistics to achieve independence. Independence is stronger than uncorrelatedness, as if two random variables are independent they are uncorrelated but the vice versa is not always true. In Figure 2.7 there is given an example of two independent source signals, for which PCA finds two corresponding orthogonal vectors in contrast to ICA which finds two independent vectors and is thus able to restore the original sources. The fact that PCA components are both spatially and temporally orthogonal is an unrealistic constraint for real EEG sources, which arise in domains (spatial regions) of partially synchronous activity in electrically oriented cortical neurons (and possibly glia). The scalp projections of actual brain EEG sources, are nearly always overlapping and non-orthogonal, contrary to the assumption of PCA. [14],[17],[19]
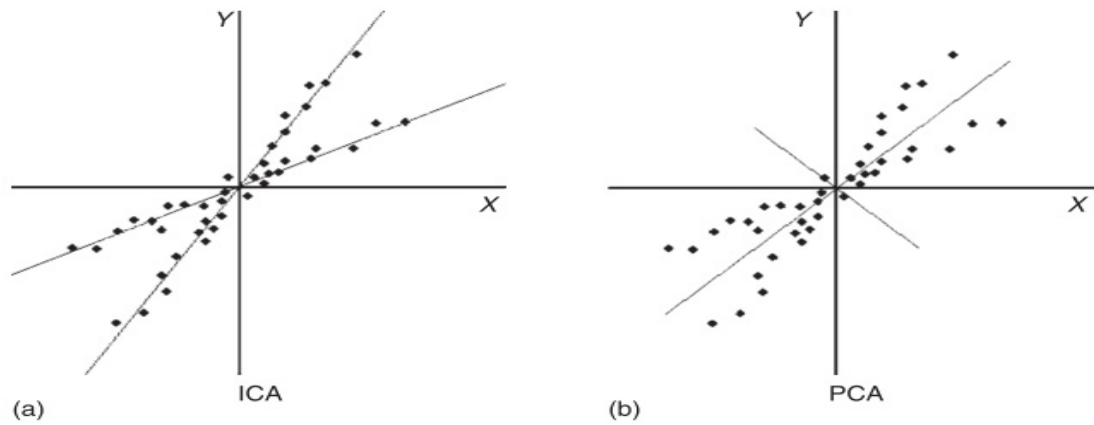
Figure 2.7: The differences between ICA and PCA.[20]

In an ICA model, it is usually assumed that the source signals cannot be observed and also that they are non-Gaussian, statistically independent and that they are mixed with an unknown but linear mixing process. Consider an observed M–dimensional random vector denoted by $x = [x_1(t), x_2(t), \dots, x_M(t)]^T$, which is generated by the ICA model:

$$x = As \tag{2.12}$$

where $s = [x_1(t), x_2(t), \dots, x_M(t)]^T$ is an N-dimensional vector whose elements are the random variables that refer to the independent sources and $A_{M \times N}$ is an unknown mixing matrix. Typically M≥N, so that A is usually a full rank matrix. What ICA tries to succeed is the estimation of an unmixing matrix $W_{N \times M}$ such that y given by:

$$y = Wx \tag{2.13}$$

Is a good approximation of the true sources s. According to the linear algebra we have that:

$$x = W^{-1}y \tag{2.14}$$

where W^{-1} is an estimation of the unknown mixing matrix A. It has to be mentioned that the ith column of W^{-1} gives the so-called (in EEG analysis) scalp topography of the corresponding component because it extracts channel weights for component i. Those topographies can be visualized in topography maps for which the source locations of independent components are assumed to be stationary, not changing in space during time of recording. An example of the raw EEG signal, the independent components and the corresponding topographies is given in the following figure. [14], [17], [20]
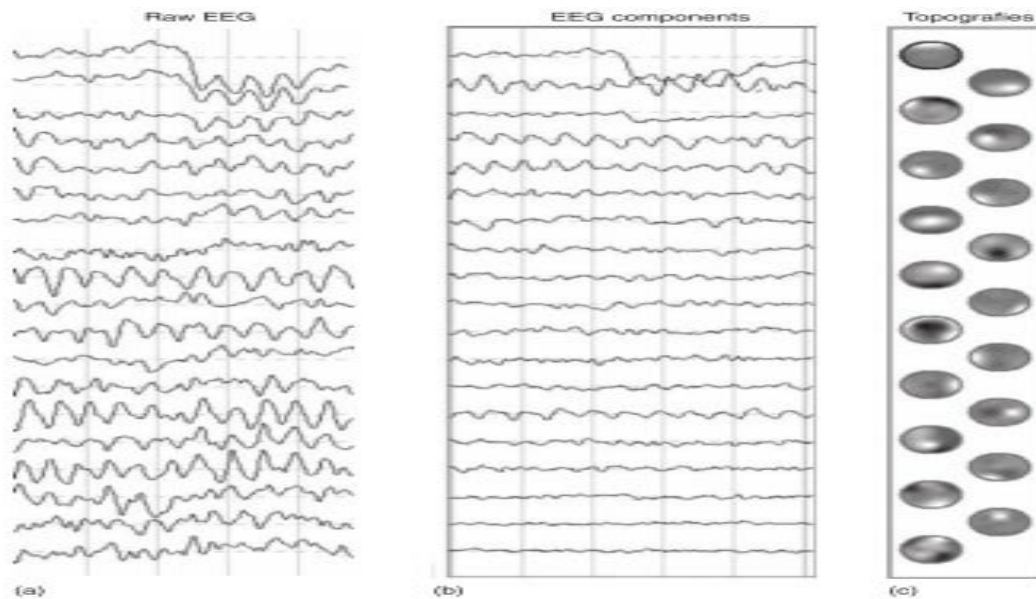
Figure 2.8: Raw EEG signal (a), its independent components (b) and the corresponding topographies (c). [20]

The waveforms of the independent components are considered as the activations sources. It has to be mentioned that the only meaningful value is that of the raw EEG (scalp recording). We can multiply both topographies (the mixing matrix columns) and the independent components (estimated sources, rows of y) by -1 without changing the value of the raw EEG. This creates the ambiguity in defining polarities of waveforms and topographies. So, neither the sign of the topography nor the sign of the waveform are meaningful in themselves. [19], [20]

As we previously mentioned, in order to achieve ICA there needs to be used higher order statistics, generated using either non-linear functions or explicitly calculated. The most popular ICA approaches have been those algorithms with non-linear functions to generate higher-order statistics. Most of these algorithms are based on maximum likelihood estimation, maximization of information transfer, mutual information minimization (maximize joint entropy), and maximization of non Gaussianity. The first three approaches are equivalent to each other, and they coincide with maximization of non Gaussianity when the unmixing matrix W is constrained to be orthogonal. This mathematical concept corresponds to the fact that ICA's goal is to find a coordinate frame in which the data projections have minimal temporal overlap. Some commonly used ICA algorithms within are Infomax, FastICA and joint approximate diagonalization of eigenmatrices (JADE) which relies on explicit computation of fourth order statistical information. [14], [17], [19]

Infomax, which is widely used in EEG analysis, is derived from the infomax principle which states that in an input- output system, independence at the output is achieved by maximizing the information flow that is the mutual information between inputs and outputs. This makes sense only if some noise is introduced into the system:

$$X = AS + N \tag{2.15}$$

where $\mathbf{N}$ is an unknown white Gaussian random vector. One can show that in the noiseless limit ($|\mathbf{N}| \rightarrow 0$) Infomax corresponds to maximizing the output entropy. Often input-output systems are modeled using neural networks. A single-layered neural network output function reads as:

$$y = \Phi(\boldsymbol{B}x) \tag{2.16}$$

where $\Phi = \varphi_1 \times \varphi_n$ is a componentwise monotonously increasing nonlinearity and $\mathbf{B}$ is the weight matrix. In this case, the entropy can be written as:

$$H(\boldsymbol{y}) = H(\boldsymbol{x}) + E\left(\log \left|det\, \frac{\partial \Phi}{\partial \boldsymbol{B}}\right.\right) \tag{2.17}$$

where x is the input vector. Then:

$$H(\boldsymbol{y}) = H(\boldsymbol{x}) + \sum_{i=1}^{n} E\left(log\varphi_i(\boldsymbol{b}_i^T \boldsymbol{x})\right) + \log |det\boldsymbol{B}| \tag{2.18}$$

Since $H(\boldsymbol{x})$ is fixed, comparing this with the logarithmic likelihood function shows that Infomax directly corresponds to maximum likelihood, if we assume that the componentwise nonlinearities are the cumulative densities of the source components (i.e. $\varphi_i = p_i$). [14], [17], [19]

2.4. Measures of Evoked/Induced Activity

One of the most important and studied brain responses is the so-called ERP. Its origins and the functional meaning of its components (N100, P300, etc.) have been greatly debated. The ERP analysis is basically based in two different approaches. The classical approach considers that the ERP response is generated by fixed latency, phase-locked responses [21]. Its underlying assumption implies that the interesting ERP response is evoked by the task and can be detected by averaging the so called evoked responses over trials, which increases the signal-to-noise ratio (SNR) in the average signal [7]. The second (alternative) approach, states that ERP and ongoing EEG oscillations may be closely interacting with each other, reflecting different aspects of the brain response to the event. In this direction, targeted experiments have revealed activities that are time but not phase-locked to the stimulus, suppressed in averaging operations. Furthermore, EEG non-phase-locked oscillations have been associated with a variety of different functions related to perception and different types of cognitive processes [3]. This form of non-phase-locked activity, referred to as induced response, is quantified and measured with techniques motivated by the time-locked nature of its envelope.

The evoked and induced responses are concerned to have separate neurophysiological origins. This is the reason why they are assumed to have different functional roles [22] and nature [23] even though they may correlate with similar cognitive events. Evoked and induced oscillations may be considered as coupled

processes progressing in time, with different spatial localization of origin and partially overlapping frequency content [23]. Thus, the separation, identification and analysis of independent activities of different nature and origin are of primary importance in considering alterations in EEG recordings due to brain pathologies or in characterizing the neurophysiological origin of brain processes.

Taking into consideration both scenarios about the ERP evaluation there have been developed measures for the quantization of phase locked and not phase-locked activity. There follows a brief presentation of these measures

2.4.1. Spectral Energy

As it was previously mentioned, the similarity or consistency of components across trials has been initially addressed in ERP studies through the average signal across trials or the spectral energy of the intertrial average. Based on that concept and going further to TF analysis using wavelets the first measure we use is the widely used spectral energy (SE) of the ERP.

For the TF representation of a component $X_i[k,n]$, with k and n indicating the frequency and time ticks, respectively, and i corresponding to the ith trial, the SE measure is defined as:

$$SE[k,n] = \left| \sum_i X_i[k,n] \right|^2 \tag{2.19}$$

In this measure there is estimated the average spectral energy. Nevertheless, spectral energy does not reflect synchronization across the trials, since a strong activity in just a few trials can induce significant spectral energy, but without providing any indication of synchronization among trials. There follows a figure showing all the procedure from the trials to the SE measure.

This measure is expected to show activation in most phase-locked EEG scenarios. In the case of phase-locked EEG with phase resetting we expect to have SE activity both when the phase resetting is linked to a power increase (activity due to the phase-locking + increased power effect) and when the power does not change (activity due to the phase-locking effect). Also, in the case of partial phase resetting, where in only part of the trials we have the phase resetting phenomenon, if those trials power contribution is efficient, the SE measure detects the activity. Finally, in the case where we have phase locked activity due to an additive activity (not phase resetting) which eventually results in power increase, here also the SE measure shows the relevant activity.

30 EEG trials in time

30 EEG trials in frequency

FT

Averaging

The corresponding ERP (time)

The ERP Fourier (frequency)

FT

Wavelets

The corresponding SE

Average (wavelets) ic. 2
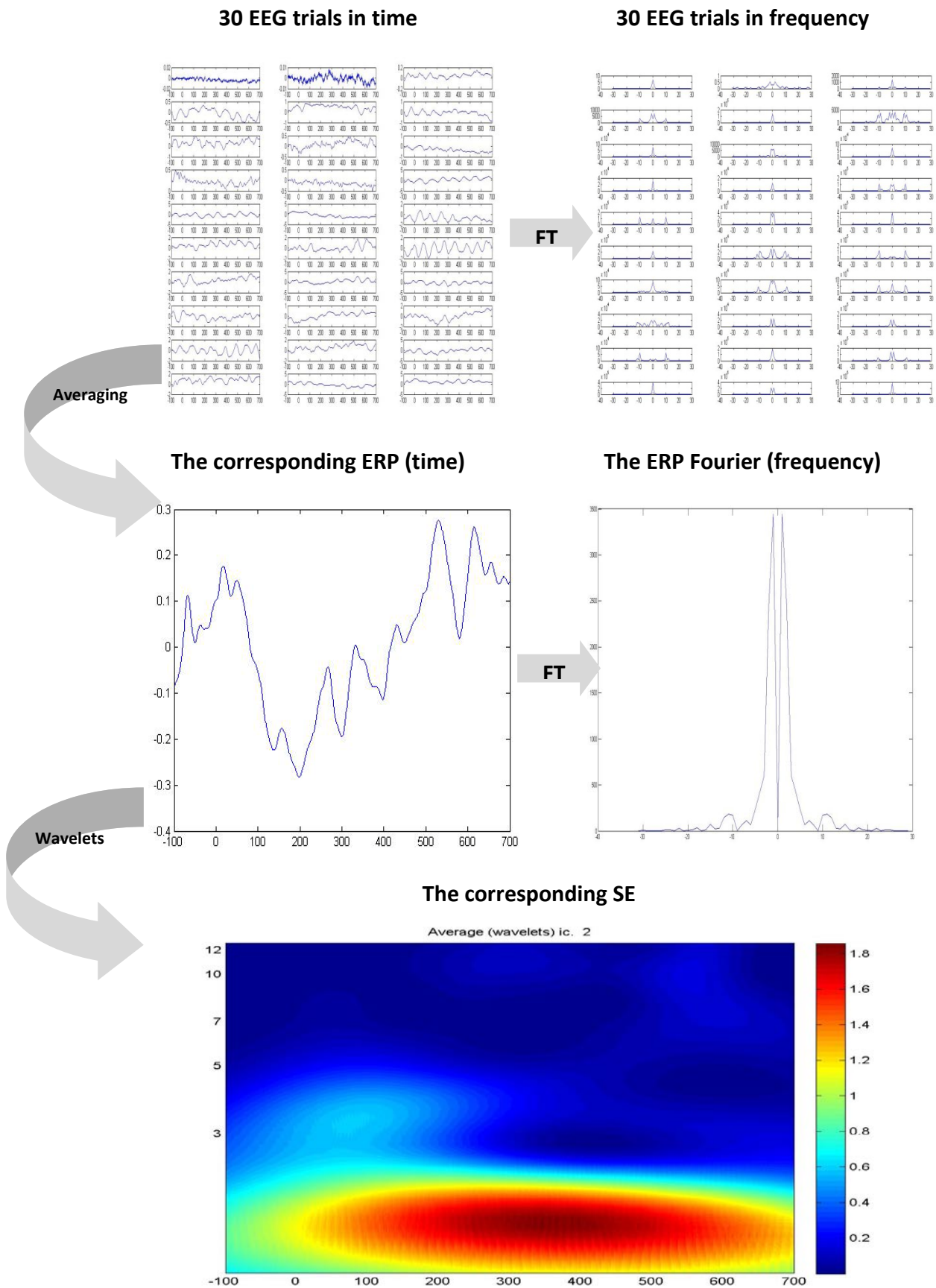
Figure 2.9: An extended example of the EEG trials (in time and frequency), the evolving ERP (in time and frequency) and the corresponding SE.

2.4.2. Phase Intertrial Coherence

As we previously mentioned the SE measure can detect phase locked activity without the certainty of synchronization among the trials. For phase locked synchronization we use the phase intertrial coherence (PIC) measure, which considers phase alignment for the evaluation of component consistency among trials [24], [25]. This metric is defined as:

$$PIC[k,n] = \frac{|\sum_i X_i(k,n)|}{\sum_i |X_i(k,n)|} \leq 1 \qquad (2.20)$$

with equality holding if and only if the trials resonate in phase. Thus, if all 'i' trials are phase-locked to the same phase shift at a certain frequency band, then the PIC measure will have large values at the corresponding frequency range. The PIC measure is a variant of the ITC measure given by:

$$ITC[k,n] = \left| \frac{1}{T} \sum_i \left(\frac{X_i(k,n)}{|X_i(k,n)|} \right) \right| \qquad (2.21)$$

Where T is the total number of trials [22]. More specifically, the PIC measure can be rewritten as: $PIC[k,n] = \sum_i \left[\left(\frac{X_i(k,n)}{|X_i(k,n)|} \right) \left(\frac{|X_i(k,n)|}{\sum_j |X_j(k,n)|} \right) \right]$ where the first part relates to the ITC measure. In this form, PIC measures the uniformity of distribution of angles (first part) weighted by the relative amplitudes (second part), in contrast to the ITC that measures the uniformity of pure angles. Based on the study performed in [26], the ITC measure alters the distribution of TF wavelet coefficients (Xi[k, n]) from multiple trials in the complex plain, projecting them all to the unit circle with no respect to amplitude. Alternatively the PIC measure preserves the structure of the cloud of coefficients (amplitude and phase) performing just scaling, so that it measures uniformity on a mixed product term involving both the angle and amplitude of coefficients. Certain trials of little amplitude in a frequency band affect the ITC measure exactly the same as trials with significant activity (amplitude), but this is not true for PIC which is proportionally affected by the amplitude of phase-locked trials. Thus, PIC is less sensitive to intertrial variations and forms a more stable measure than ITC for the discrimination of phase-locked oscillatory activity in ERP.

The PIC measure just like the SE measure is expected to show the relevant activation in most phase locking scenarios. Only for the case of partial phase locked activity in the EEG trials it is not certain that the PIC measure will detect the activity, since we have phase-locking in a group of trials and not in all of them.

SE measure	PIC measure	ITC mesure
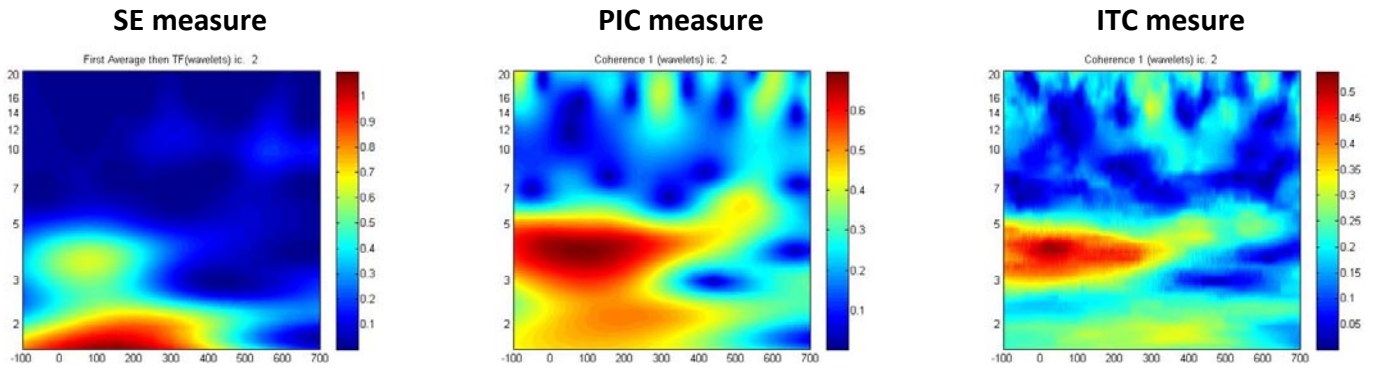
Figure 2.10: An example on real EEG data of the three phase-locked measures: SE, PIC and ITC.

In the figure above, we give an example of the three phase locked measures in order to compare and contrast their behavior. From the SE measure we see that the activation (~1) is mainly gathered from -100 to 300 ms in the low frequencies (<3Hz) and there is a smaller activation (almost half the main activation ~0.5) between 0 to 200ms in the 3 to 5Hz frequency region. On the other hand, the two synchronization measures show the main activation in the opposite way SE does which means that trials are more synchronized in theta than in delta. Comparing the two synchronization measures (PIC and ITC), we see that ITC which does not take into consideration the amplitude but only the phase synchronicity, has a greater difference in theta synchronization compared to delta than the PIC measure which also takes the amplitude into consideration.

2.4.3. Phase-shift Intertrial Coherence

Phase-shift intertrial coherence is a measure used for the evaluation of the non phase locked activity. What PsIC metric actually does is the utilization of the signal's energy instead of its value so that the phase effect is eliminated. More specifically, in case of the same basic signal with different shifts from trial to trial, there is a different exponential (phase) term remaining in the TF wavelet coefficients of each trial which is not helpful when we want to detect non-phase locked activity. So, for phase-shift responses, this metric eliminates the complex phase effects and compares the intertrial content of the signal based only on its energy in specific frequency bands. The definition of PsIc is given by:

$$PsIC[k,n] = \frac{\sum_i |X_i(k,n)|^2}{max_{k,n}(\sum_i |X_i(k,n)|^2)} \leq 1 \qquad (2.22)$$

where equality implies the same magnitude for all trials, even though they may have different phase. From this formula we understand that when we have persistent power within the trials the PsIC measure will give results close to 1. The

disadvantage of this measure is that also phase locked trials with coherent powers could have high PsIC, so we cannot be sure to characterize the underlying activity.

It should be noted here that PsIC due to the low temporal resolution at low frequencies (delta band), the wavelet coefficients present little variation in amplitude, so that the specificity of the measure decreases. Thus, the reliability of this measure at very low frequencies must be carefully handled, similar to the cone of interest for the energy analysis of WT coefficient [27].

2.4.4. Event Related Synchronization/Desynchronization

The ERD/ ERS measure represents a mean increase or decrease in event- related power. It is defined as the percentage of increase or decrease in mean trial power from a mean power baseline (usually the pre-stimulus mean power), time-locked to an event [28]. There is an assumption behind this measure implying that there are brain sources which are inactive in the pre-stimulus period and triggered by the event. In other words, it is assumed that the ongoing brain processes, pre-stimulus, are unaffected by the event and retain the same state in all trials. For the definition of ERD/ERS we give the following formula:

$$\text{ERD/ERS}[\text{k}, \text{n}] = \frac{A[k,n] - R[k]}{R[k]} \times 100 \qquad (2.23)$$

where $A[k,n]$ is the power of the kth and n^{th} frequency and post-stimulus time instant correspondingly and $R[k]$ is the power in frequency k averaged in all the pre-stimulus time instants. It is obvious that in the non phase locked scenarios where we have either power increase or decrease ERD/ERS is expected to detect the activity showing the associated synchronization or desynchronization correspondingly. Here it has to be noted that a phase locked scenario with power increase is also expected to give activation in ERD/ERS measure if it is comparable or greater that the corresponding non phase locked activity.
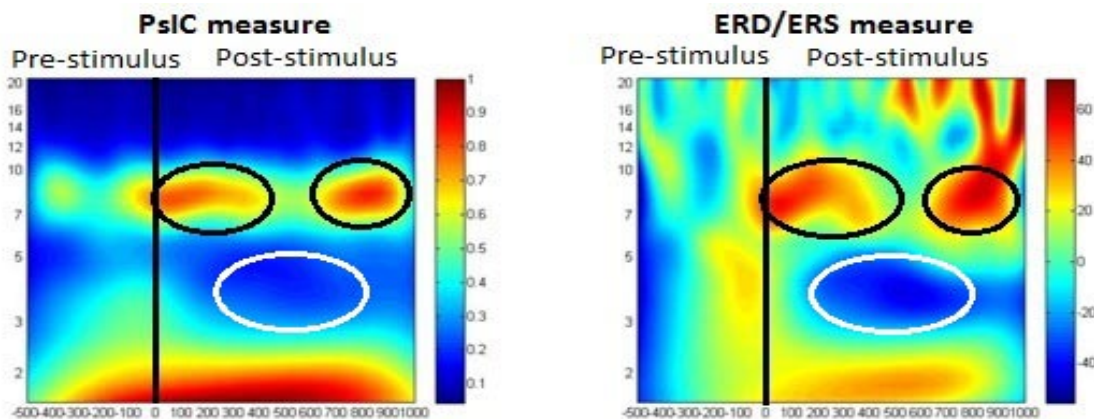

Figure 2.11: An example on real EEG data of the two non phase locked measures: PsIC and ERD/ERS. The black line in 0ms shows where the stimulus is located in time.

In the figure above we give an example of the two measures used for the detection and evaluation of the non phase locked activity. In the PsIC measure, there seems to be a profound activity in the low frequencies (delta) and in the frequencies 7-10Hz (low alpha). We have previously marked that delta activity given by PsIC has to be encountered with skepticism and in combination with ERD/ERS results. The ERD/ERS measure mainly shows a ~60% power increase in alpha (0-300ms and 700-900ms postimulus) in accordance with PsIC which shows power synchronization among trials in the same region of interest. There is also ERD/ERS detects a desynchronization activation (~40%) in 300-700ms in theta (between 3-5Hz) which could be implied by PsIC because we see that the pre-stimulus power synchronization in theta is greater than postimulus in the region of interest.

2.5. Tests of Statistical Significance

A statistical significance/hypothesis test is a method of making decisions using data, either from a controlled experiment or an observational study. In statistics, a result is called statistically significant if it is unlikely to have occurred by chance alone, according to a pre-determined threshold probability, the significance level. In order to solve any statistical problem there have to be defined some basic aspects as the followings.

A very important feature in any statistical investigation is the population. We define as population, the aggregate of evidence (animate or inanimate objects) under study. The number of units in any population, known as population size, can be either finite or infinite. Any finite, small subset of units of a population is called a sample and the number of units in a sample is called sample size. Every member of a sample is called sample unit and the numerical values of such sample units are called observations. If each unit of population has an equal chance of being included in it, then such a sample is called random sample. The process of selecting a sample is known as sampling. Statistical measures such as mean, standard deviation, variance etc. calculated based on the population are called parameters. [29], [30]

The process of ascertaining or arriving valid conclusions to the population based on a sample or samples is called statistical inference and has two major divisions: estimation and testing of hypothesis. In the case of estimation, the parameters are estimated using their respective statistics based on their samples. On the other hand, hypothesis testing begins with an assumption or hypothesized value that we make about the unknown population parameter. Then using the statistics coming from the data, we test whether the assumption made about the parameter is valid. The acceptance or rejection of the hypothesized value for the population parameter is not intuitive but based on the statistical test or test of significance which determines whether the difference between the hypothesized value and the actual

value of the sample statistic or the difference between any set of sample statistics is significant. [29], [30]

The statistical tests for testing the parameters of the population are called parametric tests. In the parametric tests we have the concept of the null hypothesis usually denoted by H_0 which refers to a tentative statement about the unknown population parameter. Any hypothesis, which is complementary to the null hypothesis, is called an alternative hypothesis. The null hypothesis is to be tested, for possible rejection under the assumption that it is true. Another very important aspect in statistical tests, is the level of significance. It has to be noted that there is no standard or universal level of significance for testing hypotheses. Nevertheless, five or one percent significant levels are very commonly used. The usage of a higher level of significance leads to a higher probability of rejecting the null hypothesis. [29], [30]

A region corresponding to a statistic t in the sample space S which amounts to rejecting of H_0 is termed as region of rejection or critical region. If ω is the critical region and t is a statistic based on a sample of size n then $P(t \in \omega | H_0) = \alpha$. That is, the null hypothesis is rejected, if the observed value falls in the critical region. The boundary value of the critical region is called as critical value Z_α. Concerning that Z is the observed value of the test statistic we have arrive at the following conclusions. If $Z \leq Z_a$ then there is no evidence against the null hypothesis H_0 and thus we accept it. In the opposite case we assume there is evidence against the null hypothesis H_0 and thus we reject it and we accept the alternative hypothesis. [29], [30]

There are many different statistical tests, each testing different parameters such as, the distribution, the mean, the variance, the median or other statistical aspects of the data. The appropriate test for each situation depends on the assumptions the test requires for the dataset which have to be satisfied. The parametric tests take use of statistical parameters of the data, while non-parametric tests do not need such evidence because they instead use medians, ranks and other methods to evaluate the data.

2.5.1. One-way Analysis of Variance

One-way analysis of variance (ANOVA) is a widely used parametric statistical test, developed by the great British statistician R. A. Fisher in the 1920s. It actually is an inferential method for comparing several means of different groups. ANOVAs basic requirements involve, independent observations, normally distributed data in each group, and equal variances for all groups and difficult to be found in raw biomedical data. Even though the method compares populations' means, it is called analysis of variance because the test statistic compares two estimates of variance. The first uses the variability between the different groups and the second uses the variability

within the groups. The basic concept of ANOVA is that the variability between groups mean is large and the variability within the groups is small. The F-test is used for comparisons of the components of the total deviation. For example, in one-way ANOVA, statistical significance is tested for by comparing the F test statistic:

$$F = \frac{\text{Between groups estimate of variance (BGEV)}}{\text{Within groups estimate of variance(WGEV)}} \qquad (2.24)$$

This is called the analysis of variance F statistic, or ANOVA F statistic for short. The degrees of freedom for the between groups estimate of variance is N-g where N is the total sample size and g is the number of groups. The BGEV is given by:

$$\text{BGEV} = \frac{\sum_i (n_i - 1)s_i^2}{N - g} \qquad (2.25)$$

Where N is the sum of the populations' samples, i is the group n_i is the population of group i and s_i^2 is the estimate of σ^2 using only the group i. s_i^2 is given by:

$$s_i^2 = \frac{\sum (y - \bar{y}_i)^2}{n_i - 1} \qquad (2.26)$$

Where y are the observations of group i and $\bar{y}_i$ is the mean of this group observations. Finally, the degrees of freedom for the between groups estimate of variance is g-1 and the WGEV formula is given by:

$$\text{WGEV} = \frac{\sum_i n_i (\bar{y}_i - \bar{y})^2}{g - 1} \qquad (2.27)$$

2.5.2. Kruskal-Wallis Test

A non-parametric version of ANOVA is the Kruskal–Wallis test. It does not require the data to be normally distributed, but just them to follow a continuous distribution in each of the groups and, the samples to be independent. The same hypotheses as in the ANOVA case are tested, but now the median values of the groups are compared. It should be noted that the non-parametric test is more reliable because it is dependent on fewer assumptions, and thus more trust should be placed on its results. The Kruskal–Wallis test starts by substituting the rank in the overall data set for each measurement value. The smallest value gets a rank of 1, the second-smallest gets a rank of 2, etc. Tied observations get average ranks, so for example if there were two identical values occupying the tenth and eleventh smallest places, all would get a rank of 10.5. The sum of the ranks is calculated for each group, then the test statistic, H, is calculated. H is given the following formula:

$$H = \left[\frac{12}{N(N-1)} \sum_i \frac{R_i^2}{n_i} \right] - 3(N + 1) \qquad (2.28)$$

Where N is the sum of the populations samples, i is the group, R_i the sum of ranks for group i and n_i is the population of group i. That basically represents the

variance of the ranks among groups, with an adjustment for the number of ties. H is approximately chi-square distributed, meaning that the probability of getting a particular value of H by chance, if the null hypothesis is true, is the P value corresponding to a chi-square equal to H and the degrees of freedom is the number of groups minus 1. If the sample sizes are too small, H does not follow a chi-squared distribution very well, and the results of the test should be used with caution. Each group should contain more than 5 samples in order not be considered too small.

3. Dataset 1: Methodology and Results

3.1. Introduction

The brain mapping of activity during task performance gives important information about the organization of the brain, which can be exploited for clinical purposes [31], [32], [33] such as disease diagnosis or for application developments as in brain computer interfaces [34]. Towards this direction many studies have been published considering EEG activation under specific tasks. Simple 2-d brain mapping is often used for qualitative comparisons. This essentially reflects a mapping of EEG amplitude distribution on a 2-D circular head map, where the electrodes are projected and the areas among electrodes are filled up by means of spatial interpolation. In order to quantify the activity and provide objective comparisons among tasks, several measures of activation (such as band power and electrode synchronization) and statistical comparison test (Kruskal-Wallis test) have been exploited. Comparison among different tasks has also been investigated by other studies either among control population [35], [36], [37] or between a control population and pathological subjects [33], [38] .

The main goal here is to consider multiple measures for differentiation of brain activity during the performance of different tasks. In particular, we consider the power spectrum at different bands and its localization in brain regions, as well as the dynamic coherence of these brain regions during the performance of each task. The derivation of significant differences is then achieved through between-task comparisons with appropriate statistical measures. The development of this chapter proceeds as follows. Firstly, the experimental protocol and the analysis tools are presented. Then, we have the presentation of the experimental results in terms of activation and synchronization of brain lobes. The results are discussed and compared with other relevant references, which also concludes this chapter.

3.2. Experimental Procedures

3.2.1. Participants

In this experiment, there participated 25 graduate or postgraduate students (14 male, 11 female) of the medical school of Iraklion/Greece who voluntarily participated in the current study. Their age ranged from 19 to 32 years. The study was approved by the local ethical committee and written informed consent was obtained from each participant.

3.2.2. EEG Recording and Test Description

The EEG signals were recorded using 30 electrodes according to the international 10/20 system. The electrode positions used are: FP2, F4, FC4, C4, CP4, P4, O2, F8, FT8, T4, TP8, PO8, Fz, FCz, Cz, CPz, Pz, Oz, FP1, F3, FC3, C3, CP3, P3, O1, F7, FT7, T3, TP7, PO7, and A1 +A2 as reference. Vertical and horizontal eye movements and blinks were monitored through a bipolar montage from the supraorbital ridge and the lateral canthus. A connected ear- lobe electrode (A1 + A2) was used as reference electrode. The A1 and A2 electrodes were positioned on ear-lobed far from the scalp electrodes (and far from muscles). The signals were filtered online with a 0.1–200 Hz band pass and digitized at 500 Hz.

During the acquisition, the subjects were performing one of the two arithmetic tasks: Simple addition of one digit numbers (fundamental task for students) i.e. 3 + 2 and comparison of three digit numbers i.e. 123 vs. 232. There was also recorded a control EEG during a passive viewing of simple digit numbers (control task). 1 person was discarded from the control task and another person was discarded from the compare task because of incomplete data (1 channel was problematic). Stimuli were presented on an LCD screen located in front of the participants at a distance of approximately 80 cm, subtending 2–4◦ of horizontal and 2– 3◦ of vertical visual angle. The recorded EEG was under inspection on a PC screen and the recording was stopped when there were pieces of proper length free of artifacts. The EEG signals were further inspected offline for artifacts (especially eye artifacts) using EEGLAB tools such as ICA for component rejection and backprojection to the channels, or rejection by eye of continuous part of the EEG signal. Also the EEG signal was re-referenced to an average reference instead of the default common reference using the tools of EEGLAB, since, this selection could influence significantly the subsequent computations of power spectrum and coherence [39], [40].

3.2.3. EEG Analysis

The EEG signals (~8 sec. duration) were transformed from the temporal domain to the time-frequency domain by means of the wavelet transform using the complex Morlet wavelet functions. The WT has developed into an important tool for the analysis of time series that contain non-stationary activity at multiple different frequencies such as the EEG signal. Instead of frequencies, the WT employs the alternative notion of scales, resulting to the so called time-scale representation [41].

The Complex Morlet Wavelets are denoted as $W_t(s)$, where t denotes the discretized-time (sample) number and s indicates the scale. In our analysis we use the power spectrum $|W_t(s)|^2$ for each EEG signal. There exists a concrete

relationship between scales and equivalent Fourier frequencies, often known as pseudo-frequencies. The correspondence of the scales to the frequency-bands used in our analysis is demonstrated on Table 3.1 (a total of 56 scales).

Band	Frequency (Hz)	Scales
Delta	1-4	37-56
Theta	4-8	27-36
Alpha	8-13	20-26
Beta	13-30	8-19
Gamma	30-45	1-7

Table 3.1: The matching of frequency band to wavelet scales.

After the EEG is zero-mean normalized for each task (control, addition and comparison), channel and frequency band, we estimate from the power spectrum the average power spectrum for all the participants. The estimation of the power spectrum through wavelets has also been used in other studies [37].

$$\overline{PS}(f) = \frac{1}{P}\sum_{p=1}^{P}\left(\frac{1}{ms - ls}\sum_{s=ls}^{ms}\left(\frac{1}{T}\sum_{t=1}^{T}|W_t(s)|^2\right)\right) \qquad (3.1)$$

where f is the frequency band, s is the wavelet-scale (ls and ms are the scales corresponding to the appropriate frequency band), t is the time instant (T is the last time instant) and p corresponds to the participant index (P is the number of participants).

After estimating $\overline{PS}$ for every electrode, band and task we subtract pair wisely all the different combinations of the PSs of the different tasks (a total of 3 combinations (e.g. $\overline{PS}_{control\ task} - \overline{PS}_{addition\ task}$) for the corresponding electrodes and bands so as to detect significantly different power differences (via Kruskal-Wallis significance test) in the brain activation between the different mathematical thinking tasks and in contrast to a control condition.

Different groups of electrodes were selected so as to be representatives of the different brain regions taking also representing the left and right hemisphere. This was important in order to reduce the degrees of freedom in the non-parametric analysis of PS and since entire cortical regions are assumed to function in a similar manner. We use non-parametric analysis because our data do not follow a Gaussian distribution. The considered groups of electrodes are: Frontal left (FL): FP1, F3, F7, FC3, FT7, Frontal right (FR): FP2, F4, F8, FC4, FT8, Temporal left (TL): FT7, T3, TP7, Temporal right (TR): FT8, T4, TP8, Central left (CL): FC3, C3, CP3, Central right (CR): FC4, C4, CP4, Parietal left (PL): P3, TP7, PO7, Parietal right (PR): P4, TP8, PO8, Occipital left (OR): O1, PO7 and Occipital right (OR): O2, PO8. For the significance of the power increase or decrease the resulting power spectrum of each task in the groups of electrodes were submitted to Kruskal-Wallis one way analysis of variance

significance test so as to examine the significance between the distributions of the different pairs of tasks, for the different frequency bands and regions. Kruskal-Wallis test is a non-parametric version of the classical one-way ANOVA. We consider as significant the p-values which are under 0.05 ($p < 0.05$).

In addition to the previous analysis, we also examine the magnitude squared coherence (MSC) of the EEG electrode groups. The MSC is calculated for all the different pairs of electrodes in the region group which we evaluate through Kruskal-Wallis test and then for the significant regions we take the average within the group for the different tasks. After the MSC is computed, it is averaged for all participants in every frequency band. MSC is a normalized cross-spectral density function and measures the strength of association and relative linearity between two stationary stochastic processes on a scale from zero to one. The coherence will be zero when the processes are independent and absent a linear time-invariant relationship [42].

$$MSC(f) = \frac{P_{x,y}(f)^2}{P_{x,x}(f)P_{y,y}(f)} \tag{3.2}$$

Where $P_{x,y}(f)$ is the cross-spectral density, and $P_{x,x}(f), P_{y,y}(f)$ are the autospectral densities of x and y correspondingly at frequency f. The spectral density function is given by the Fourier of autocorrelation function $R(\tau)$ and the cross-correllation by the Fourier of the corresponding cross-correlation function. The coherence results are examined for their significance via Kruskal-Wallis one way analysis of variance significance test for the different regions and tasks.

3.3. Results

The outcome of our analysis in terms of power on the experimental datasets is summarized in Figure 3.1 and Table 3.2. The tabulated brain lobes are the significant ones extracted from the five frequency bands under investigation. Figure 3.1 depicts the topographies which show the power-activation differences between the different tasks and in we have the regions in which there exist significant differences. In addition to power, the coherence behavior is also explored in terms of different bands, regions and tasks. The results for the coherence differences between the tasks are summarized in Table 3.3.

3.3.1. Power

As observed in Table 3.2, there are no significant results concerning the theta band. In terms of power values (Figure 3.1) reflects that the comparison task has an

increase of delta both in FL and FR regions (mostly in FL) compared to the control (p<0.05 for FL and FR); the same is also observed in addition (p<0.05 for FL).

We observe from Table 3.2 that the most significant results occur for the alpha band, where we have power decrease for the more demanding tasks, in agreement to other studies [3]. In both tasks of addition and comparison, we have alpha decrease mostly in central, occipital and parietal regions (addition: p<0.01 for PL, PR, and CL and p<0.05 for OL, OR; comparison: p<0.001 for PL, PR, CL, CR and p<0.01 for OL, OR). The actual power distribution is presented in detail in Figure 3.1. Comparing the two mathematical tasks, it appears that number comparison has an alpha power decrease in contrast to the addition task in the central-parietal regions (p<0.001 for PR, p<0.01 for CL and CR, and p<0.05 for PL). The comparison task shows a greater power decrease especially in the central-parietal region of the left hemisphere (an asymmetry can be easily distinguished). This can be clearly observed in Figure 3.1 in agreement with [43].

For the gamma band we do not observe significant differences in Table 3.2. In beta band, the addition task shows a power decrease in contrast to the control task in the PR site (p<0.05). The comparison task expresses power decrease compared to the control task in the central-parietal sites (p<0.01 for CL, and p<0.05 for PR, PL and CR). From Figure 3.1 we observe a slight asymmetry in the power decrease, with larger decrease in the right hemisphere both in addition and comparison task as compared to the control task. Asymmetries in the two hemispheres are also reported by other studies [44].

$$\overline{PS}_{addition} - \overline{PS}_{control} \qquad \overline{PS}_{compare} - \overline{PS}_{control} \qquad \overline{PS}_{addition} - \overline{PS}_{compare}$$

$$\overline{PS}_{compare} - \overline{PS}_{control} \qquad \overline{PS}_{addition} - \overline{PS}_{control} \qquad \overline{PS}_{compare} - \overline{PS}_{control}$$
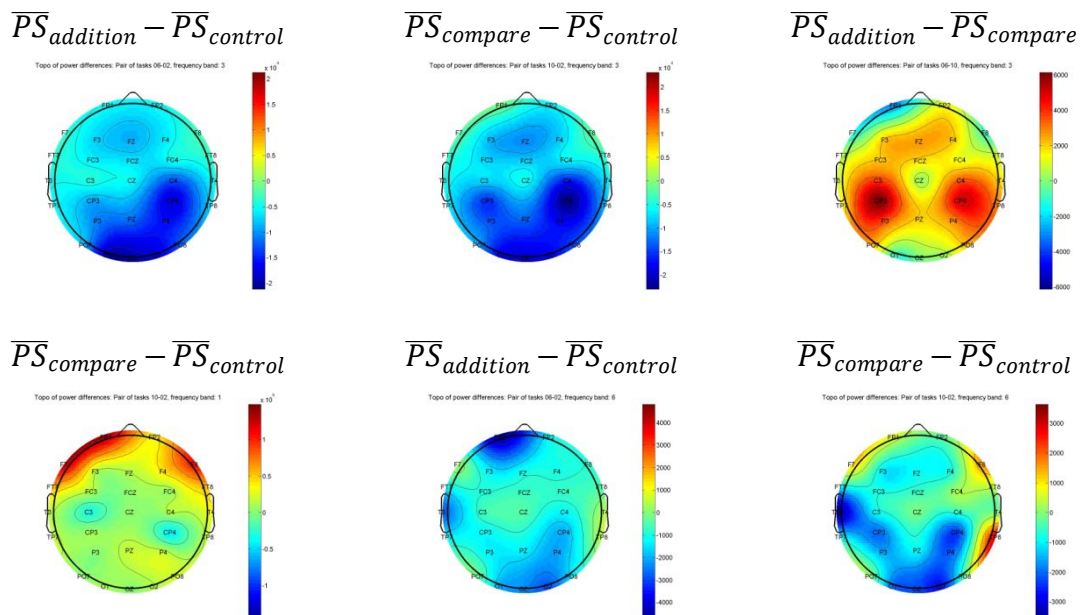

Figure 3.1: Power differences between the tasks for Alpha in the 1st row, Delta band in the 2nd row, 1st column and Beta in the 2nd row, 2nd and 3rd column (topographic representation).

Band	Addition-Control Task	Comp.-Control Task	Comp.-Addition Task
Delta	-	FL↑, FR↑, TL↑, TR↑	FL↑, TL↑, TR↑
Theta	-	-	-
Alpha	FL↓, PL↓, PR↓, OL↓ ,OR↓ , CL↓ , CR↓	FL↓, FR↓, TL↓, TR↓, PL↓, PR↓, OL↓, OR↓, CL↓, CR↓	PL↓, PR↓, CL↓, CR↓
Beta	PR↓	PL↓, PR↓, CL↓, CR↓	-
Gamma	-	-	-

Table 3.2: The tabulated results for significant power differences between the tasks. The arrows denote either an increase or a decrease in the power of the first task compared to the second.

3.3.2. Coherence

In Table 3.3 we present the coherence differences found to be significant (p<0.05) for the three different tasks. The brain regions in bold are those also found to be important in Table 3.3 in terms of power changes. In particular, the coherence differences appear to be consistent with power differences. For example, in the addition compared to the control task we have a power and coherence decrease for PR region in alpha and beta bands. Only for the pair (comparison, control) tasks in beta band for the CR region we have a decrease in power and an increase in coherence. This could imply phase-locked activity in CR (increase of coherence despite the power decrease) in beta, in contrast to the other regions (decrease both in power and coherence).

In general, we have the following behavior in the coherence differences: For the coherence of addition compared to control task we have a power decrease in theta, alpha, beta, and gamma bands for the regions (a) TL, (b) PR, (c) PL, PR, TR, OL, and (d) PR, OL, OR, whereas we observe a power increase for beta and gamma in the regions (e) TL, CL, CR and (f) FL, TL, PL. For the coherence of the (compare, control) pairs we have a power decrease in delta, theta, alpha, beta and gamma for the regions (a) PL, OL, (b) TL, TR, (c) FL, FR, TR, PL, PR, OL, OR, (d) PL, PR, FR, TR, OL, OR and (e) PL, OL, OR, while we have a power increase for beta and gamma in the regions (f) CR, FL, TL and (g) FL, CR. Finally, for the coherences of the compare compared to the addition task we have a power increase for theta, alpha, beta, and gamma for the regions (a) TR (b) TR, PL, PR, OR (c) FR, TL, TR, PL, OR, CL and (d) FR, PL, OR, and we have a power increase for delta and gamma for (e) FL, (f) PR, CR.

The coherence behavior for the addition and comparison compared to the control task are similar for the common regions, except from PL coherence in gamma which has an increase in the addition and a decrease for compare task.

Band	Addition-Control Task	Comp.-Control Task	Comp.-Addition Task
Delta	-	PL↓, OL↓	**FL↑**
Theta	TL↓	TL↓, TR↓	TR↓
Alpha	**PR↓**	**FL↓, FR↓, TR↓, PL↓, PR↓, OL↓, OR↓**	TR↓, PL↓, PR↓, OR↓
Beta	**PR↓,** TL↑, TR↓, PL↓, OL↓, CL↑, CR↑	**PL↓, PR↓, CR↑,** FL↑, FR↓, TL↑, TR↓, OL↓, OR↓	FR↓, TL↓, TR↓, PL↓, OR↓, CL↓
Gamma	FL↑, TL↑, PL↑, PR↓, OL↓, OR↓	FL↑, PL↓, OL↓, OR↓, CR↑	FR↓, PL↓, PR↑, OR↓, CR↑

Table 3.3: The tabulated results for significant coherence differences between the tasks. The bold results correspond to the common regions which both have significant power and coherence differences.

3.4.Discussion

There are some key findings to notice in our data. First, the two mathematical tasks are associated with: (a) reduced power in the alpha (mostly) and beta band, primarily over the central-parietal regions in agreement with, [3], [35], [36]. Alpha oscillation is associated by many studies with memory retrieval processes. More specifically, alpha power has been found to decrease with increasing retrieval demands (alpha ERD) [3]. It is also reported that alpha decrease in mathematical tasks is mainly localized in central and parietal regions [35]. (b) a power increase of delta in the frontal regions for the task of comparison in agreement with [36], [40]. A delta increase has been reported in some experiments during mental arithmetic or other mental tasks, especially at frontal or central regions [36]. (c) A larger power decrease in alpha along with a larger increase in delta for the compare task in contrast to the addition task. To the best of our knowledge, there is no, literature study relating such band effects at those specific mathematical tasks. Though, these differences could be an implication for the different functionalities in the two mathematical tasks (addition, comparison).

At this point it is important to observe that the power decrease often reflects a coherence decrease. For example in the alpha band for the comparison and addition task, in contrast to the control case, we observe a power and coherence decrease for

the corresponding regions. The only exception is for the case of comparison task compared to the control in beta, for which we have a decrease in power and an increase in coherence in CR. However, this could be explained as an indication of phase-locked activity. We also observe a common tendency in the coherence differences of the two mathematical tasks compared to the control task. The only exception is for PL in gamma, which could imply a different functionality for the two mathematical tasks in this region. We should emphasize that these results need extensive verification, since there exist only a few studies relating tasks in terms of coherence [35]. Nevertheless, the joint consideration of power and coherence (or other measures of dynamic synchronization) can shed light to the complex organization of brain operation during mental tasks, in terms of both source activations and interactions. For instance, power measures can differentiate between evoked and induced activations, whereas coherence can characterize the effects of phase resetting in ongoing EEG oscillations [45].

At this point, it has to be noted that the findings of this work can be found at [46].

4. Dataset 2: Methodology and Results

4.1. Introduction

The internal or external stimulus, evoke brain activity which is caused by the firing of different neural assemblies in different locations of the brain. These activations are captured in the scalp electrodes either as phase-locked (evoked) or non-phase-locked (induced) oscillations.[47] Phase-locked and non-phase locked responses have differences because of their neurophysiologic origins.[7], [48] They also have different functional roles, even though they may reflect similar cognitive events and correlate in their various parameters.[22], [49] In order to extract phase locked activity from the EEG signal, we need to average EEG single trials, which results to the well known ERP.

The ERP is one of the brain response most widely and extensively studied as it has been proven extremely useful in clinical and physiological research. There is a rich literature about the functional meaning of the different peaks of ERP (such as the P100, N100 and P300), which are thought to reflect different aspects of information processing in the brain. This classical point of view states that ERPs are generated by fixed latency, phase-locked responses. Its underlying assumption implies that the interesting ERP response is evoked by the task and can be detected by averaging the recorded signals over trials, which increases the signal-to- noise ratio (SNR) in the average signal.[7], [21], [50]

Targeted experiments have revealed activities that are time but not phase-locked to the stimulus, which are suppressed in averaging operations. Such activities are exemplified by the increase or decrease of energy in a specific band post-stimulus, denoted as event related synchronization (ERS) or desynchronization (ERD), respectively.[28] Non phase-locked oscillations have been associated with a variety of different functions related to perception and different types of cognitive processes.[3] Extensive findings correlate alpha energy and alpha phase, on stimulus onset with the ERP amplitude, indicating that the ERP and EEG oscillations interact and relate to each other.[51] Evoked and induced oscillations may be considered as coupled processes progressing in time, with different spatial localization of origin and partially overlapping frequency content [7], [48], [22], [50], [24]. Thus, the separation, identification and analysis of independent activities of different nature and origin are of primary importance in considering alterations in EEG recordings due to brain pathologies or in characterizing the neurophysiological origin of brain processes. Efficient decomposition frameworks include wavelet analysis and independent component analysis (ICA) [52] followed by a variety of methods to characterize the nature of derived components in terms of their TF activity.

In this part of the study ICA, wavelets and measures reflecting the phase-locked and not-phase locked activity were used in a population of dyslexic and control subjects having a Wechsler experiment, in order to find possible significant differences for the different ERP components regions (P50, N100, P300 and P600) and frequencies (delta, theta and alpha).

4.2. Background

Often children of average intelligence even though they do not have general learning difficulties, they show symptoms of difficulty in reading not connected to extraneous factors such as socioeconomic disadvantage. These children manifest difficulties in acquiring basic reading sub-skills such as word identification and phonological decoding [53]. There is a 10-15% of school aged children showing these symptoms accompanied by specific deficits in cognitive abilities related to reading skills. This symptom pattern is called 'dyslexia', or, alternatively, 'specific reading disorder' [according to the 10th edition of the International Classification of Diseases].[54] This is the main diagnosis of the general diagnostic category: specific developmental disorders of scholastic skills (DDSS) [53].

It is not clear what the pathophysiological mechanisms underlying DDSS are and there is a long way till they are identified, though researchers have made some interesting suggestions in the fields of biological and cognitive research. There have been implicated deficits of the working memory operation and attention within the patterns of cognitive characteristics of dyslexia. [53] ,[55] Contemporary neuropsychological thinking defines working memory as the capacity to keep information on line, as necessary, for an ongoing task [56]. According to this view, working memory is not for 'memorizing' in itself, but is used for complex cognitive activities such as language, reasoning, problem solving and decision-making [54].

There have been various studies comparing control to dyslexic subjects under the basis of ERP methodology and more specifically relating information processing deficiency with patterns of N100 component. In many of these studies it has been found that dyslexics have reduced N100 amplitude [57], [58], [59] and prolonged latency [60] as compared to controls. Though, there were also studies which failed to detect differences between the two populations [61] or made the opposite conclusions. Such inconsistencies appear due to the variability of the experiments methodology.

For the particular dataset, previous research on the time-frequency of the channels has reported differences between the group of dyslexics and controls lying mainly in the time period 50-200msec after the warning stimulus, most prominently around the N100 ERP component, and containing frequencies 5- 20Hz [11]. More specifically the analysis showed reduced mean peaks for the N100 ERP components

[11]. The attenuation of the N100 ERP component [62] and prolonged latency of the P50 ERP component [54] for the group of dyslexics did also emerge from the analysis of this dataset in time. Furthermore, research on the Wechsler experiment in heroin addicts showed significant differences for the P300 [63] and P600 [64] ERP components.

4.3.Experimental Procedures

4.3.1. Participants

In this experiment, there participated 57 children from which 38 (26 boys and 12 girls) were outpatient cases who had been diagnosed as having dyslexia according to the 10th edition of the International Classification of Diseases (ICD-10) and the rest 19 children (7 boys and 12 girls) were control sibling of the dyslectic group. The mean ages and the standard deviations for the dyslectic children and for the controls were 11.47±2.12 and 12.21±2.25 years, respectively and did not have significant differences. In each case, the following assessments were performed: child psychiatric examination, psychological examination and educational evaluation. The Wechsler Intelligence Scale for Children – Third Edition (WISC-III) was used to obtain the IQ of each child. Also, the participants did not enter the study if they had (1) clinically notable neurological disease (including seizure disorder), (2) a history of head injury, (3) hearing difficulties and (4) attention deficit disorder and hyperkinetic syndrome. Prior to participation in the examination, parents were informed about the aims of the study, received a full description of the procedure, and provided written consent. Children were tested individually and the investigators explained to each child the procedure and the children also gave their consent. The study was approved by the local ethical committee. For more experimental information see Papageorgiou et al [54].

4.3.2. EEG Recording and Test Description

The children's EEG/ERP signals were recorded at 15 electrodes (Fp1, F3, C5, C3, Fp2, F4, C6, C4, O1, O2, P4, P3, Pz, Cz, Fz) according to the 10–20 international system, referred to both earlobes. Ag/AgCl electrodes were attached to the scalp with adhesive cream in order keep the electrode resistance below 5 kΩ. An electrode placed on the subject's forehead served as ground. The pass band of the amplifiers was set from 0.05 Hz to 35 Hz. During the recordings the subjects had their eyes closed in order to minimize eye movements and blinks. Eye movements were

recorded through electrooculogram (EOG) and recordings with EOG higher than 75 μV were rejected. Warning stimuli, as well as learning material (i.e. the numbers to recall), were presented binaurally via earphones at an intensity of 65 dB sound pressure level. The evoked biosignal was submitted to an analog-to-digital conversion, at a sampling rate of 1 kHz and the total procedure consisted of 52 repetitions. [10], [62]

During the acquisition, the subjects were evaluated with the digit span Wechsler auditory test [65]. There was a warning stimulus of either high (3kHz) or low (0.5kHz) frequency presented through earphones to the participants, who were asked to memorize the numbers that followed in the same or opposite order correspondingly. Firstly, there was a warning stimulus (100ms) and 1sec after the stimulus onset the numbers to be memorized were presented by a male voice. If the frequency of the signal tone was low, the participants had to recall the numbers in the same order as presented else the participants had to recall the numbers in the opposite order. At the end of the number sequence presentation, the same signal tone was repeated. Before the procedure was followed in the participants, practice trials were administered until the participants could clearly discriminate the warning stimuli (tones). The ERPs were recorded during the 1.1-s interval between the warning stimulus and the first administered number.[54], [62]

| Time period	Action
AB (500ms)	Recording of EEGs.
BC (100ms)	Warning stimulus (500 or 3000Hz, 65dB)
BD (1000ms)	Recording of ERP signal.
DE (varies) (Not in scale)	Computerized administration of the sequence of numbers
EF (100ms)	Repetition of warning stimulus (500 or 3000Hz, 65dB)
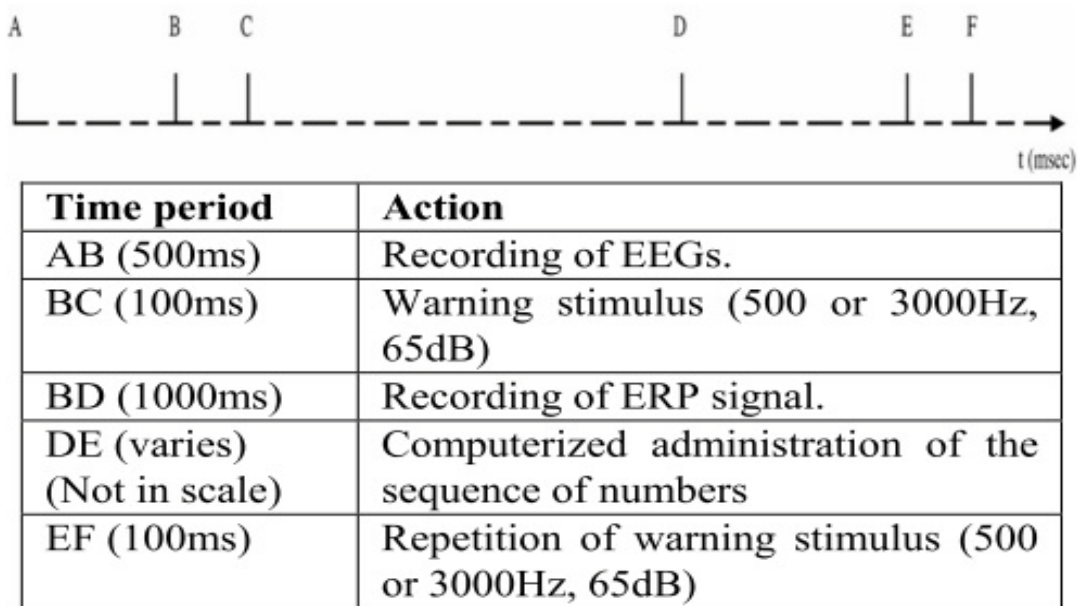
Figure 4.1: Outline of the experimental procedure. [10], [62]

4.4. EEG Analysis

The EEG signals (~1.5s) were zero-mean normalized and then ICA was applied on them. Previous research on the dataset focused on its analysis in time [54] or time-frequency [11] giving results specifically for each channel. We used ICA, in order to investigate the overall activity of the EEG signals of this dataset, so instead of channels have components of activity. ICA was applied on the entire collection of concatenated (one trial after the other) EEG signals $e_i(n), i = 1, \ldots, L$ and $n = 1, \ldots, N$, where L indicates the number of channels on the scalp and N denotes the number of data points in the signal. Thus the estimated de-mixing matrix W is assumed to initially produce the EEG signals $e_i(n)$ based on mutually independent sources $s_i(n)$: $\boldsymbol{s} = \boldsymbol{We}$

In our approach we use ICA on concatenated trials (all the trials of both high and low frequency acquisition) under the assumption of similar decomposition across trials, which can effectively recover the intertrial variability of sources (derived components) [66] while preserving stability and avoiding overtraining of the inversion process [67]. Concatenated ICA also has the advantage that the ordering of components in the various trials is preserved, so that similar components can be statistically studied over trials.

In this analysis we use the Infomax ICA algorithm [19], which minimizes the mutual information among the data projections in order to achieve independence. The column elements of the inverse matrix W^{-1} reflect the projection intensity of each independent component back to the electrodes and form the basis of topographic mapping of this component.

After we had the ICs coming from the original EEG channel data, we applied the well-known wavelet transform on them using in specific the complex Morlet wavelet function which has been extensively studied in EEG analysis [68]. We have already emphasized that in the second chapter that wavelets form a great tool for the presentation of the EEG signal to the time-frequency domain. More specifically, in the wavelet approach, we have the signal decomposition into constituent time–frequency ranges of energy based on the notion of scale applied to a set of basis functions. There is a tradeoff between frequency and time in the wavelet analysis as we have small scale (high-frequency) intervals with shorter time windows and large scale regions (low-frequency) with longer time windows. Due to this fact, there is a higher resolution in frequency (but not in time) for the low frequencies and a higher resolution in frequency (but not in time) for the high frequencies.

In order to evaluate the activity of the TF transformed ICs, we apply on then measures revealing the evoked and induced activity. That way, we extract the phase locked and induced characteristics of the ICs in the time-frequency domain. The first measure we use is the widely used spectral energy (SE) of the ERP. For the TF representation of a component $X_i[k,n]$, with k and n indicating the frequency and

time ticks, respectively, and i corresponding to the ith trial, the SE measure is defined as:

$$SE[k,n] = \left| \sum_i X_i[k,n] \right|^2 \qquad (4.1)$$

In this measure there is estimated the average spectral energy. Nevertheless, spectral energy does not reflect synchronization across the trials, since a strong activity in just a few trials can induce significant spectral energy, but without providing any indication of synchronization among trials. For phase locked synchronization we use the phase intertrial coherence (PIC) measure, which considers phase alignment for the evaluation of component consistency among trials [24], [25]. This metric is defined as:

$$PIC[k,n] = \frac{|\sum_i X_i(k,n)|}{\sum_i |X_i(k,n)|} \leq 1 \qquad (4.2)$$

with equality holding if and only if the trials resonate in phase. More details on the measure are given in chapter 2. For the quantification of the event-related but non phase-locked activity there is used the so-called phase-shift intertrial coherence (PsIC) and the ERD/ERS measures. PsIC is based on the energy of single-trial decompositions and highlights frequency bands of increased energy in all trials. The PsIC measure reflects persistent activity in all trials and is defined as:

$$PsIC[k,n] = \frac{\sum_i |X_i(k,n)|^2}{max_{k,n}(\sum_i |X_i(k,n)|^2)} \leq 1 \qquad (4.3)$$

where equality implies the same magnitude for all trials, even though they may have different phase. The disadvantage of this measure is that also phase locked trials with coherent powers could have high PsIC, so we cannot be sure to characterize the underlying activity [24], [25]. On the other hand, ERD/ERS measure is defined as the percentage of increase or decrease in mean trial power from a mean power baseline (usually the pre-stimulus mean power), time-locked to an event [28]:

$$ERD/ERS[k,n] = \frac{A[k,n] - R[k]}{R[k]} \times 100 \qquad (4.4)$$

where $A[k,n]$ is the power of the kth and t^{th} frequency and post-stimulus time instant correspondingly and $R[k]$ is the power in frequency k averaged in all the pre-stimulus time instants. These measures are analyzed in detail in the second chapter of this essay.

After some indicative components were examined in order to evaluate the activity of the subjects in response to the specific memory experiment they attenuate, from the TF maps of the measures applied on the ICs of the two groups (controls, dyslexics) there were collected evidence for their comparison via Kruskal-Wallis significance test. Statistical significance was set at the 0.05 level in all cases. We considered as evidence the 'main activity' (or main components) of each TF map. More specifically, per each TF map there were chosen those regions whose value

were up to 20% lower than the maximum value of the overall TF map. Such an example is presented in the following figure.
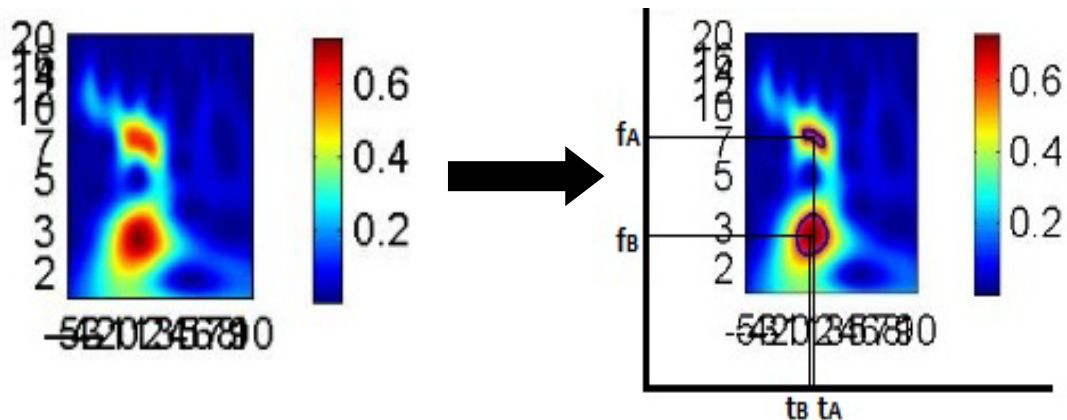

Figure 4.2: An example for the component area selection. On the left there is the TF map of an IC and on the right the 'important' areas of the IC have been circled with blue and the frequency and time instants of the centroids of those areas have been projected on the axis as (t$_A$,f$_A$) and (t$_B$,f$_B$).

After that, the centroid of those areas was computed so as to have a central time and frequency instant for each area. There was also estimated their average value over the points meeting the previously described criteria. Then, the time, frequency and average value evidence coming from the TF maps were compared via Kruskal-Wallis significance test for the control and dyslexic subjects for the *different ERP component regions* and *frequency bands*. The ERP component regions considered were: P50 (30ms-80ms postimulus (ps.)), N100 (70-150ms ps.), P300 (240-500ms ps.) and P600 (500-800ms ps.), and the frequency bands considered were: delta (1.6-3Hz), theta (3-7Hz), low alpha (8-10Hz), high alpha (10-12Hz) and overall alpha (8-12Hz). Thus, there took place 60 distinct significance tests for all the combination of characteristics (time, frequency, value), ERP regions and frequency bands for each measure. It was only possible to compare the main activity of the components and not separate the TF map in grids and compare the corresponding component grids like [28] did in channels because ICs are not comparable the way channels are. There follows a diagram showing an outline of the procedure.
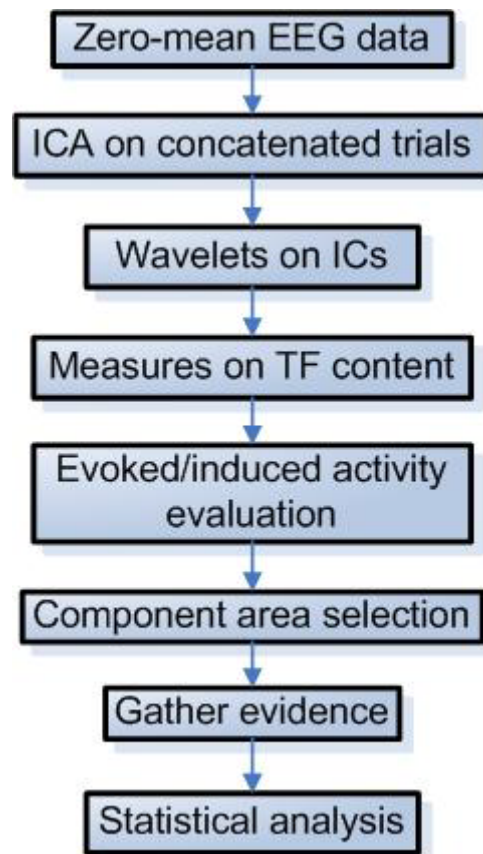
Figure 4.3: An outline of the process.

4.5. Results

4.5.1. Activity Evaluation via Synchronization Measures

At this point it should be mentioned that there is still going on a debate about the underlying mechanisms causing the ERP. Two are the main alternatives proposed. In the first alternative it is assumed that stimulation induces a partial phase resetting of ongoing EEG rhythms in each trial, and averaging these phase-coherent rhythms produces the ERP [47], [69]. The additive ERP alternative view suggests that stimulation elicits a neural population response with fixed polarity and latency in each trial which is additive to and independent from ongoing activity and that averaging these evoked responses produces the ERP [28],[69]. In former studies [47], [70] it has been stated that a pure phase-reset of ongoing activity would be indicated by changes in evoked activity and phase locked activity without a change in signal power in single trials. This is not true though because of the background oscillations which exhibit modulations of amplitude to a stimulus at the same time [69].

In our analysis we consider three scenarios in the phase locked case, the phase resetting, the partial phase resetting and the additive activity. We consider both phase resetting and partial phase resetting assuming the cases that the majority of the trials get the phase resetting effect or just a minority of them accordingly. In the phase resetting case, we have the alternative of power increase or no power increase and in the additive activity we expect a power increase due to the fact that a new activity is added to the existent one. In the partial phase resetting it is more likely that we will not have any power increase due to the fact that the activity concerns a few trials. In all those case we basically expect the phase locking measures to detect the activity. Nevertheless in the case where a power increase accompanies the phase locked activity, ERD/ERS (a classical measure used for the non phase locked activity evaluation) is expected to detect it.

On the other hand, induced activity is a measure of oscillatory power in single trials which captures signals that are not phase-locked to stimulus onset. We make three possible assumptions for the generation of the induced activity, oscillations causing power increase, power decrease or additive activity to the existing oscillations. The measures revealing non phase locked activity are ERD/ERS and PsIC which in combination help us make a clearer interpretation of the results. There follows a figure summing up the ERP activations with all the possible scenarios we assumed for the phase locked and non phase locked case and also the most significant measures expected to reveal the activity per case.
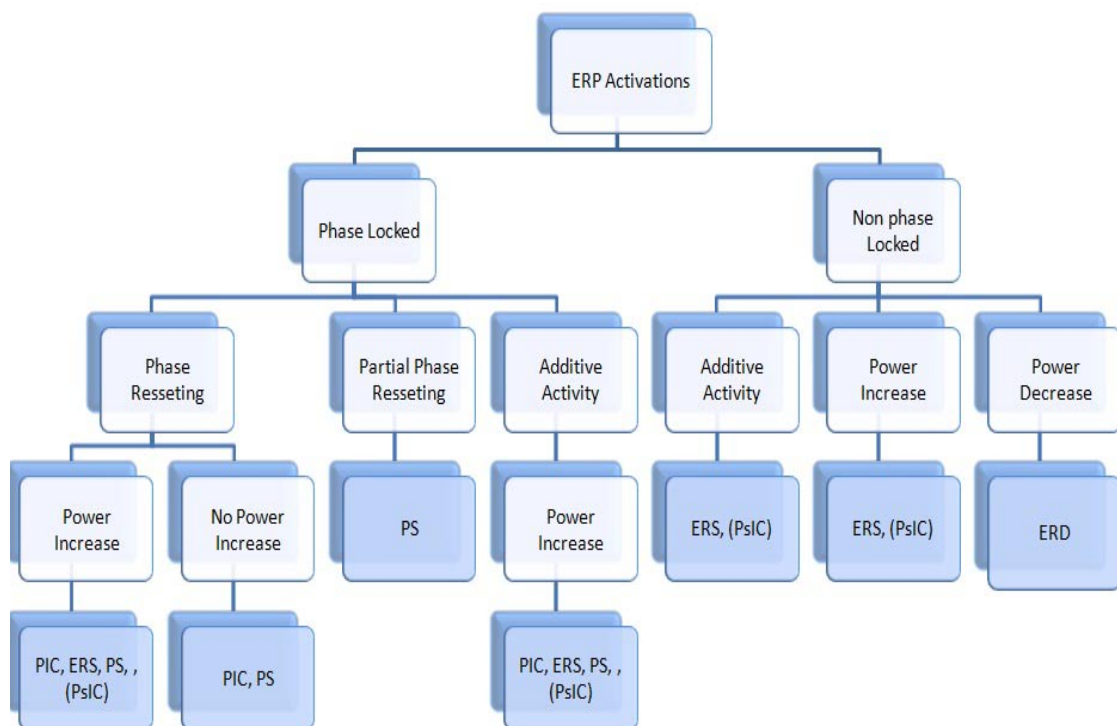

Figure 4.4: The ERP activations scenarios and the measures expected to point them out.

Taking these into consideration, we randomly picked three control subjects in order to see what kind of activation (evoked/induced) the specific memory experiment brings out and how we can use the measures in order try to decode it. In the figure below there are presented the tabulated results showing the different phase locked activity scenarios detected in those subjects using the four measures we previously described (SE, PIC, PsIC and ERD/ERS).

In the first component picked, we observe that we have a phase locked delta in ~100-400ms indicated by both SE and PIC. In the case of this component we seem to have power increase clearly implied by the ERD/ERS measure. Also in the PsIC there seems to be power synchronization in the region of the activity described greater than the prestimulus power activity. In this case we could either assume that this phase locked activity is due to phase resetting or due to an additive activity. We chose the phase resetting scenario taking into consideration the long duration of the activity implied by all measures. The thought behind this assumption is that an additive activity provoked by the event (stimulus) would stop some ms after the event stopped in contrast to a phase resetting of an existent activity which could remain longer in the new phase state. The particular component could also be discussed on its secondary activity marked by an orange arrow. We characterize it as alpha induced activity in ~50-100ms with power increase mostly brought out by ERD/ERS, implied by PsIC's greater power synchronization in the area having a small phase locked part shown not very loudly by the two phase locked measures (SE and PIC).

The second selected component shows a phase locked theta activity concerning the 50-150ms region with no power increase (ERD/ERS does not show power increase evidence in the area). This could be characterized as pure phase-reset according to [70],[47]. This component also has a secondary activity pointed by an orange arrow showing theta desynchronization in the ERD/ERS measure in the ~400-700ms region. The third and fourth components are both examples of partial phase resetting. In both the third and fourth component there is pronounced phase locked delta activity shown by SE measure and very less (~0.3) in PIC measure. This implies that just a few trials are phase locked (due to the PIC results). The difference in those two components is that for IC #3 we do not have any evidence for non phase locked activity in the specific area (ERD/ERS and PIC measure) in contrast to IC #4 which seems to have a pronounce non phase locked activity in the specific area brought out clearly by both non phase locked measures (ERD/ERS and PsIC). Both these ICs also have secondary phase locked activity in theta in ~50-100ms which in the case of IC #3 has no power increase in contrast to IC #4 which also shows a power increase.

The last component we picked has phase locked theta in ~50-150ms with power increase and it is clearly seen in all the measures. We characterize it as additive phase locked activity because of its relatively small duration, knowing that such a characterization might need deeper skepticism. In this component there is also

another non phase locked activity in ~100ms basically expressed from the ERD/ERS measure and less from the PsIC measure.

#IC	SE	PIC	PsIC	ERD/ERS

Phase Locked Activity

Phase Resetting→ Power Increase → SE, PIC, PsIC, ERS
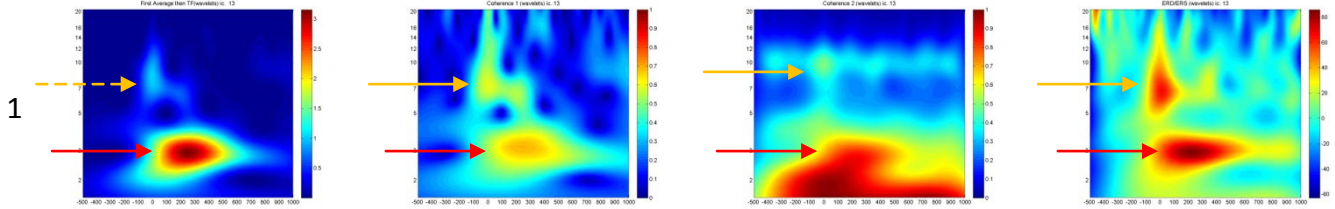
Phase Resetting→ No Power Increase→ SE, PIC
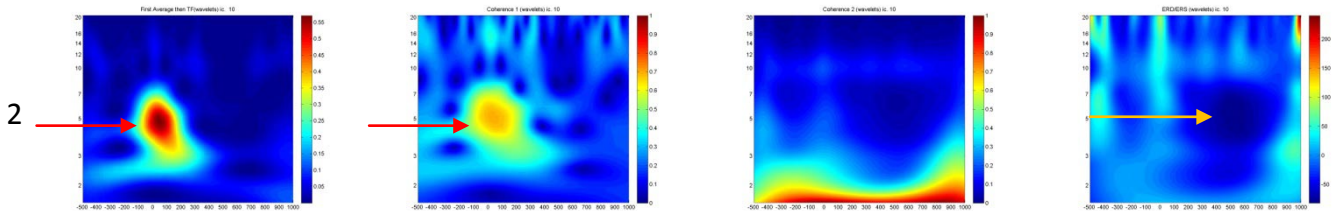
Partial Phase Resetting→ SE
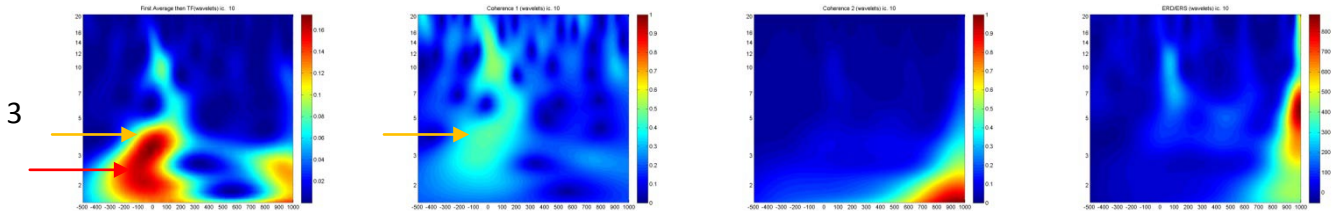
Partial Phase Resetting→ SE, PsIC
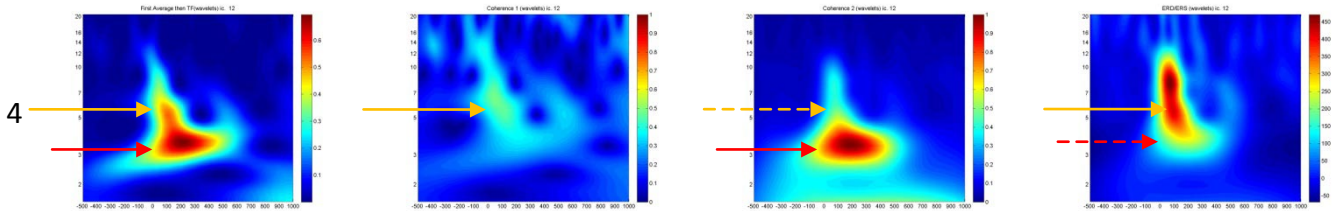
Additive → power increase→ SE, PIC, ERS, PsIC
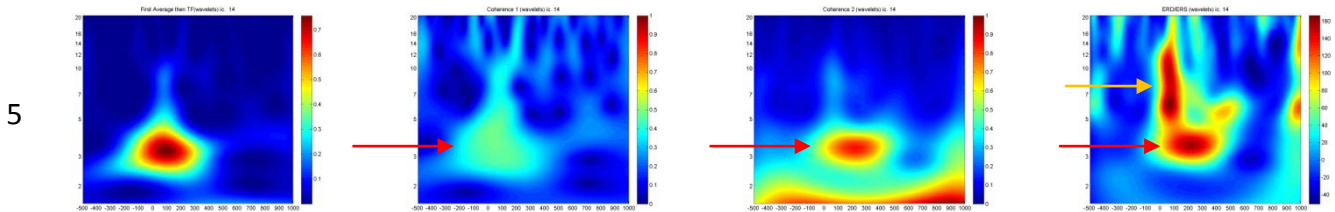
Figure 4.5: Selected ICs from 3 random control subjects to evaluate phase locked activity. The activity described above each component group is pointed by a red arrow. Possible other activities in parallel to the described one are pointed by an orange arrow.

Non-Phase Locked Activity

#IC	SE	PIC	PsIC	ERD/ERS

Additive→ PsIC, ERS

1

Power Increase→ ERS

2

Power Increase→ ERS, PsIC

3

Power Decrease→ ERD

4
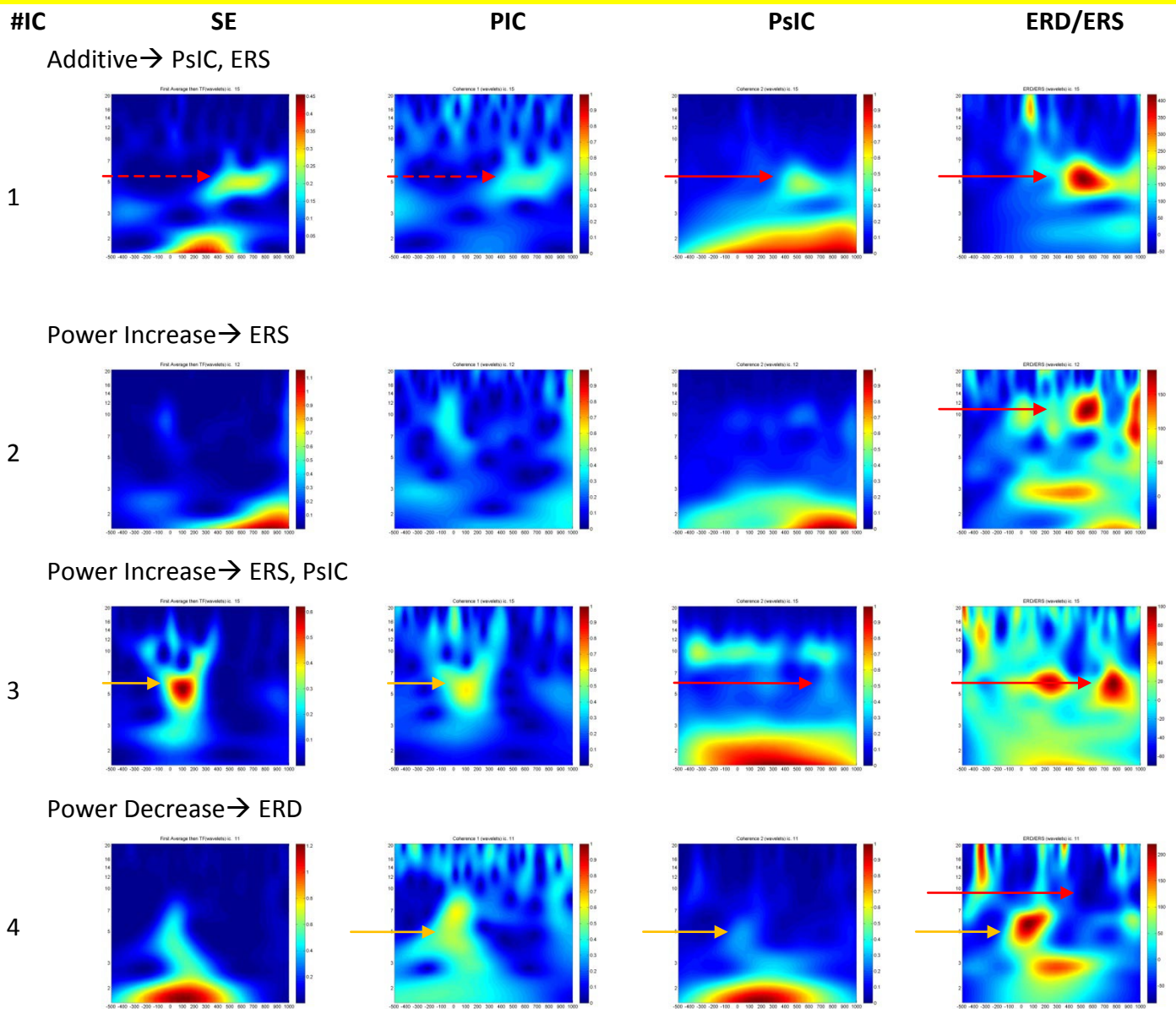
Figure 4.6: Selected ICs from 3 random control subjects to evaluate non phase locked activity. The activity described above each component group is pointed by a red arrow. Possible other activities in parallel to the described one are pointed by an orange arrow.

In the figure above there are exposed the component selections we made in order to evaluate the non phase locked activity brought out by this experiment. The first IC picked we have non phase locked theta in the ~400-700ms clearly shown by both ERD/ERS and PsIC. Some of this activity is also observed in the SE and PIC measure but it is not as strong so we could say that maybe a few trials are phase locked (partial phase locking). We characterize this activity as additive non phase locked activity considering its relatively small duration.

Both the second and third component show non phase locked activity resulting in power increase. The second one has non phase locked upper alpha in mainly ~500-700ms (it starts though less intense just after the stimulus onset and peaks in

~600ms) mostly shown by ERD/ERS and less by PsIC. This activity seems to be pure non phase locked as we do not see any interesting activity by the phase locked measures. The third IC has non phase locked theta staring from ~100-200ms as phase locked (SE and PIC) and evolving as non phase locked in ~700-900ms (no SE or PIC).

The last component we choose has non phase locked activity in ~500-800ms in alpha shown very clearly by the ERD/ERS measure. This could be considered a very interesting component as it also has ~0-100ms phase locked theta (SE, PIC) with power increase (ERS). This is a typical example of activity in a working memory experiment.

4.5.2. Population Evidence

Taking into consideration the activity evaluation of selected components we presented in the previous section, gathered evidence the populations of controls and dyslexics in the P50, N100, P300 and P600 region in delta, theta, low and high alpha and also overall alpha. Based on these and [11], evidence were gathered the way or procedure briefly explains, and we investigated the percentage of appearance of 'main activity' for the different ERP component regions, frequency bands and measures for both the population of controls and dyslexics. The results are demonstrated in Table 4.1. Most of the subjects' activity, both for the controls and the dyslexics, is gathered in the measures showing phase locked activity (SE and PIC). It should be mentioned that the phase locked activity mostly concerns delta and theta band. There is also some low alpha mainly in the PIC measure. The percentages for the two populations are relevant, with the controls percentages being higher in most of the cases. The non phase-locked measures are generally more interesting for alpha or maybe theta. In overall alpha there seem to be a few components of activity mainly for the control population and mostly by the PsIC measure. In theta there are also some non phase-locked components revealed by the two measures (PsIC and ERS). In both non phase locked measures controls outreach dyslexics by having a greater percentage of non phase locked activity. It is remarkable that there is a ~20% of controls having non phase locked activity in alpha (PsIC measure) for the N100 ERP component in contrast to the dyslexics whose percentage is zero in the corresponding case. Also, in theta controls have ~30% more P50 ERP components than dyslexics in the SE measure. In the only case dyslexic outreach dyslexics by ~20% is theta P50 ERP component.

	Controls%				Dyslexics%			
				Delta				
	P50	**N100**	**P300**	**P600**	**P50**	**N100**	**P300**	**P600**
SE	37	68	58	58	32	53	42	42
PIC	26	26	42	42	18	47	47	34
PsIC	Ni	Ni	Ni	Ni	Ni	Ni	Ni	Ni
ERS	Ni	Ni	Ni	Ni	Ni	Ni	Ni	Ni
				Theta				
	P50	**N100**	**P300**	**P600**	**P50**	**N100**	**P300**	**P600**
SE	58	74	42	16	29	71	37	13
PIC	84	89	95	63	74	89	87	68
PsIC	11	11	16	5	0	8	11	5
ERS	32	53	32	26	13	47	29	13
				Alpha1				
	P50	**N100**	**P300**	**P600**	**P50**	**N100**	**P300**	**P600**
SE	11	0	5	0	3	3	3	8
PIC	37	26	26	21	24	18	21	13
PsIC	5	11	11	11	3	0	8	11
ERS	11	0	5	0	3	5	3	3
				Alpha2				
	P50	**N100**	**P300**	**P600**	**P50**	**N100**	**P300**	**P600**
SE	0	0	5	11	3	3	0	3
PIC	11	5	0	26	21	18	11	13
PsIC	0	11	5	11	0	0	0	11
ERS	5	5	0	11	0	0	3	5
				Alpha				
	P50	**N100**	**P300**	**P600**	**P50**	**N100**	**P300**	**P600**
SE	11	0	11	11	5	5	3	11
PIC	42	32	26	42	39	32	32	24
PsIC	5	21	16	21	3	0	8	18
ERS	16	5	5	11	3	5	5	8

Table 4.1: The percentage of appearance for the specified activity. The results in red concern cases found to be significant in Table 4.2 and results in purple to percentage differences between the two groups greater than 20%. Ni refers to not interested.

4.5.3. Significance Test

In Table 4.2 we have the tabulated results found to be significant via Kruskal-Wallis significance test. The first letter of the table results corresponds to the frequency band (D for delta, T for theta, A1 for low alpha, A2 for high alpha) and the second letter corresponds to the characteristic (t for time, f for frequency and a for amplitude). The arrows ($\uparrow$ and $\downarrow$) correspond to an increase or a decrease for the corresponding value of the controls compared to this of the dyslexics. For example TT$\downarrow$ corresponds to a prolonged latency in time for the dyslexics compared to the controls (the time instant of the controls is previous to that of the dyslexics).

Controls-Dyslexics				
Measure	**ERP Region**			
	P50	**N100**	**P300**	**P600**
SE	-	Tt$\downarrow$	Df$\downarrow$	Df$\downarrow$
PIC	-	Tt$\downarrow$,A1a$\uparrow$	Df$\downarrow$	Df$\downarrow$
PsIC	-	-	-	-
ERS	-	-	-	-

Table 4.2: The tabulated statistically significant results. The arrows denote an increase ($\uparrow$) or decrease ($\downarrow$) of the corresponding value for the controls compared to the dyslexics.

There were differences found between the controls and dyslexics mainly for the N100 component for the mean latency values and the amplitudes. More specifically, the dyslexics had a significantly prolonged latency in theta for both ERP SE and PIC measure. There was also significantly reduced amplitude for the dyslexics in low alpha for the PIC measure. For the P300 and P600 ERP components, delta was significantly lower in both ERP SE and PIC measure. From the results in Table 4.2 it is obvious that there is not found any significant activity for the P50 component and the non-phase locked measures. From the fact that we did not have significant results for the two non phase-locked measures (PsIC and ERS) we assume that they may are not the most appropriate measures for our data as they were for other datasets such as [24]. Thus, the differences of our population are not detected in the non phase-locked activity, but they are detected in the phase locked activity.

4.6.Discussion

The purpose of this analysis was the evaluation of the differences between the population of controls and dyslexics using measures of phase locked (SE and PIC) and non phase-locked (PsIC and ERS) activity. In order for the evaluation to be achieved a statistical framework was introduced. The analysis took place using the ICs instead of the original channels so as to achieve proper decomposition of the data as well as characterization of the overall channels' activity (instead of channel-by-channel activity). The measures were applied on the TF content of the ICs from which there was then made an analysis concerning what kind of activity we are given by this memory experiment based on selected components of three random control subjects. Then, in means of percentage we examined what kind of activation the control and dyslexic populations have in the different measures for the different frequency bands and ERP components based on the collection of evidence (main activity) from all the subjects. The gathered evidence where then used in the statistical analysis concerning time, frequency and amplitude features. The statistical analysis took into consideration the different ERP components and frequency bands.

In this analysis we tried to decode the activation of the independent components using measures of synchronicity for phase locked and non phase locked activity. Doing this we found phase locked activity mainly in theta in the ~100ms region and non phase locked activity both in theta (mainly late theta ~700ms) and alpha (mainly late alpha ~600ms both ERS and ERD cases). There was also recognized in those components the very interesting case of ERS in theta followed by alpha ERD, met in the majority of working memory experiments like this one. Examining the different scenarios of ERP activation concerning different expressions of phase locked and non phase locked activity, we can say we distinguished representatives of every possible scenario. It has to be noted here that further research has to be made in order to make safe conclusions for the origination of an activity.

Furthermore, by the quantification of the evidence we gathered from the two populations, we showed that both groups mainly had phase locked activity and just a few had non phase locked activity. Generally the controls had a greater contribution in both phase locked and non phase locked activity in most of the cases. More specifically, for the PsIC measure we had ~20% of the controls having non phase-locked alpha in the N100 ERP component in contrast to the dyslexics who did not have any non phase-locked alpha in the N100 ERP component. Also, for the SE measure we had ~60% of the controls having phase locked theta in contrast to ~30% of dyslexics having phase locked theta in the P50 ERP component. The only case dyslexics outreached controls by a great percentage is for the SE in delta where ~50% of them had phase locked (via SE) N100 ERP components in contrast to ~25% of controls.

Our analysis showed that the dyslexic group demonstrated significantly prolonged latency in theta for both phase-locking measures and reduced amplitudes in low alpha for PIC of the N100 ERP component. Our results are in accordance with relevant studies on dyslexic populations such as [57], [58], [59] and [61] which also noticed the prolonged latency and reduced amplitude of dyslexics compared to controls for the N100 ERP component. In particular, studies on the specific dataset using channel TF maps showed reduced mean peaks of the N100 ERP components in the 5-20Hz range for the majority of the channels [11]. Also, other studies on this dataset in time, also found significantly reduced amplitudes for dyslexics in N100 ERP component [62]. The reduced amplitude and prolonged latency of N100 ERP component has been connected with impairments in 'attentional operation' of information processing in such cases [62]. In addition to this, we found that the frequency ticks in delta were significantly higher in the dyslexic group compared to the controls for both phase-locking measures in the latter ERP components (P300 and P600).

5. Conclusions

5.1.Work Review & Conclusions

In this study two individual datasets consisting of ongoing and evoked responses accordingly were analyzed and evaluated using well known EEG analysis tools and distinct methodological patterns.

The main goal in the first dataset was to compare the different mathematical thinking tasks by means of power and coherence. In this context, the measures of power spectrum (PS) and magnitude squared coherence (MSC) were applied on the EEG electrodes of this dataset. The PS was estimated for each electrode and presented using a topographic mapping and the MSC was estimated for the neighbor channel pairs of selected topographic regions. The selected topographic regions were finally the ones used for the evaluation of the differences between the tasks using Kruskal-Wallis statistical significance test.

The key findings of this dataset considered significant differences for both power and coherence measures in specific frequency bands and topographic regions matching in support and additional to previous research in this area. There were also indications of correlation between the power and coherence results. More specifically, the findings show, (a) reduced power in the alpha (mostly) and beta band for the mathematical thinking tasks compared to the control task (b) power increase of delta in the frontal regions for the task of comparison (c) larger power decrease in alpha along with a larger increase in delta for the compare task in contrast to the addition task. We also noticed that (d) the power decrease often reflected a coherence decrease and (e) power and coherence for the two mathematical tasks had relevant behavior compared to the control task.

The second dataset consists of ERPs from a working memory experiment for a group of controls and dyslexics. The concept in this case was the application of synchronization measures on the TF maps of the ICs of the EEG signals in order to evaluate the activation evoked by the stimulus and furthermore try to find significant differences between the populations using Kruskal-Wallis statistical significance test.

An evaluation of the evolving activity was performed here, which verified the emergence of statistical significant ERP components in specific frequency bands for certain synchronization measures. In particular we had (a) phase locked activity basically in theta and delta, (b) non phase locked activity basically in theta and alpha, recognized by the analysis made on three random control subjects. Also, using the evidence we gathered in the whole of the populations we observed that (c) there was a greater percentage of phase locked components than non phase locked

components and (d) generally the activity components of the controls outreached those of the dyslexics in most of the cases. Furthermore, by the statistical analysis made on the evidence gathered for the synchronization measures we found (e) prolonged latency of the N100 ERP component in theta for SE and PIC measure and (f) reduced amplitude of N100 ERP component in low alpha for PIC measure for the dyslexics compared to the controls as well as (g) higher central frequency in delta for SE and PIC measure in the latter ERP components (P300, P600).

In both datasets we had finding which are verified by previous research and also some complementary findings. More specifically, our findings in the first dataset concerning alpha and delta for the two mathematical thinking tasks compared to the control task are verified by [3], [35], [36], [40]. On the other hand the comparison we made between the two mathematical thinking tasks and the correlation of the power and coherence results of the electrodes are tasks not quite investigated in the relevant bibliography and as such they might need further verification. On the second dataset, it is not of our greatest knowledge that a relevant methodology has not been followed for the specific working memory experiment. Previous analysis on the dataset in time [62] or time-frequency [11] on the channels though has shown relevant significant ERP components as the ones we found in our analysis. We additionally, tried to get evidence concerning the generation of the ERP components.

5.2. Future Work

In the first dataset there can also be investigated the coherence between channels of neighbor or distant lobes except from the inter-lobe coherences. Furthermore the synchronization of the channels could be further investigated using non-linear coherence measures or even graph techniques. Also the correlation of power and coherence could be 'deeper' established using more subjects for the investigation and stricter mathematical formulas. It would also be very interesting to redesign the experiment for many trials so as to combine this analysis with a corresponding ERP analysis which is the analysis followed for the second dataset.

We applied synchronization measures on the ICs of the second dataset which could be expanded by using the measures on the channels and compare the results to these of the ICs. This set of results could be combined and reviewed with the results of previous publications concerning the analysis of the specific dataset in time. Also, more effort must be devoted to the decoding of the synchronization measures, by using and examining more datasets on the measures and also trying out specially designed simulations. In addition the evidence from the measures used in the statistical analysis could be gathered in different ways, for example taking into consideration the special characteristics of the ERP activity. For further analysis we

could also use the topographic maps of the components in order to also extract head location complementary to the synchronization measures. Finally, the working memory experiment could be rerun using a variety of pathological groups for verification of abnormalities.

APPENDIX

In order to have a better picture of the EEG data behavior of the second dataset we developed a preliminary evaluation of the signals in time. From the channel ERPs of the individual subjects and from the grand average ERPs of all the subjects for both controls' and dyslexics' populations the ERP components which can be easily distinguished are P50, N100 and maybe P300. According to these observations and considering the fact that these components are also examined by relative analysis [62] we also used these component areas in our analysis. The analysis in time and the evaluation of the results has been considered in detail in [62].
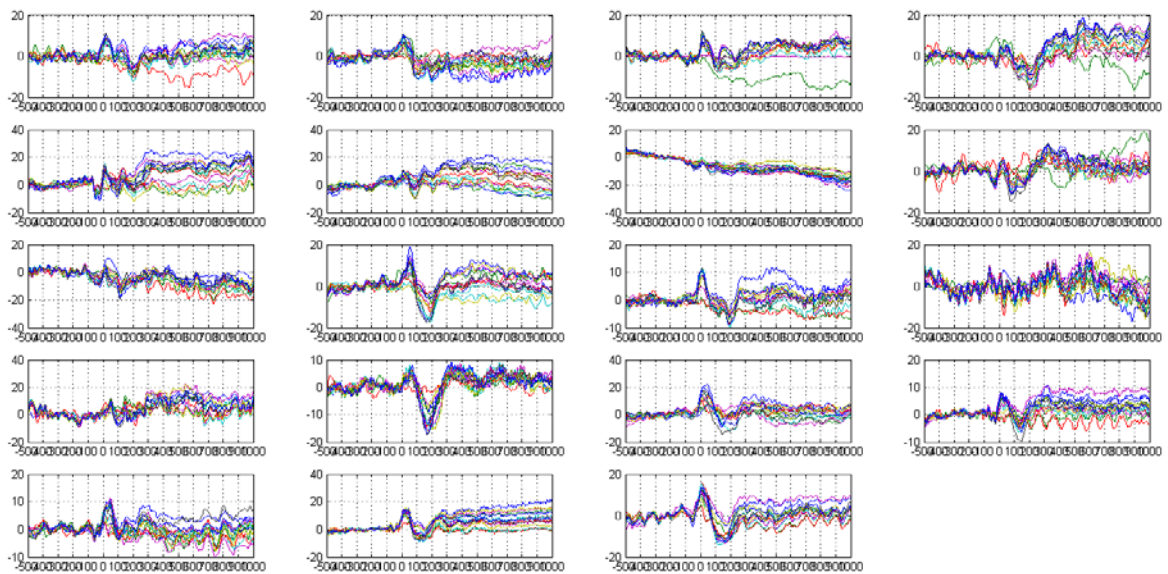
Figure 0.1: The time representation of the EEG signals of the 19 control subjects for all 15 electrodes. Each subplot represents a subject's channel content.
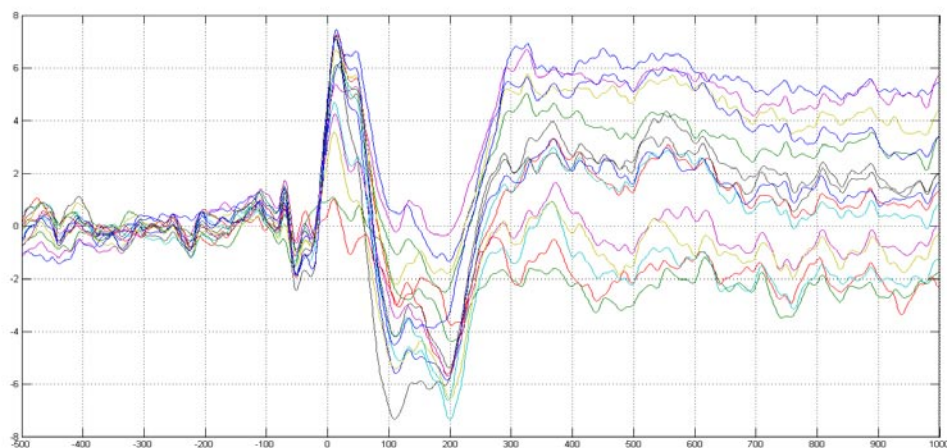
Figure 0.2: Grand average ERPs of controls for each channel.
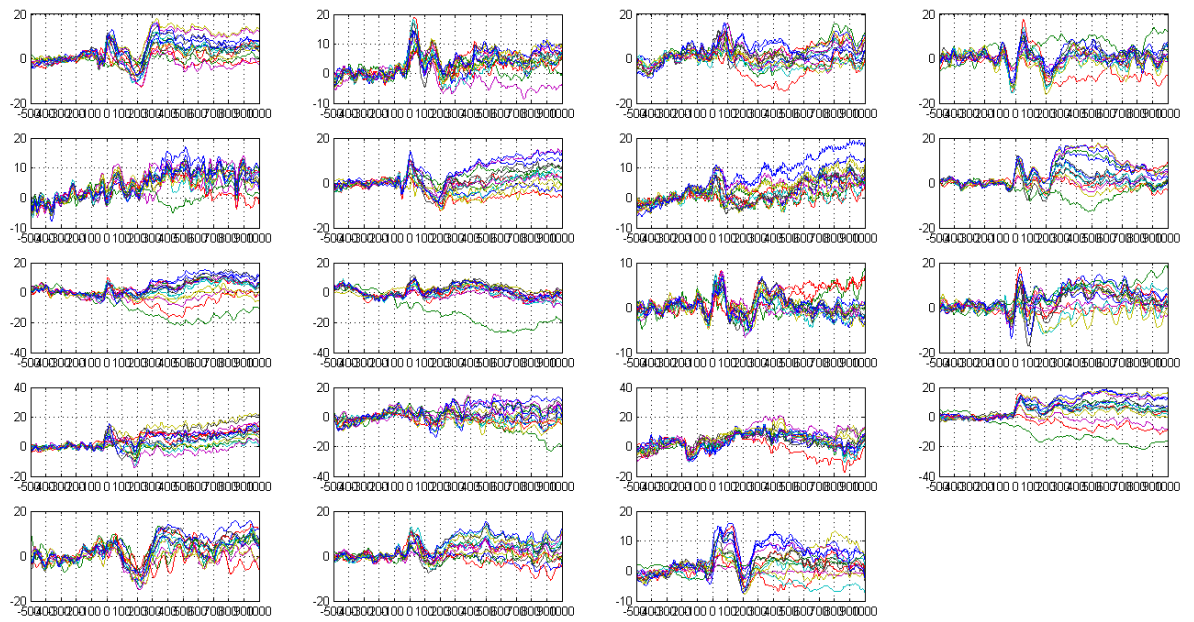
Figure 0.3: The time representation of the EEG signals of the 19 dyslexic subjects for all 15 electrodes. Each subplot represents a subject's channel content.
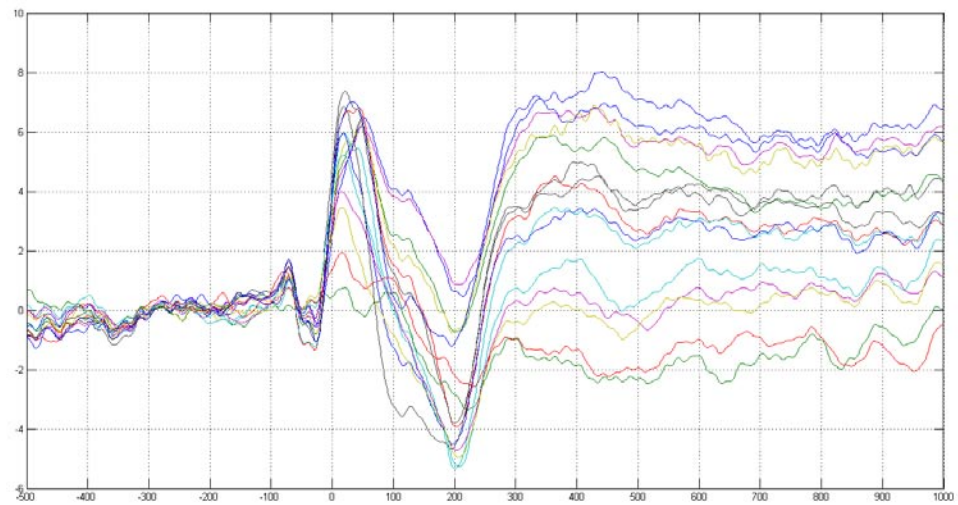
Figure 0.4: Grand average ERPs of dyslexics for each channel.

There are also included all TF maps for two selected controls and two selected dyslexics for all the synchronization measures. More specifically, we give the TF map of the phase locked measures (SE and PIC) and also the TF map of the non phase locked measures (PsIC and ERD/ERS) for all 15 ICs. Each subplot concerns a TF map of the corresponding IC for the specific measure. The order of the components is kept for all the measures concerning the specified subject.

SE
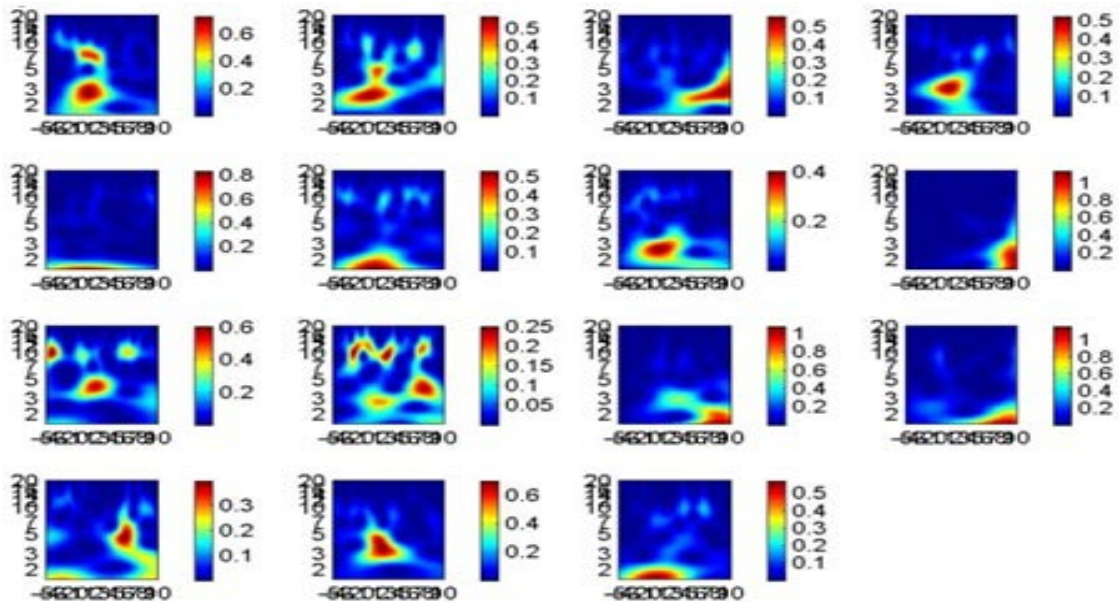
PIC
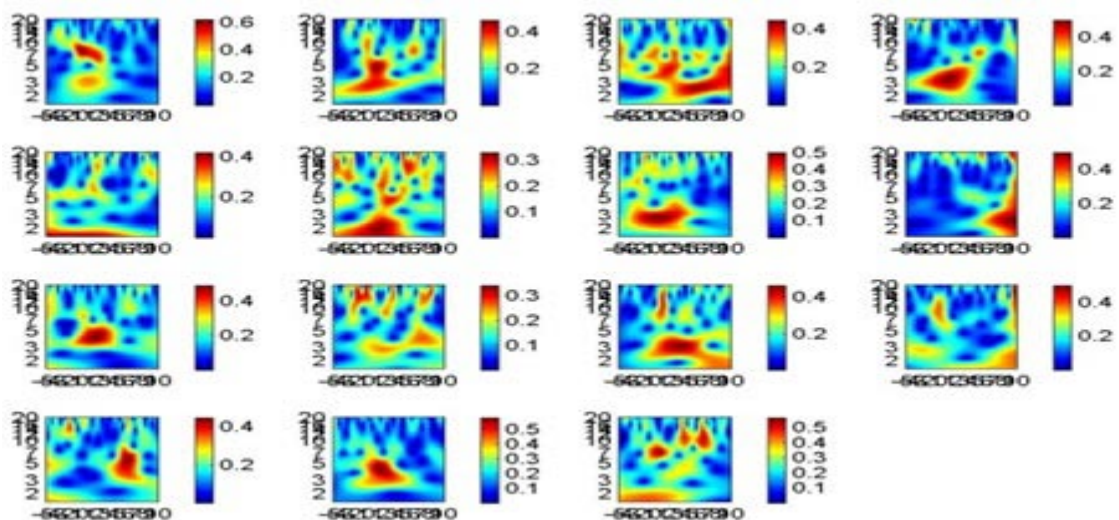
Figure 0.5: Control subject 1, phase locked measures on its 15 ICs.
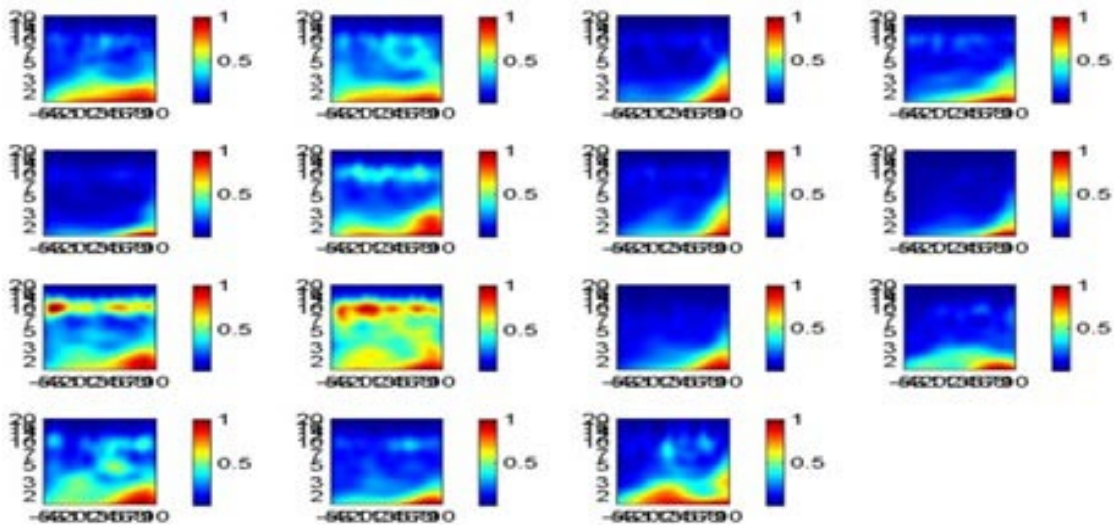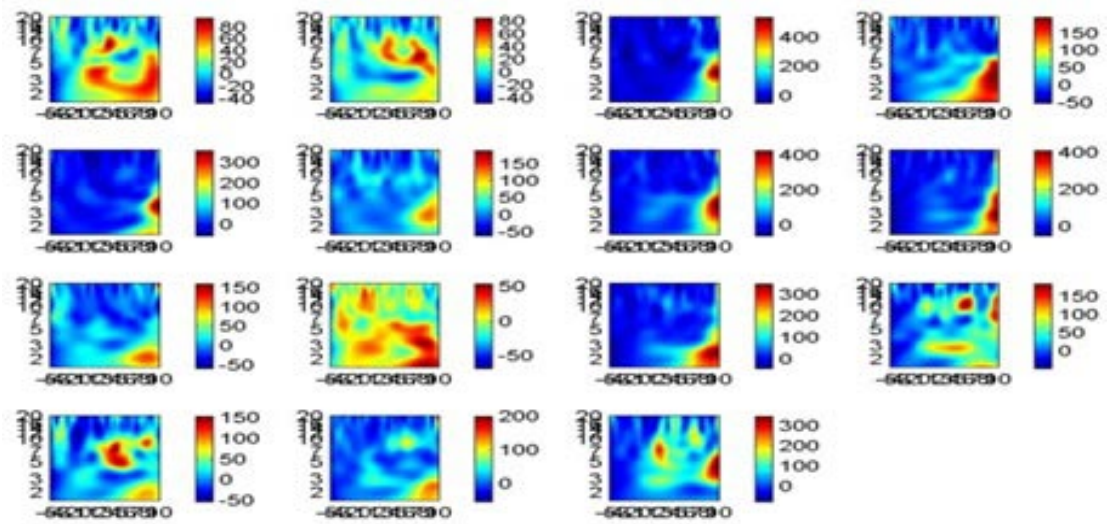
PsIC

ERD/ERS

Figure 0.6: Control subject 1, non phase locked measures on its 15 ICs.

SE
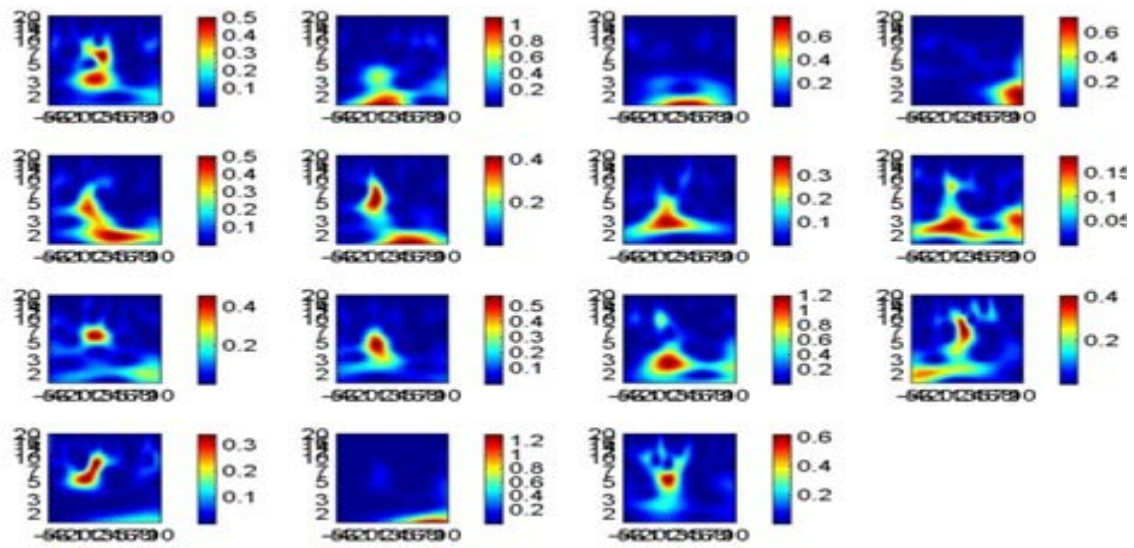
PIC
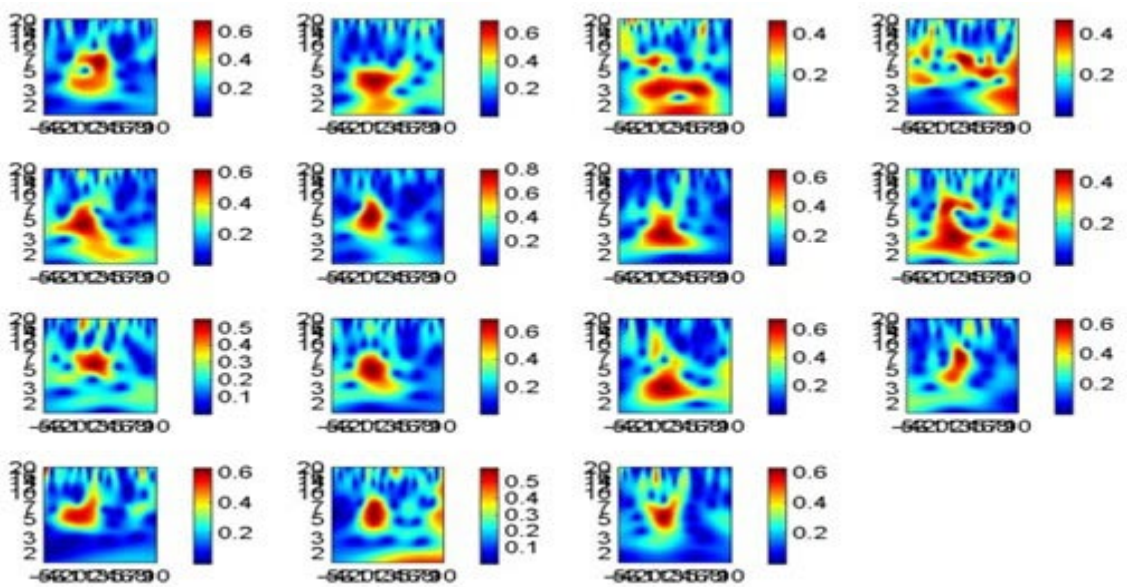
Figure 0.7: Control subject 2, phase locked measures on its 15 ICs.
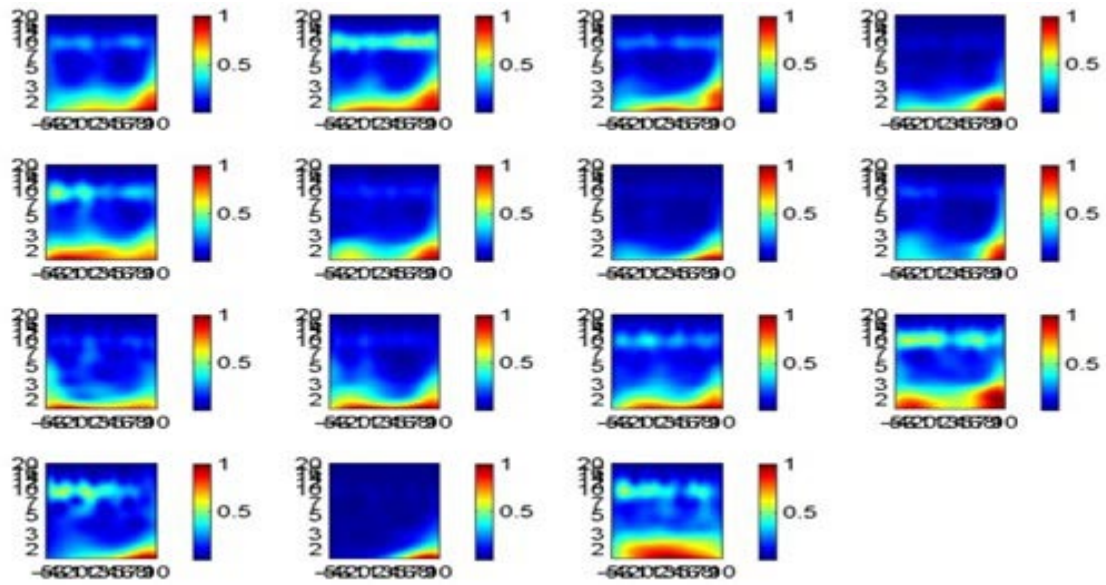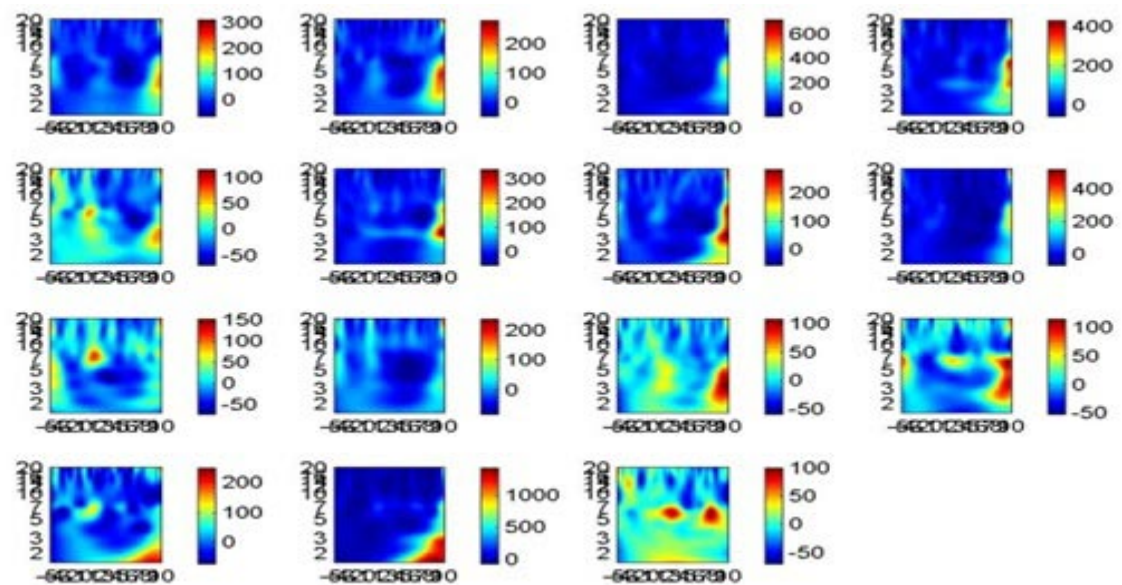
PsIC

ERD/ERS

Figure 0.8: Control subject 2, non phase locked measures on its 15 ICs.

SE
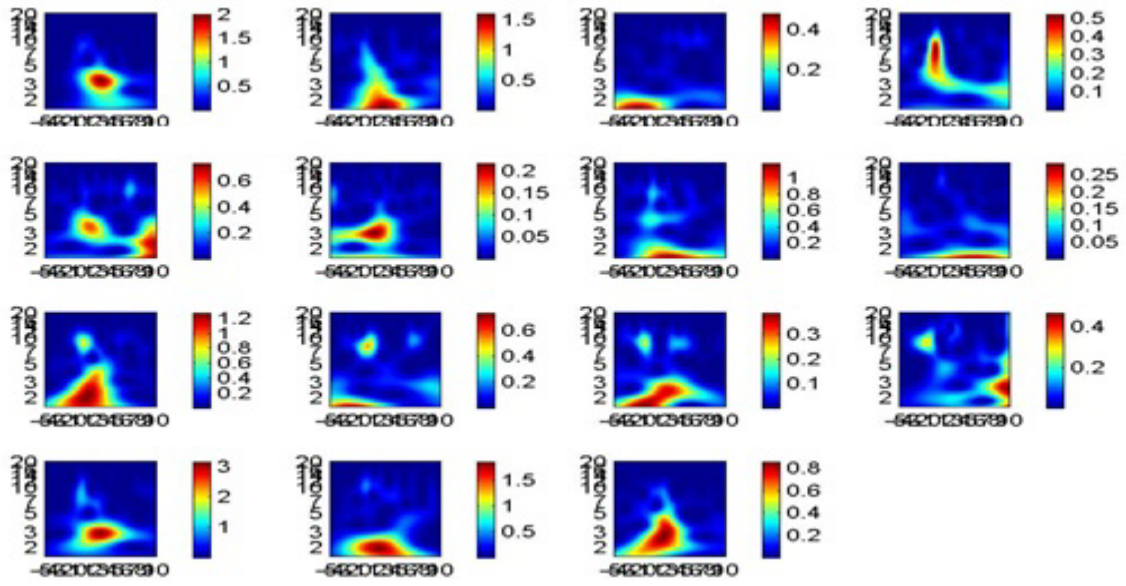
PIC
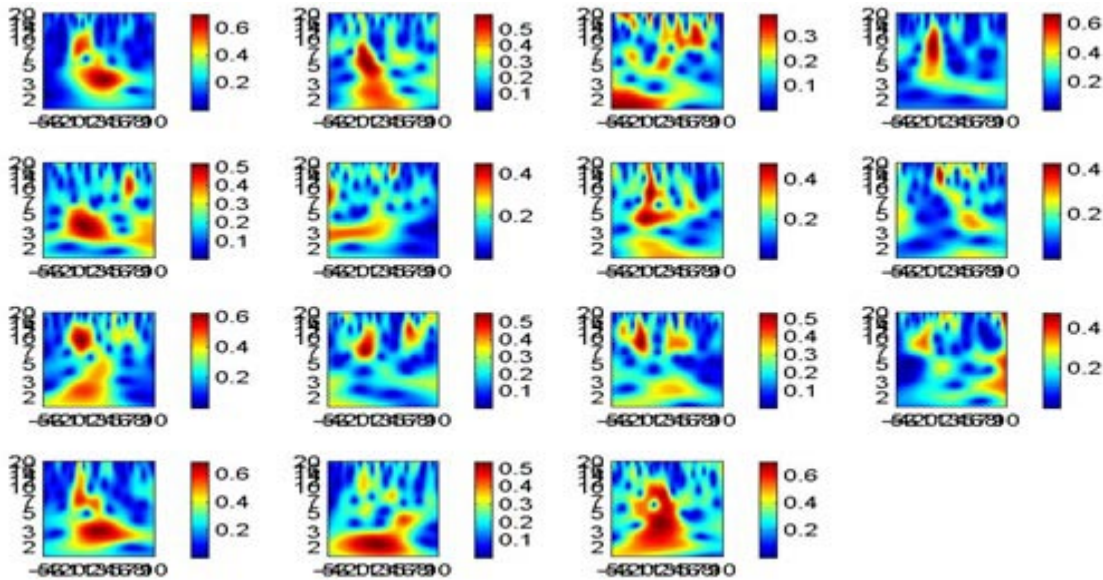
Figure 0.9: Dyslexic subject 1, phase locked measures on its 15 ICs.
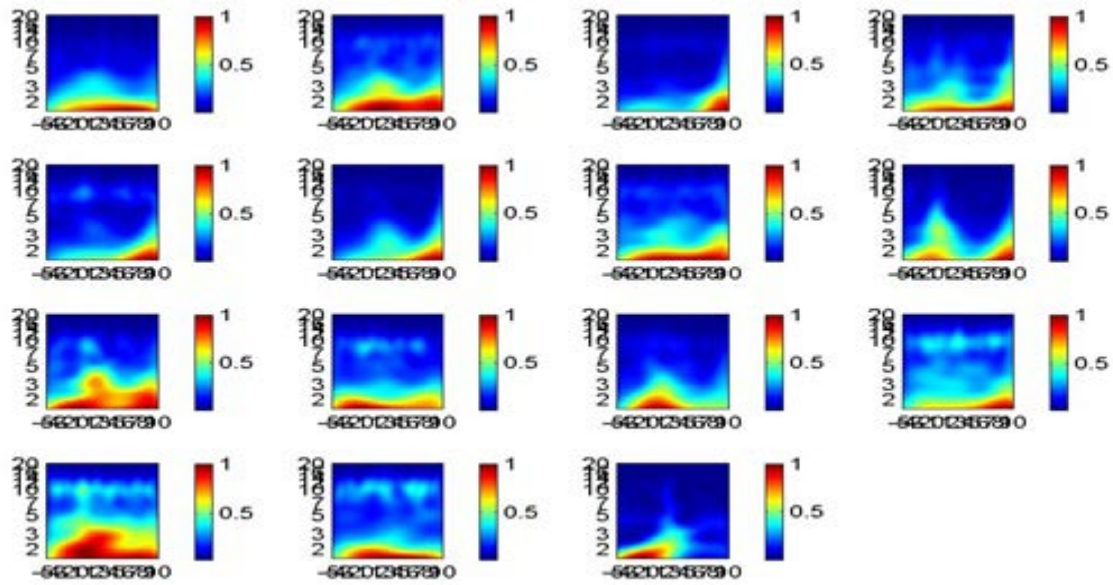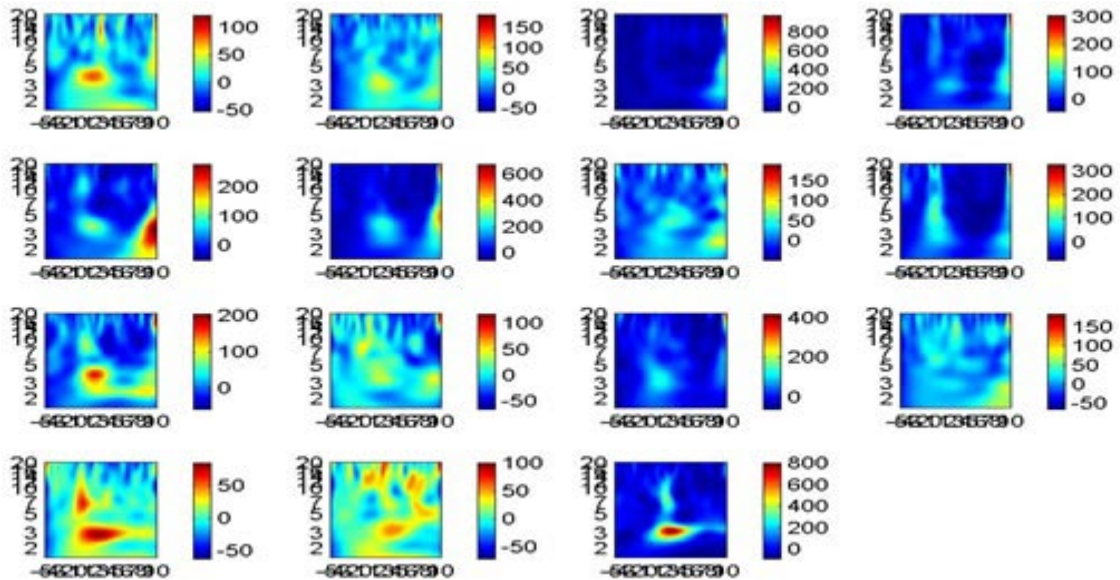
PsIC

ERD/ERS

Figure 0.10: Dyslexic subject 1, non phase locked measures on its 15 ICs.

SE
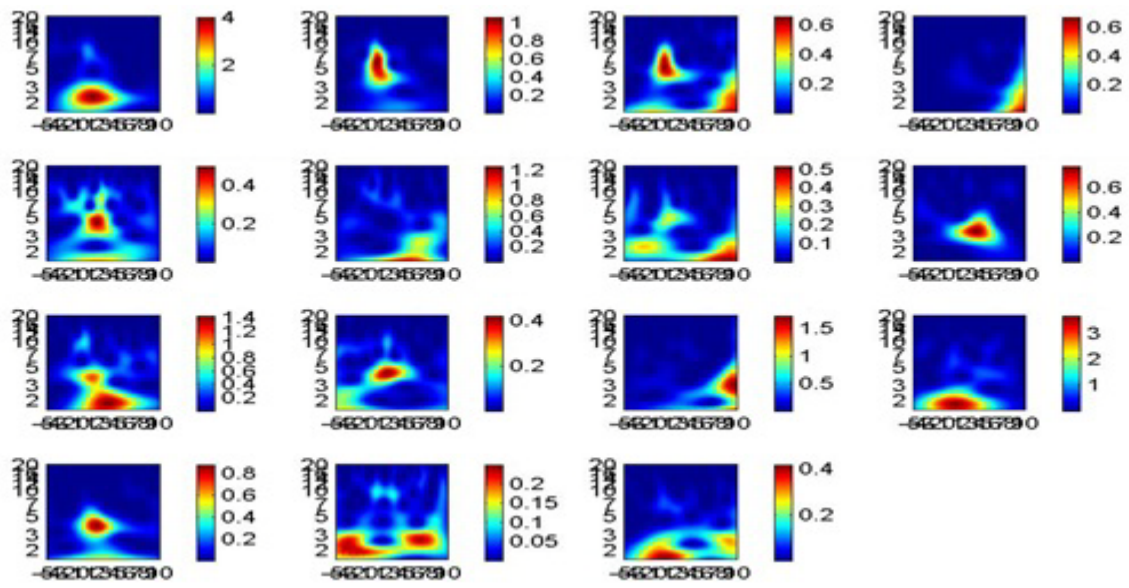
PIC
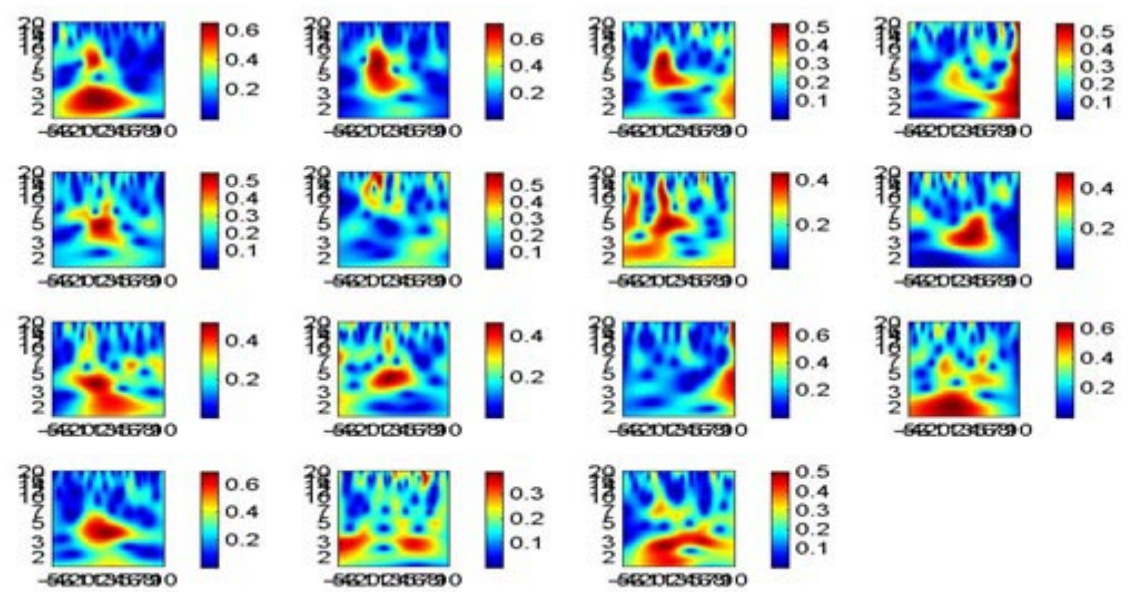
Figure 0.11: Dyslexic subject 2, phase locked measures on its 15 ICs.

**PsIC**
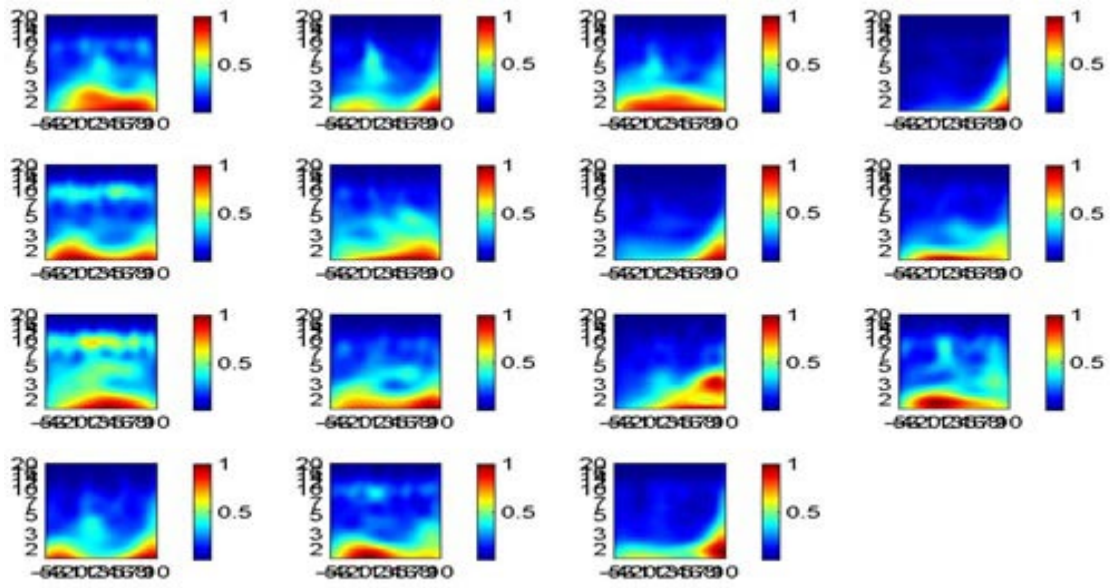
ERD/ERS
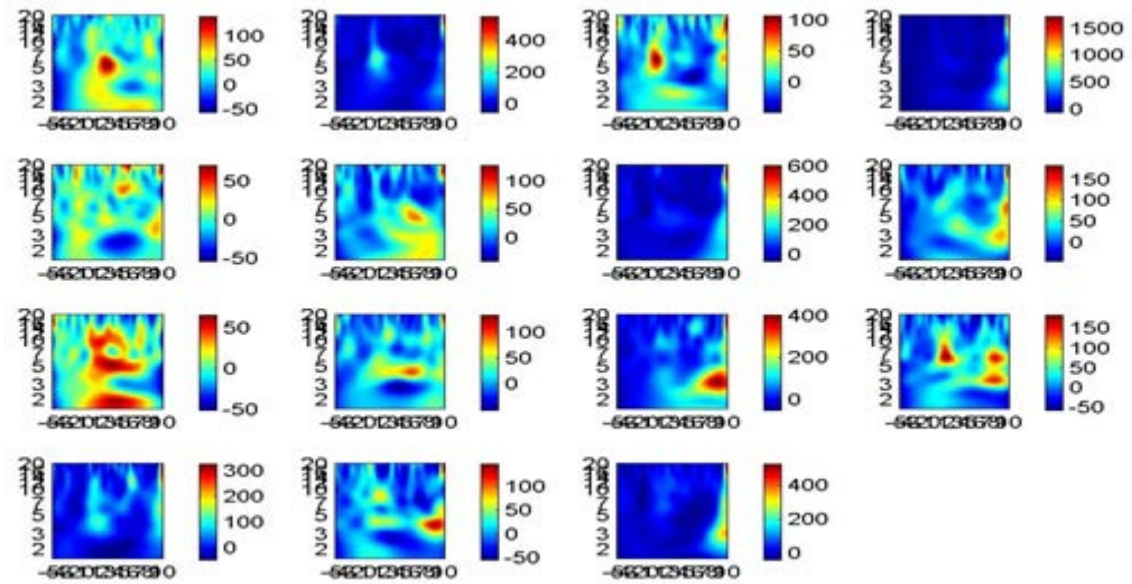
Figure 0.12: Dyslexic subject 2, non phase locked measures on its 15 ICs.

REFERENCES

[1]   J. Cacioppo, L. Tassinary, and G. Berntson, *The Handbook of Phychophysiology*, Third. Cambridge University Press, 2007.

[2]   R. B. Reilly and T. C. Lee, "Electrograms (ECG, EEG, EMG, EOG).," *Technology and health care : official journal of the European Society for Engineering and Medicine*, vol. 18, no. 6, pp. 443-58, Jan. 2010.

[3]   W. Klimesch, "EEG alpha and theta oscillations reflect cognitive and memory performance: a review and analysis.," *Brain research. Brain research reviews*, vol. 29, no. 2-3, pp. 169-95, Apr. 1999.

[4]   E. Başar, C. Başar-Eroglu, S. Karakaş, and M. Schürmann, "Gamma, alpha, delta, and theta oscillations govern cognitive processes.," *International journal of psychophysiology : official journal of the International Organization of Psychophysiology*, vol. 39, no. 2-3, pp. 241-8, Jan. 2001.

[5]   A. K. Engel and P. Fries, "Beta-band oscillations--signalling the status quo?," *Current opinion in neurobiology*, vol. 20, no. 2, pp. 156-65, Apr. 2010.

[6]   S. P. Fitzgibbon, K. J. Pope, L. Mackenzie, C. R. Clark, and J. O. Willoughby, "Cognitive tasks augment gamma EEG power.," *Clinical neurophysiology : official journal of the International Federation of Clinical Neurophysiology*, vol. 115, no. 8, pp. 1802-9, Aug. 2004.

[7]   C. Tallon-Baudry and O. Bertrand, "Oscillatory gamma activity in humans and its role in object representation.," *Trends in cognitive sciences*, vol. 3, no. 4, pp. 151-162, Apr. 1999.

[8]   S. Luck, G. Woodman, and E. Vogel, "Event-related potential studies of attention.," *Trends in cognitive sciences*, vol. 4, no. 11, pp. 432-440, Nov. 2000.

[9]   S. Makeig, A. Bell, T. P. Jung, and T. J. Sejnowski, "Independent Component Analysis of Electroencephalographic Data," *Advances in Neural Information Processing*, vol. 8, pp. 145-151, 1996.

[10]   G. A. Giannakakis, N. N. Tsiaparas, M.-filitsa S. Xenikou, C. Papageorgiou, and K. S. Nikita, "Wavelet entropy differentiations of event related potentials in dyslexia," in *8th IEEE International Conference on Bioinformatics and Bioengineering*, 2008.

[11]   G. A. Giannakakis, M. Vavatsioula, C. Papageorgiou, and K. S. Nikita, "DYSLEXIA USING MATCHING PURSUIT ALGORITHM," in *6th European Symposium on Biomedical Engineering*, 2008.

[12] K. Blinowska and P. Durka, "Electroencephalography (EEG)," in *Wiley Encyclopedia of Biomedical Engineering*, vol. 47, no. 3, .

[13] A. L. Ronald and D. W. Mills, *SIGNAL ANALYSIS TIME, FREQUENCY, SCALE AND STRUCTURE*. 2004.

[14] F. J. Theis and A. Meyer-Base, *Biomedical Signal Analysis CONTEMPORARY METHODS AND APPLICATIONS*. 2010.

[15] S. Qian and D. Chen, "Understanding the nature of signals whose power spectra change with time," *IEEE Signal Processing Magazine*, pp. 53-67, 1999.

[16] S. Mallat, *A Wavelet Tour of Signal Processing*. 2009.

[17] V. D. Calhoun, J. Liu, and T. Adali, "A review of group ICA for fMRI data and ICA for joint inference of imaging, genetic, and ERP data.," *NeuroImage*, vol. 45, no. 1, pp. S163-72, Mar. 2009.

[18] J. V. Stone, *Independent Component Analysis. A Tutorial Introduction*. 2004.

[19] A. Delorme and S. Makeig, "EEGLAB: an open source toolbox for analysis of single-trial EEG dynamics including independent component analysis.," *Journal of neuroscience methods*, vol. 134, no. 1, pp. 9-21, Mar. 2004.

[20] J. Kropotov, *Quantitive EEG, Event-Related Potentials and Neurotherapy*, vol. 1, no. 11. Wiley Online Library, 2009, pp. 1829–1841.

[21] H. J. Heinze, T. F. Münte, and G. R. Mangun, *Cognitive Electrophysiology*. 1994.

[22] C. Tallon-Baudry, O. Bertrand, C. Delpuech, and J. Pernier, "Stimulus specificity of phase-locked and non-phase-locked 40 Hz visual responses in human.," *The Journal of neuroscience : the official journal of the Society for Neuroscience*, vol. 16, no. 13, pp. 4240-9, Jul. 1996.

[23] P. J. Yordanova J, Kolev V, "P300 and alpha event-related desynchronization (ERD)," *Psychophysiology*, vol. 38, pp. 143-152, 2001.

[24] M. Zervakis, K. Michalopoulos, V. Iordanidou, and V. Sakkalis, "Intertrial coherence and causal interaction among independent EEG components," *Journal of Neuroscience Methods*, vol. 197, no. 2, pp. 302-314, 2011.

[25] K. Michalopoulos, V. Sakkalis, V. Iordanidou, and M. Zervakis, "Activity Detection and Causal Interaction Analysis among Independent EEG Components from Memory Related Tasks," *Neuroscience Letters*, pp. 2070-2073, 2009.

[26] E. Martinez-Montes, E. Cuspineda-Bravo, W. El-Deredy, J. Sanchez-Bornot, A. Lage-Castellanos, and P. Valdes-Sosa, "Exploring event-related brain dynamics

with tests on complex valued time – frequency representations," *Statistics in Medicine*, no. 2007, pp. 2922-2947, 2008.

[27]   C. Torrence and G. Compo, "A practical guide to wavelet analysis," *Bull Am Meteorol Soc*, vol. 79, pp. 61-78, 1998.

[28]   G. Pfurtscheller and F. H. Lopes da Silva, "Event-related EEG/MEG synchronization and desynchronization: basic principles.," *Clinical neurophysiology : official journal of the International Federation of Clinical Neurophysiology*, vol. 110, no. 11, pp. 1842-57, Nov. 1999.

[29]   V. Rajagopalan, *Selected Statistical Tests*. 2006.

[30]   C. Reimann, P. Filzmoser, R. G. Garrett, and R. Dutter, *Statistical Data Analysis Explained*. 2008.

[31]   J. P. John et al., "Differentiate Positive and Negative Subgroups in Schizophrenia Patients," *Journal Of Neuropsychiatry*, pp. 160-172, 2009.

[32]   M. J. Hogan, G. R. J. Swanwick, J. Kaiser, and M. Rowan, "Memory-related EEG power and coherence reductions in mild Alzheimer ' s disease," *International Journal of Psychophysiology*, vol. 49, pp. 147-163, 2003.

[33]   Z.-yan Jiang, "Study on EEG power and coherence in patients with mild cognitive impairment during working memory task.," *Journal of Zhejiang University. Science. B*, vol. 6, no. 12, pp. 1213-9, Dec. 2005.

[34]   C. Guger, G. Edlinger, W. Harkam, I. Niedermayer, and G. Pfurtscheller, "How many people are able to operate an EEG-based brain-computer interface (BCI)?," *IEEE transactions on neural systems and rehabilitation engineering : a publication of the IEEE Engineering in Medicine and Biology Society*, vol. 11, no. 2, pp. 145-7, Jun. 2003.

[35]   S. Micheloyannis, V. Sakkalis, M. Vourkas, C. J. Stam, and P. G. Simos, "Neural networks involved in mathematical thinking: evidence from linear and non-linear analysis of electroencephalographic activity.," *Neuroscience letters*, vol. 373, no. 3, pp. 212-7, Jan. 2005.

[36]   T. Fernfindez et al., "EEG activation patterns during the performance of tasks involving different components of mental calculation," *Electroencephalography and Clinical Neurophysiology*, vol. 94, pp. 175-182, 1995.

[37]   V. Sakkalis, M. Zervakis, and S. Micheloyannis, "Significant EEG features involved in mathematical reasoning: evidence from wavelet analysis.," *Brain topography*, vol. 19, no. 1-2, pp. 53-60, Jan. 2006.

[38]   E. M. Whitham et al., "Thinking activates EMG in scalp electrical recordings.," *Clinical neurophysiology : official journal of the International Federation of Clinical Neurophysiology*, vol. 119, no. 5, pp. 1166-75, May 2008.

[39]   G. Fein, J. Raz, F. F. Brown, and E. L. Merrin, "Common reference coherence data are confounded by power and phase effects," *Electroencephalography and clinical Neurophysiology*, vol. 69, pp. 581 -584, 1988.

[40]   S. I. Dimitriadis, N. a Laskaris, V. Tsirka, M. Vourkas, and S. Micheloyannis, "What does delta band tell us about cognitive processes: a mental calculation study.," *Neuroscience letters*, vol. 483, no. 1, pp. 11-5, Oct. 2010.

[41]   M. Farge, "WAVELET TRANSFORMS AND THEIR APPLICATIONS TO TURBULENCE," *Annual Reviews*, vol. 24, pp. 395-457, 1992.

[42]   S. Wang and M. Tang, "Exact Confidence Interval for Magnitude-Squared Coherence Estimates," *Signal Processing*, vol. 11, no. 3, pp. 326-329, 2004.

[43]   K. Moeller, G. Wood, M. Doppelmayr, and H.-C. Nuerk, "Oscillatory EEG correlates of an implicit activation of multiplication facts in the number bisection task.," *Brain research*, vol. 1320, pp. 85-94, Mar. 2010.

[44]   a Gundel and G. F. Wilson, "Topographical changes in the ongoing EEG related to the difficulty of mental tasks.," *Brain topography*, vol. 5, no. 1, pp. 17-25, Jan. 1992.

[45]   S. Makeig, S. Debener, J. Onton, and A. Delorme, "Mining event-related brain dynamics.," *Trends in cognitive sciences*, vol. 8, no. 5, pp. 204-10, May 2004.

[46]   V. Iordanidou, K. Kanatsouli, K. Michalopoulos, S. Michelogiannis, and M. Zervakis, "Investigation of both power and coherence differences of brain lobes in two mathematical thinking tasks," in *2011 10th International Workshop on Biomedical Engineering*, 2011, pp. 1-4.

[47]   S. Makeig et al., "Dynamic brain sources of visual evoked responses.," *Science (New York, N.Y.)*, vol. 295, no. 5555, pp. 690-4, Jan. 2002.

[48]   V. Wyart and C. Tallon-Baudry, "Neural dissociation between visual awareness and spatial attention.," *The Journal of neuroscience : the official journal of the Society for Neuroscience*, vol. 28, no. 10, pp. 2667-79, Mar. 2008.

[49]   T.-P. Jung, S. Makeig, M. J. McKeown, A. J. Bell, T.-W. Lee, and T. J. Sejnowski, "Imaging Brain Dynamics Using Independent Component Analysis.," *Proceedings of the IEEE. Institute of Electrical and Electronics Engineers*, vol. 89, no. 7, pp. 1107-1122, Jul. 2001.

[50]   K. Michalopoulos, V. Iordanidou, G. A. Giannakakis, K. S. Nikita, and M. Zervakis, "Characterization of evoked and induced activity in EEG and

assessment of intertrial variability," *2011 10th International Workshop on Biomedical Engineering*, 2011.

[51]   W. Klimesch, P. Sauseng, S. Hanslmayr, W. Gruber, and R. Freunberger, "Event-related phase reorganization may explain evoked neural dynamics.," *Neuroscience and biobehavioral reviews*, vol. 31, no. 7, pp. 1003-16, Jan. 2007.

[52]   D. Iyer and G. Zouridakis, "Single-trial evoked potential estimation: comparison between independent component analysis and wavelet denoising.," *Clinical neurophysiology : official journal of the International Federation of Clinical Neurophysiology*, vol. 118, no. 3, pp. 495-504, Mar. 2007.

[53]   F. R. Vellutino, J. M. Fletcher, M. J. Snowling, and D. M. Scanlon, "Specific reading disability (dyslexia): what have we learned in the past four decades?," *Journal of child psychology and psychiatry, and allied disciplines*, vol. 45, no. 1, pp. 2-40, Jan. 2004.

[54]   C. Papageorgiou et al., "Preattentive deficits in developmental disorders of scholastic skills.," *Neuroreport*, vol. 16, no. 16, pp. 1829-32, Nov. 2005.

[55]   R. H. Fitch and P. Tallal, "Neural mechanisms of language-based learning impairments: insights from human populations and animal models.," *Behavioral and cognitive neuroscience reviews*, vol. 2, no. 3, pp. 155-78, Sep. 2003.

[56]   A. Baddeley, "Recent developments in working memory.," *Current opinion in neurobiology*, vol. 8, no. 2, pp. 234-8, Apr. 1998.

[57]   F. Pinkerton, D. R. Watson, and R. J. McClelland, "A NEUROPHYSIOLOGICAL STUDY O CHILDREN WITH READING , WRITING AND SPELLING DIFFICULTIES," *Developmental Medicine and Child Neurology*, vol. 31, pp. 569-581, 1989.

[58]   N. Brunswick and G. Rippon, "Auditory event-related potentials, dichotic listening performance and handedness as indices of lateralisation in dyslexic and normal readers.," *International journal of psychophysiology : official journal of the International Organization of Psychophysiology*, vol. 18, no. 3, pp. 265-75, Dec. 1994.

[59]   M. L. Bonte and L. Blomert, "Developmental dyslexia: ERP correlates of anomalous phonological processing during spoken word recognition.," *Brain research. Cognitive brain research*, vol. 21, no. 3, pp. 360-76, Nov. 2004.

[60]   D. L. Molfese, "Predicting dyslexia at 8 years of age using neonatal brain responses.," *Brain and language*, vol. 72, no. 3, pp. 238-45, May 2000.

[61] C. D. Yingling, D. Galin, G. Fein, D. Pelzman, and L. Davenport, "Neurometrics does not detect 'pure' dyslexics," *Electroencephalography and clinical neurophysiology*, vol. 63, pp. 426-430, 1986.

[62] C. Papageorgiou, G. a Giannakakis, K. S. Nikita, D. Anagnostopoulos, G. N. Papadimitriou, and A. Rabavilas, "Abnormal auditory ERP N100 in children with dyslexia: comparison with their control siblings.," *Behavioral and brain functions : BBF*, vol. 5, p. 26, Jan. 2009.

[63] C. C. Papageorgiou et al., "Long-term abstinence syndrome in heroin addicts: indices of P300 alterations associated with a short memory task.," *Progress in neuro-psychopharmacology & biological psychiatry*, vol. 28, no. 7, pp. 1109-15, Nov. 2004.

[64] C. Papageorgiou et al., "Abnormal P600 in heroin addicts with prolonged abstinence elicited during a working memory test.," *Neuroreport*, vol. 12, no. 8, pp. 1773-8, Jun. 2001.

[65] D. Weschler, *Manual for the Weschler Adult Intelligence Scale*. 1955.

[66] A. C. Tsai et al., "Mapping single-trial EEG records on the cortical surface through a spatiotemporal modality.," *NeuroImage*, vol. 32, no. 1, pp. 195-207, Aug. 2006.

[67] A. Delorme, S. Makeig, M. Fabre-thorpe, and T. Sejnowski, "From single-trial EEG to brain area dynamics," *Neurocomputing*, vol. 46, pp. 1057-1064, 2002.

[68] T. Demiralp, a Ademoglu, M. Comerchero, and J. Polich, "Wavelet analysis of P3a and P3b.," *Brain topography*, vol. 13, no. 4, pp. 251-67, Jan. 2001.

[69] B.-K. Min et al., "The best of both worlds: phase-reset of human EEG alpha activity and additive power contribute to ERP generation.," *International journal of psychophysiology*, vol. 65, no. 1, pp. 58-68, Jul. 2007.

[70] W. Klimesch, M. Schabus, M. Doppelmayr, W. Gruber, and P. Sauseng, "EVOKED OSCILLATIONS AND EARLY COMPONENTS OF EVENT-RELATED," *International Journal of Bifurcation and Chaos*, vol. 14, no. 2, pp. 705-718, 2004.